**Programa de Doctorat en Ciències**

**Escola de Doctorat de la Universitat Jaume I**

# Relaxin 3/ Relaxin Family Peptide Receptor 3 (RXFP3) system impact over spatial memory and social behaviour

(Papel del sistema Relaxina-3/ Receptor 3 de la Familia peptídica de las relaxinas (RXFP3) sobre la memoria espacial i el comportamiento social)

Memoria presentada per Hèctor Albert Gascó per optar al grau de doctor per la Universitat Jaume I.

Hèctor Albert Gascó Francisco Olucha Bordonau Ana María Sánchez Pérez

Castello de la Plana, Agost, 2018

## Finançament rebut

Agencies finançadores del doctorand

- Contracte predoctoral FPI UJI amb codi PREDOC/2014/35 (2015 – 2018)
- Pla de Promoció de la Investigació de l'UJI (2014-2017) P1.1A2014-06
- Consellería de Educación, Cultura y Deporte (2015-2016) AICO/2015/042

# ACKNOWLEDGMENTS

Quiero agradecer a mis dos directores de tesis, Ana María Sánchez Pérez y Francisco Olucha Bordonau por aceptarme en su laboratorio hace ya casi 7 años. Es de agradecer su aceptación porque como buen estudiante de licenciatura al finalizar mis estudios carecía de experiencia alguna en el laboratorio. Así pues ellos me lo enseñaron todo y contagiaron la pasión por la Neurociencia. Pero su aportación no ha sido solo profesional sino también personal, aportándome y transmitiéndome la importancia de la ética y valores en la ciencia y en la vida.

También quiero agradecerles el apoyo que durante todo este tiempo me ha dado mi familia; mi hermana Laura mi padre, mi madre, mi primo Joan y mis tíos.

En el día a día, sumido en jornadas de mucho trabajo, operando, haciendo comportamiento o simplemente estando en el laboratorio sin duda los miembros/amigos de mí grupo de investigación han sido fundamentales. Esto incluye a miembros pasados como Álvaro y Nisrin y presentes como Sandra, Cristina, Alberto, Nuno, Ernestina, Paco Ros, Vero, Mari. Gracias Cinta por tu inestimable apoyo trifásico que siempre toca mi alma y que echaré de menos seguro.

También mis amigos. Amigos en el sentido de “toda la vida”, esos que te definen y moldean con el paso del tiempo. Esos amigos como Marc Lluch, Andrea, Julia, Irene, Jade, Victor o Marc Perez.

Finally I would like to thank both Andrew and Sherie who helped, showed me and guided me during my stay in Melbourne. Both of them contributed greatly in making my stay a unique experience which always shall keep in my mind.

# SUMMARY

Different brain areas work together as a result of intricate connections allowing the expression of different behaviours. A major challenge in neuroscience research is to decipher the specific mechanisms of how different brain areas are inter-related to work together and what modulates them. Important lines of research focus on understanding how specific molecules, such neuropeptides, are key modulators of neuronal activity with deep implications in behavioural outcomes.

Many neuropeptidergic systems have been described and affect a wide range of behaviours. Some, such as hypocretin/orexin are synthesized only on a single region of the brain while others are synthesised on several locations. Oxytocin and vasopressin are but an example of the existing modulatory effects on the central nervous system, they are known for their role modulating socially related behaviours; others like ghrelin, leptin insulin regulate appetite and are also known as the “hunger hormone”, or neuropeptide Y; known for its role in circadian rhythm modulation; are other cases which illustrate the importance of neuropeptides on behaviour. Neuronal activity modulation studies reveal a complex interaction between slow-acting neuromodulators (neuropeptides) and fast-acting amino acid transmitters in the control of homeostasis, drug addiction, mood and motivation, sleep-wake states and neuroendocrine function.

This work focuses on the study of another neuropeptide, Relaxin-3. Since the discovery of Relaxin-3 and its cognate receptor, Relaxin Family Peptide Receptor 3, almost two decades ago, this system has been widely distributed throughout the brain, including hippocampus, septum and amygdala. Moreover, Relaxin-3 system has been shown to affect appetite, alcohol seeking, arousal and anxiety. Given the high expression of receptor and Relaxin-3 fibres in brain areas regulating memory and social behaviour we hypothesized that this system could have an important modulatory role in the fine tuning of these behaviours. In order to test our hypothesis we infused a

specific agonist of the Relaxin Family Peptide Receptor 3 intracerebroventircularly (icv) and tested the effect in specific behavioural paradigms.

Specifically, we hypothesized that the Relaxin3/ Relaxin Family Peptide Receptor 3 system has an impact on spatial memory through its Relaxin3 projections and Relaxin Family Peptide Receptor 3 expression in the septal area. We first tested the effect of the activation of Relaxin Family Peptide Receptor 3 in a T-maze two trial delayed paradigm. To do so we icv infused the agonist Relaxin-3 analogue 2. Subjects with agonist infusion did not distinguish between novel and familiar arms, meaning that spatial short-term memory was impaired compared to controls. Further studies revealed that agonist-infused subjects presented increased phosphorylated ERK at the septal area that colocalized with hippocampus-projecting cholinergic neurons. In addition, by means of In situ hybridization assays we observed that at the medial septum most Relaxin Family Peptide Receptor 3 expressing neurons also expresses vesicular GABA transporter and Parvalbumin. While colocalization with Parvalbumin is limited to the midline region of medial septum exclusive GABA transporter coexpression occurs on the outer parts of medial septum.

In conclusion, these results confirm a specific role of Relaxin-3 receptor in hippocampal dependent behaviour, and strongly suggested that this regulation could be achieved through modulation of septal specific neurons. In addition, it adds some new interesting features regarding memory processes which had not been tested until now. Nonetheless, time specific effect of the system on these neuronal phenotypes still need additional experiments to fully understand the underlying circuitry.

Results published in Brain Structure and Function, (Albert-Gascó et al. 2017) and Frontier in Neuroanatonomy, (Albert-Gascó et al. 2018).

We also hypothesised that the Relaxin 3/ Relaxin Family Peptide Receptor 3 system has an impact on social behaviour through its Relaxin 3 projections and Relaxin Family Peptide Receptor 3 expression in the amygdala. To assess its impact on social behaviour, a traditionally amygdala–dependent behaviour task, animals were subjected to a two trial social interaction three

chamber behavioural paradigm. Rats with agonist infusions had no social interaction impairment, but reduced social recognition memory compared to controls. Furthermore, agonist infused subjects showed increased number of phospho ERK (pERK) positive neurons in the amygdala compared to controls. Specifically in medial amygdala, ventral part of the bed nucleus of the stria terminalis and oval nucleus. pERK positive neurons in agonist treated animals had somatic contacts with relaxin-3 fibres and coexpressed Relaxin Family Peptide Receptor 3 in a significant higher ratio than controls. Moreover, complementary in situ hybridization assays revealed that Relaxin Family peptide Receptor 3 coexpresses oxytocin receptor at both anterodorsal and posterioventral medial amygdala. Interestingly, approximately 50% of total oxytocin receptor neurons coexpress the Relaxin Family Peptide Receptor 3.

Given oxytocin/oxytocin receptor signalling important role regulating social recognition memory, our results strongly suggests a possible mechanism underlying social recognition memory impairment by relaxin-3 agonist infusion. Furthermore, these results show how different neuropetidergic systems may interact with each other in fine tuning of behaviour.

Results sent to publication to Brain Structure and Function.

# RESUM

Diferents regions del cervell treballen a l'uníson com a conseqüència de connexions d'alta complexitat per donar lloc a l'expressió de diferents comportaments. Un del majors reptes de la recerca a la neurociència és saber diferenciar els mecanismes específics que modulen les interconnexions de les àrees que treballen juntes per regular un comportament. Línies de recerca importants es focalitzen com molècules específiques, com els neuropèptids, són moduladors clau de l'activitat neuronal i del comportament.

S'ha provat que molts sistemes nerupetidèrgics estan implicats i afecten a un rang elevat de comportaments. Alguns neuropèptids, com la hipocretina/orexina, són sintetitzats en una única regió del cervell, mentre que d'altres estan expressats a diverses localitzacions. L'oxitocina i la vasopressina són un exemple, entre molts, que presenten efectes moduladors sobre el sistema nerviós central. Són especialment importants pel seu paper modulant comportaments d'índole social. Altres casos a destacar són la grehlina, la leptina o la insulina que regulen l'apetit i per això també s'ha nomena com "l'hormona de la fam" o el neuropèptid Y que regula els ritmes circadians. Estudis de la modulació de l'activitat neuronal revelen que existeix una interacció complexa entre neuromoduladors d'acció lenta (neuropèptids) i els d'acció ràpida (aminoàcids). La interacció entre aquests dos components és d'especial importància per a mantindre l'homeostasis, addicció a drogues, motivació, estats de vigília/son i funció neuroendocrina.

Aquest estudi es focalitza a un altre neuropèptid, la relaxina-3. Des del descobriment, fa ja dos dues dècades, de la relaxin-3 i el seu receptor, receptor peptídic de relaxina 3 (RXFP3), aquest sistema està distribuït per tot el cervell amb hipocamp, sèptum i amígdala inclosos. A més, les fibres de relaxin-3 afecten l'apetit, cerca d'alcohol, ansietat i comportaments atencionals i actius. Tenint en compte l'alta expressió de la relaxina-3 en fibres i RXFP3 a les àrees que regulen la memòria i el comportament social vàrem hipotetitzar que aquest sistema podria tindre un rol modulador important per afinar trets específics

d'aquests comportaments. Per a corroborar la nostra hipòtesi vàrem infusionar una agonista específic de RXFP3 de manera intracerebroventricular (icv) per a després testar el seu efecte al comportament.

El primer objectiu era comprovar si l'activació de RXFP3 tenia un efecte en un paradigma en laberint T en dos tests. Per a dur-ho a terme vàrem infusionar l'agonista relaxin-3 analogue 2. La infusió de l'agonista, alhora que els animals realitzen el paradigma experimental, provoca que en el segon test els animals no podien diferenciar entre quin era el braç del laberint en T conegut i quin era el braç familiar, comparat amb els controls. La interpretació d'aquest comportament és que els animals amb infusions d'agonista no codifiquen la memòria espacial a curt-termini. Estudis posteriors varen revelar que aquests animals infusionats presentaven una densitat augmentada d'ERK fosforilat a l'àrea septal. Específicament, aquestes neurones pERK positives colocalitzaven amb neurones colinèrgiques de projecció hipocàmpica. D'altra banda es va comprovar amb la tècnica d'hibridació in situ que al sèptum medial RXFP3 es coexpresa amb el transportador de GABA i el de parvalbumina. La colocalització d'RXFP3 amb parvalbumina es limita a la regió pròxima a "línia mitja" mentre que el transportador de GABA es distribueix a les regions laterals del sèptum medial.

En resum, aquests resultats confirmen un rol específic de RXFP3 en els comportaments depenents d'hipocamp i suggereix que aquesta modulació podria ocórrer a través de l'acció específica de neurones del sèptum medial. Cal afegir a l'anterior, que aquests experiments afegeixen nous paràmetres interessants respecte al processament de memòria espacial que no s'havien testat fins ara. No obstant això, per conèixer el temps d'acció òptim del sistema i els diferents circuits que interactuen encara són necessaris experiments addicionals.

Els resultats varen estar publicats a Brain Structure and Function, (Albert-Gascó et al. 2017) i a Frontiers in Neuroanatonomy, (Albert-Gascó et al. 2018).

El segon objectiu era comprovar l'efecte sobre el comportament social, un comportament tradicionalment depenent d'amígdala. Per avaluar l'efecte, diferents exemplars varen realitzar un test social a un laberint de tres habitacions a dos fases. A la primera fase, s'analitzava el grau d'interacció social dels exemplars i a la segona fase, la memòria de reconeixement social. Les rates amb infusions d'agonista no presenten una interacció social reduïda, però no podien reconèixer ni diferenciar a un animal coespecífic conegut d'un desconegut, quan es comparava amb individus controls. A més, individus amb infusions d'agonista presentaven una densitat augmentada de fosforilació d'ERK a l'amígdala i amígdala estesa, comparat amb els exemplars del grups no experimentals. L'augment és específicament significatiu a l'amígdala medial, part ventral del nucli de l'stria terminalis i el nucli oval. Les neurones pERK positives als animals tractats amb l'agonista de RXFP3 presentaven contactes somàtics amb fibres de Relaxina-3 i coexpressaven RXFP3 en un ràtio més alt que exemplars controls. Estudis complementaris d'hibridació in situ mostren que RXFP3 es coexpressa amb el receptor d'oxitocina tant a la part anterodorsal, com posteroventral de l'amígdala mitjana. De totes les neurones que expressen el receptor de oxitocina, el 50% expressa RXFP3.

Tenint en compte el rol tan determinant que el sistema oxitocina/receptor d'oxitocina té regulant la memòria de reconeixement social, els nosaltres resultats suggereixen un possible mecanisme per explicar la no codificació de memòria de reconeixement social causat per infusió de l'agonista d'RXFP3. A més, aquests resultats encara reforcen més el paper regulador neuropeptidèrgic sobre el comportament.

Els resultats han estat enviats per a publicar-se a Brain Structure and Function.

# TABLE OF CONTENTS

# FIGURE AND TABLE LIST

# ABBREVIATIONS

| | |
|---|---|
| **Aca** | anterior commissure |
| **Ach** | acetylcholine |
| **aCSF** | artificial cerebrospinal fluid |
| **CaBP** | calcium binding protein |
| **cAMP** | Cyclic adenosine monophosphate |
| **CB** | calbindin |
| **CeA** | central nucleus of the amygdala |
| **ChAT** | Cholin Acetyltransferase |
| ***ChAT*** | Cholin Acetyltransferase gene |
| **CR** | calretinin |
| **CRE** | cAMP response elements |
| **Crf** | Corticotropin releasing factor |
| **DG** | Dentate gyrus |
| **dSN** | dorsal área to the Substantia nigra |
| **ERK** | externaly regulated kinase |
| **GABA** | gamma Aminobutyric acid |
| **GLU** | glutamate |
| **GPCR** | G protein–coupled receptor |
| **GPCR135** | Relaxin peptide receptor 3 |
| **Hb** | habenula |
| **HDB** | horizontal diagonal band |
| **HYPO** | hyothalamus |
| **ICV** | intracerebro ventricular |
| **IGL** | Intergeniculate leaflet |
| **IR** | immunoreactive |
| **LSI** | intermidiate lateral septum |
| **LSV** | ventral Lateral septum |

| | |
|---|---|
| **LTP** | long-term potentiation |
| **MeA** | anteromedial amygdala |
| **MeAD** | dorsomedial MeA |
| **MeAV** | anteroventral MeA |
| **MePD** | posterodorsal MeA |
| **MePV** | posteroventral MeA |
| **MnPo** | median preoptic nu |
| **MOB** | main olfactory bolb |
| **MS** | medial septum |
| **MS/DB** | medial septum/ diagonal band |
| **NI** | nucleus incertus |
| **NPY** | Neuropeptide Y |
| **Orx** | orexin |
| **OT** | oxytocin |
| **OV** | oval nucleus |
| **OXTR** | oxytocin receptor |
| ***Oxtr*** | oxytocin receptor gene |
| **PAG** | periaqueductal gray area |
| **PeP** | peptidergic system |
| **pERK** | phosphor externally regulated kinase |
| **PFA** | paraformaldehyde |
| **PFC** | prefrontal cortex |
| **PnR** | pontine raphe nucleus |
| **PV** | parvalbumin |
| ***PV*** | parvalbumin gene |
| **R3/I5** | human relaxin-3 /INSL5 chimeric peptide |
| **RLN3** | Relaxin-3 |
| **RPO** | reticularis pontis oralis |
| ***Rxfp3*** | Relaxin peptide receptor 3 mRNA |
| **RXFP3** | Relaxin peptide receptor 3 |
| **RXFP3-A2** | relaxin-3 analogue 2 |
| **Shy** | substantia Innominata |
| ***Slc32a1*** | vesicular GABA Transporter gene |

| | | | |
|---|---|---|---|
| **SOM** | somatostatine | | nucleus |
| **SRM** | social recognition memory | **TS** | triangular septal nucleus |
| **ST** | bed nucleus of the stria terminalis | **vCA1** | field CA3 of the hippocampus |
| **STLP** | posterolateral ST | **VDB** | vertical diagonal band of broca |
| **STMA** | anteromedial ST | ***vGAT*** | vesicular GABA transporter gene |
| **STMV** | ventromedial ST | **vLS** | ventral lateral septum |
| **SuM** | supramammilar | | |

# 1

# General Introduction

## 1.1. The Relaxin-3/RXFP3 system

Behaviour regulation depends on different anatomical and physiological brain systems. These systems may work in two ways, through amino acid fast-action or through slow-action modulatory regulation. The combined action of these systems results in promotion or inhibition of behaviours. Relaxin-3 (RLN3) and its cognate receptor Relaxin Family peptide receptor 3 (RXFP3), having a brain wide distribution, belong to the second group and have been proven to modulate different behaviours and potentially modulate many others. Although its behavioural importance and impact has been proven since it was first discovered, further experiments are needed to clarify the reach and ways which this behavioural system works. For instance, no information is known on what phenotypic markers are shared by RXFP3, regulation by/with other neuromodulators or the whole range of modulated behaviours.

To clarify the main defining traits of the RLN3/ RXFP3 system, we will introduce RLN3 as a neuropeptide in combination with its historical perspective, which has led from its discovery to its potential therapeutic application in neural illness.

### 1.1.1. Historical significance: Discovery of Relaxin-3, relaxin-family peptide 3 receptor (RXFP3)

Relaxin-3 (RLN3) was discovered in 2002 when searching for homologues of relaxin in different databases (Bathgate et al. 2002). Given that the expression pattern was mostly confined to the brain it was classified as a neuropeptide.

The cognate receptor for RLN3 is the relaxin-family peptide 3 receptor (RXFP3) (Bathgate et al. 2006). This receptor has also been referred to as GPCR135 (Liu et al. 2003) and had previously been named as somatostatin or angiotensin-like receptors. Given its similarity in structure with the angiotensin AT1 receptor and the somatostatin receptor-5 (Matsumoto et al. 2000).

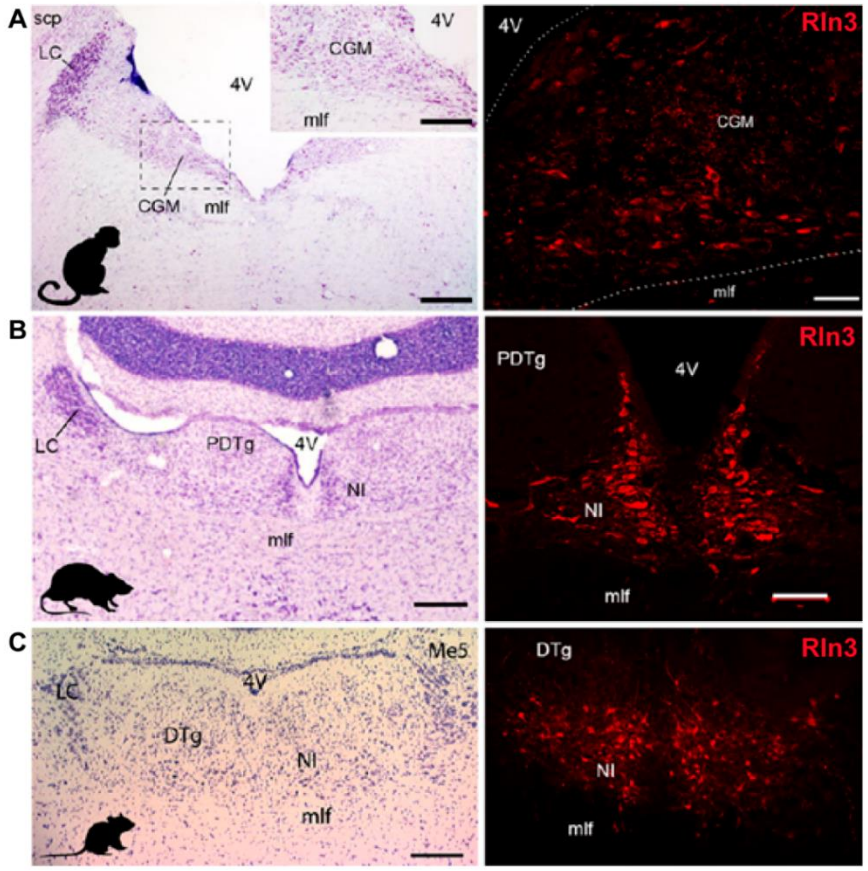


**Figure 1.1 NI across species**. Adapted from (Ma et al 2017). The nucleus incertus and its relaxin-3 neurons are similarly located in the midline periventricular central grey of non-human primate (macaque), rat and mouse brain and are conserved across species (adapted from Ma et al., 2007; 2009b; Smith et al., 2010). Nucleus incertus (NI) is the primary source of neurons expressing relaxin-3 mRNA and abundant relaxin-3 immunoreactivity, which are located in the midline periventricular central grey at the base of the fourth ventricle (4V) of (**A**) macaque, (**B**) rat and (**C**) mouse. Abbreviations: CGM, mid central grey; DTg, dorsal tegmental nucleus; LC, locus coeruleus; Me5, mesencephalic trigeminal nucleus; mlf, medial longitudinal fasciculus; PDTg, posterodorsal tegmental nucleus; scp, superior cerebellar peduncle. Scale bars, (A) Nissl, 0.6 mm, inset, 80 µm, relaxin-3, 0.2 mm; (B) Nissl, 0.3 mm, relaxin-3, 0.1 mm; (C) 0.2 mm.

Ultrastructural examinations of the rat brain have revealed that relaxin-3-like immunoreactivity (IR) is present within the endoplasmic reticulum and Golgi apparatus in the cell soma, and within dense-core vesicles adjacent to

the synapsis in nerve terminals (Tanaka et al. 2005; Ma et al. 2009a; Olucha-Bordonau et al. 2012), confirming the role of RLN3 as a neurotransmitter.

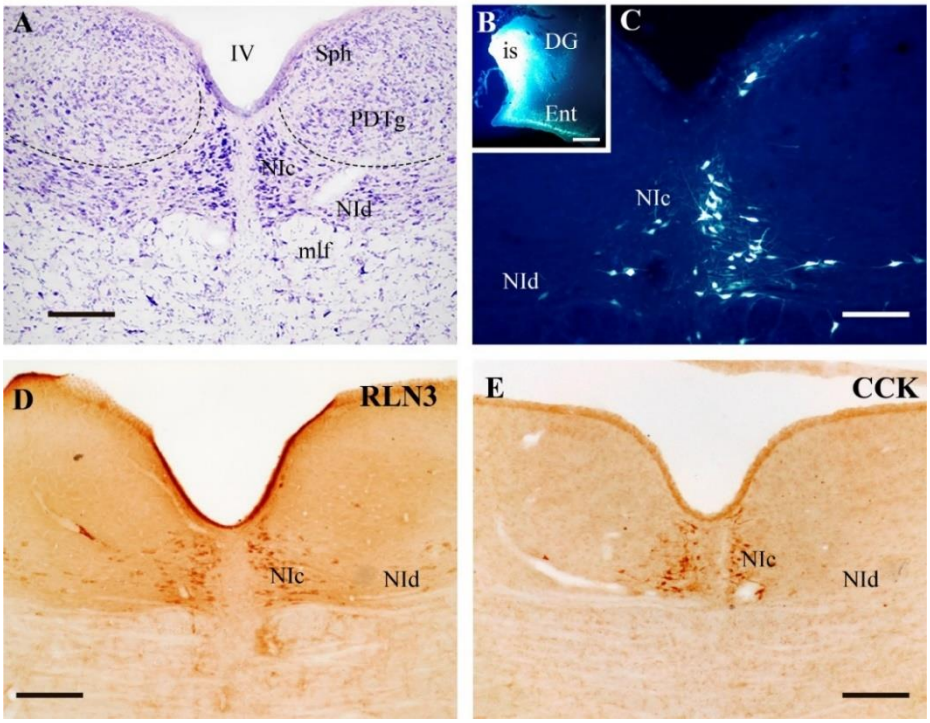


**Figure 1.2**. **Basic morphological features of the NI**. (adapted from Olucha 2018) (**A**) A giemsa stained section of the pontine tegmentum at the level of the floor of the Ivth ventricle (IV), the NI is outlined and composed of the pars compacta in the midline (Nic) and the pars dissipata (Nid), just dorsal to the medial longitudinal fascicle (mlf) dorsolateral to the NI at this level, the posterodorsal tegmentum (PDTg) and the sphenoid nucleus (Sph). (**B**) An injection site (is) of the retrograde tracer fluorogold (FG) in the dentate gyrus of the caudal hippocampus, some retrograde labeling is observed in tghe entorhinal cortex (Ent). (**C**) Retrograde labeling in the ipsilateral NI resulting from the injection in B, some retrograde labeling also appeared in the contralateral NI. (**D**) ICC of relaxin-3 (RLN3) in the NI. (**E**) ICC of colecistokinin (CCK) in the Nic. Calibration bars in A, C, D and E, 200 um, calibration bar in B, 500 um.

RLN3 positive cells distribution in brain has been studied in adult rat and mouse brain revealing an intense expression in a tight cluster of cells known as nucleus incertus (NI) (Bathgate et al. 2002; Burazin et al. 2002; Tanaka et al. 2005; Ma et al. 2007; Smith et al. 2010). In addition, this area, the NI has been identified across many other species including zebra fish (Donizetti

et al. 2008) and, macaque (Ma et al. 2009b) **(Fig 1.1)**. NI conservation throughout different species strongly suggest an important function.

In the adult rat brain the NI was estimated to contain approximately 2000 RLN3 positive neurons (Tanaka et al. 2005). The distribution of this neurons closely resembles the topography of the GABAergic NI (Goto et al. 2001; Olucha-Bordonau et al. 2003), making RLN3 a good marker for NI. Most RLN3 positive neurons are in the pars compacta (NIc) while they are more sparsely distributed on the pars disipata (NId) (Tanaka et al. 2005; Ma et al. 2007) **(Fig 1.2)**.

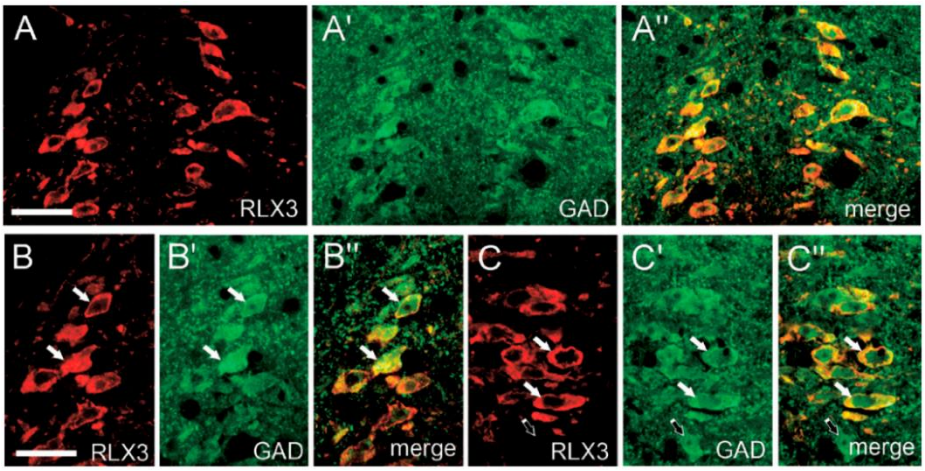


**Figure 1.3 RLN3 phenotype at NI.** Adapted from (Ma et al. 2007). Relaxin 3 positive neurons **(A)** GAD **(A')** and merge **(A'')** signal from an IF confocal image. Higher magnification images of the left NIc **(B-B'')** and right NIc **(C-C'')** to illustrate the colocalization**.** Scale bar at (A) 30µm and (B) 20µm.

Following the location of RLN3 positive neurons at NI double labelled immunofluorescence confirmed that these neurons were also positive for GABA synthase enzyme, GAD (Ford et al. 1995; Olucha-Bordonau et al. 2003; Ma et al. 2007) **(Fig.1.3)**. Several other peptides and proteins have been observed within the NI, coexpressing with RLN3 including neuromedin B, cholecystokinin, calbiding, calretinin, TrackA receptor, $CRF_1$ receptor, $CRF_2$ receptor (Kubota et al. 1983; Olucha-Bordonau et al. 2003; Justice et al. 2008; Banerjee et al. 2010).

In addition to the NI, other structures within the brain contain some RLN3 positive neurons, These areas include the pontine raphe nucleus, the anterior periaqueductal grey (medial and ventral) and in the lateral substancia nigra (Tanaka et al. 2005; Ma et al. 2007; Smith et al. 2010). RLN3 positive neurons in these areas have recently been proven to share many electrophysiological traits with the NI RLN3 positive neurons. (Tanaka et al. 2005; Ma et al. 2007; Blasiak et al. 2013).

This shared characteristics further encloses RLN3 and RXFP3 into a system and highlights how closely it resembles other neuropeptidergic systems.

### 1.1.2. Relaxin-3 and RXFP3 in comparison to other Neuropetidergic systems.

RLN3 system shares many features with other neuroptidergic systems. Thus, RLN3 storage occurs in dense core vesicles (DCV) adjacent to synapse in nerve terminals (Tanaka et al. 2005; Ma et al. 2009a; Olucha-Bordonau et al. 2012). DCV are placed nearby active synaptic sites in contrast with clear vesicles, carrying amino acid neurotransmitters (GABA, Glu), that tend to congregate in the active synaptic specialization (Dreifuss 1975; Nordmann and Morris 1984). The release of DCV is dependent on axonal high spike frequency which are efficient until they reach a *plateau* and released concentrations do not get higher. Alternatively, spike bursts followed by silent periods of stimulation seem to be even more efficient for neuropeptide release (Ludwig and Leng 2006). Changes in spike frequencies or bursts cause neuropeptide release through increased citoplasmatic calcium concentration changes within the axon terminals (Ludwig et al. 2002). DCV have a slow recycling rate (Van den Pol 2012) and could be indicative of a specific stimuli and/or context modulation. Nothing is known about the dynamics and spike frequencies regarding RLN3 release at the axonal terminals.

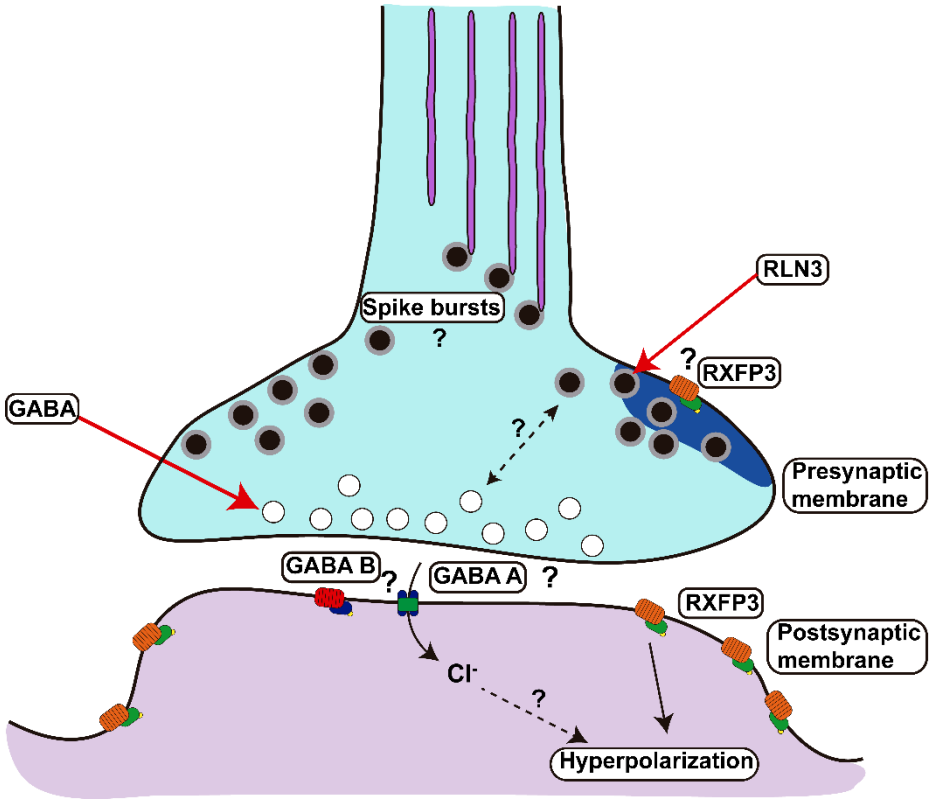


**Figure 1.4 Schematic synaptic representation of the RLN3/RXFP3 system.** Possible interaction with γ-Aminobutyric acid (GABA) are shown with doted lines and question marks untested.

Neuropeptides are usually ligands for G-protein coupled receptors (GPCRs). Upon activation, neuropetidergic GPCRs dissociate activating/inhibiting adenylyl cyclase and amplify the peptide signalling through ERK/MAPKeses and other protein kinases such as PKC or PKA (Vögler et al. 2008). GPCRs are sensitive to nanomolar ligand concentrations, while ionotropic receptors require ligand concentration in the micromolar range, (Van den Pol 2012). This is the case for RXFP3 that has been shown to be activated *in vitro* with $10^{-8}$ M of H3 (human relaxin-3) (Kocan et al. 2014).

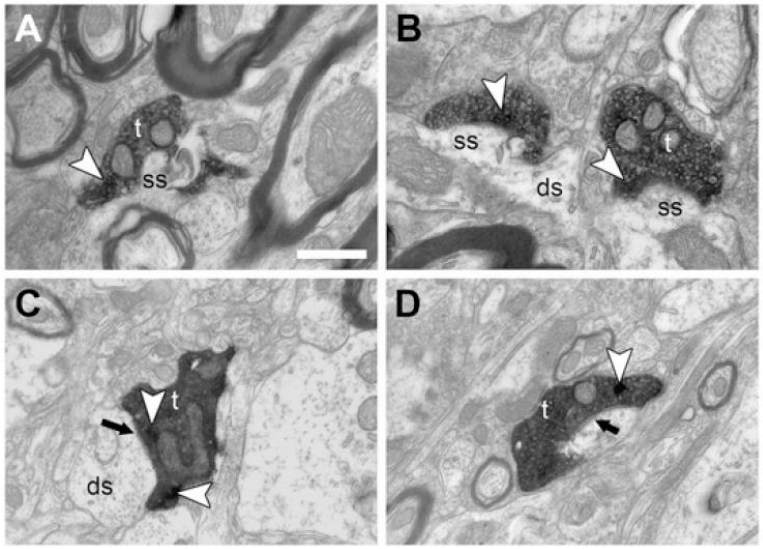


**Figure 1.5 RLN3 dense core vesicles.** (Adapted from Ma 2009) Electron photomicrographs of coronal sections of the MS following anterograde-labelling from the NI after local injection of mR.**(A–D)** Densely packed synaptic vesicles of oval morphology were observed in terminal synapses (white arrows), many of which made contact with dendritic shafts and small spines of MS neurons with clear symmetric morphology (black arrows). (ds) Dendritic shaft; (ss) small spine; (t) terminal. Scale bar, 500 nm.

Another common trait in many neuropeptide systems are mismatches between distribution of neuropeptide terminals and cognate receptors. This fact has generated an intense debate about the role that receptors in brain areas with no apparent neuropeptide terminal release (Van den Pol 2012). That is also the case in the RLN3/RXFP3 system which presents high expression of RXFP3 but scarce RLN3 positive fibres at central amygdala (CeA), paraventricular nucleus (PVN) and oval nucleus (OV) (Sutton et al. 2005; Ma et al. 2007; Santos et al. 2016). Some have argued that, given the presence of disulphide bonds binding neuropeptides together and extending their extracellular half-life (Ludwig and Leng 2006), neuropeptides may travel by diffusion throughout several microns of distance (Jan and Jan 1982). In fact, neuropeptides are known to be functional micrometres away from their release site in contrast to amino acid neurotransmitters which only act within nanometres of release (Jan and Jan 1982; Van den Pol 2012).

Finally, neuropeptides are coexpressed in neurons with other neurotransmitters like GABA, glutamate or Glycine. For instance, GABA interneurons in the hippocampus coexpress neuropeptide Y, somatostatin, vasoactive intestinal polypeptide, cholecystokinin, dynorphin, enkephalin, neurokinin B, and substance P (Freund and Buzsáki 1998; Acsády et al. 2000; Billova et al. 2007; Antonucci et al. 2012). Similarly, RLN3 positive neurons express GABA in the NI (Ma et al. 2007). Coexpression of peptides and neurotransmitter within the same neuron does not act as two defined separate systems but on most occasions peptides modulate GABAergic or glutamatergic fast synaptic activity (Colmers et al. 1988; Sperk et al. 2007). Regarding the interaction between GABA and RLN3 not much is known.

## 1.2. Distribution of Relaxin-3 and RXFP3

High resolution tracing techniques and classical in situ hybridization (ISH) techniques have been used to pinpoint the exact location for both RLN3 and RXFP3. RLN3 positive neurons have been found to arise from the pontine raphe nucleus (~350 neurons), the anterior PAG (~550 neurons), an lateral substancia nigra (~350 neurons) and within NI (~2000 neurons) (Tanaka et al. 2005). Furthermore, studies regarding RXFP3 distribution used classic ISH techniques. As such, many utilised radioligands which do not qualify to obtain sufficient cellular resolution. Nonetheless, it did show an accurate distribution throughout the brain, highlighting areas with higher levels of expression. Additionally, binding assays gave further insights from a functional perspective ([125]-R3/I5) (Ma et al. 2007; Ma et al. 2009a; Smith et al. 2010; Haidar et al. 2017).

When using Risold and Swanson (Risold and Swanson 1997) nomenclature for the septal divisions, RLN3 distribution throughout the different levels of **septum** showed that in anterior sepum bregma 1.0 mm), most prominent RLN3 labelling was found in the LSr-dl and more diffusely on the vMS. But not observed in LSc or in the septohimpocampal nucleus. At more more caudal levels (bregma 0.75, 0.5 and 0.3 mm) RLN3 fibres had increasing Immunoreactive (IR) levels within the medial septum (MS), vertical diagonal band of broca (VDB) and horizontal diagonal band of broca (HDB) while other

surrounding areas were lacking in RLN3 (LSr-dl, LSr-m, LSr-vl) (Olucha-Bordonau et al. 2012).

At posterior level of septum (Bregma 0.05 mm) fibres were mostly distributed on the LSc-v and were sparsely distributed along the triangular septalis (TS) and Septofimbrial nucleus (SFi). Interestingly, many of the RLN3 fibres have been shown in close synaptic contacts with parbalvumin (PV) calbindin (CB), calretinin (CR) and cholinergic (ChAT) positive MS neurons (Olucha-Bordonau et al. 2012).

RXFP3 on the other hand, is found highly expressed at the MS/DB in different species such as mouse, rat or macaque (Ma et al. 2007; Ma et al. 2009b; Smith et al. 2010). In mouse, binding assays showed that binding levels between RXFP3 and RLN3 are moderate at the MS/DB (Smith et al. 2010) (Smith et al. 2010).

Similar to the hippocampus, RLN3 fibres reach amygdala and extended amygdala on specific and delimited areas. Given the developmental common origin this areas were studied together (Santos et al. 2016). Specifically, at the most anterior levels of the bed nucleus of the stria terminalis (ST) (bregma +0.12 mm) RLN3 fibres are widely distributed on the medial anterior stria terminalis (STMA), ventromedial stria terminalis (STMV) and ventrolateral stria terminalis (STLV) in contrast to the dorsolateral part of the stria terminalis (STLD-LJ) or oval nucleus (OV). On mid-levels of ST (bregma -0.36 mm) most RLN3 positive fibres are present at the STMA and STMV and some diffuse fibres in the STLV and very scarce in the OV Posterior ST (bregma -0.72 mm) had fewer fibres than in anterior levels. delimited to STMP, STMPI and STMPL (Santos et al. 2016).

In the rat, the largest density of RXFP3 receptor at ST is found in the OV compared to the slightly lower distribution at STMV and STMA (Ma et al. 2007), whereas in mice the receptor is not found in this area (Smith et al. 2010).

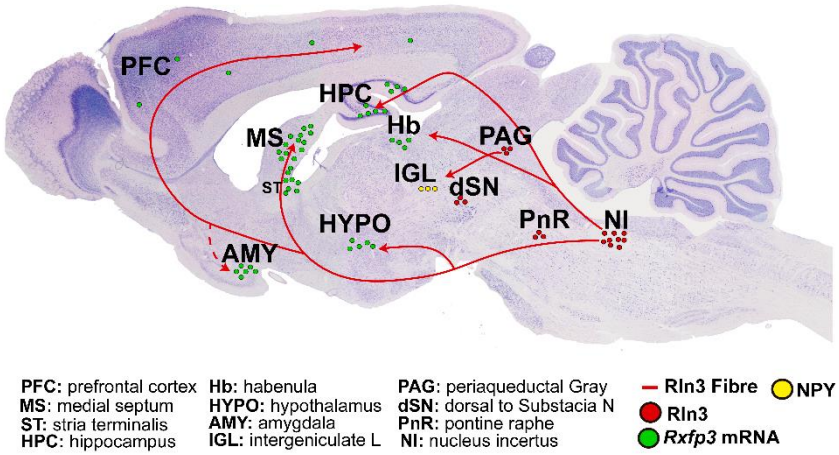


**Figure 1.6 RLN3/RXFP3 system distribution** showing the different locations of RLN3 positive neurons (red dots) and their known projections (RED). Rxfp3 mRNA positive areas are indicated with green dots.

Within the pallial amygdala (Bregma - 2.12 to - 3.80 mm) the greatest density of RLN3 positive fibres are present at the media amygdala (MeA) especially at the mid-levels (Bregma – 3.14 mm). In addition, a high density of RLN3 fibres were found at the posteriolateral cortical amygdala (PLCo), interamygdaloid stria terminalis nucleus (STIA) and some portions of the lateral amygdala (LA), whereas very few fibres entered the central amygdala (CeA) and basolateral amygdala (BLA). Furthermore, some RLN3 fibres made synaptic contacts with CR and CB positive neurons (Santos et al. 2016). Distribution of RXFP3 in rat amygdala showed high levels within the CeA and slightly lower at the BMA, MeAD and MePV (Ma et al. 2007). In contrast in mice expression levels were high at the MeA and BMA but none in the CeA (Smith et al. 2010).

RLN3 fibres distribution within the hippocampus has been found very dense at the dentate gyrus (DG), CA1 and CA3 fields, in both rats and mice; making somatic contacts with somatostatin (SST), CR and GAD positive neurons at the DG (Haidar et al. 2017). RXFP3 distribution, similarly to septal

area matched that of RLN3 fibres distribution (Ma et al. 2007; Smith et al. 2010; Haidar et al. 2017).

## 1.3. Relaxin-3 and its cognate receptor, RXFP3

RLN3 belongs to the insulin superfamily, and is a heterodimeric peptide (A chain and B chain). These two chains bind together with two interchain disulphide bonds (Liu et al. 2003; Rosengren et al. 2006). Several analysis show that the A-chain display greater sequence divergence than B-chains (Sherwood 2004). Although RLN3 binds and activates RXFP3 through the B-chain, an A-chain point mutation have been shown to alter receptor binding (Liu et al. 2003; Liu et al. 2005).

RLN3 can bind to receptors RXFP1, RXFP4 and RXFP3. In order to synthesize specific agonist of RXFP3 first strategies conjugated the human B-chain of RLN3 to the human's INSL5 A-chain. This chimeric agonist was named R3/I5 which displayed markedly reduced ability to bind to and activate RXFP1 (Liu et al. 2005). Truncation of R3/I5 B-Chain, resulted in a RXFP3 antagonist (ΔR3/I5) (Kuei et al. 2007). Some years later a second generation of agonist with specific binding for RXFP3 with no affinity over RXFP1 or RXFP4 was developed. This agonist was called RXFP3-selective analogue 2 (RXFP3-A2) [R3A(11–24,C15 → A)B] and the specificity was obtained by the deletion of 10 residues of the N terminus of the A-chain. Further truncation of the B-chain led to a high-affinity RXFP3-selective antagonist (A3) (Shabanpoor et al. 2012).

RXFP3 also known as GPCR135 and SALPR, as RXFP4 (GPCR142), is a member of the type I GPCRs family (Liu et al. 2003). Therefore, is coupled to inhibitory $G\alpha_{i/0}$ subunits and is -sensitive to the pertusis toxin inhibition of forskolin-stimulated cyclic adenosine monophosphate (cAMP) accumulation. Studies in vitro cell lines, have shown that upon binding of ligand RXFP3, like many other $G\alpha_{i/0}$ – couple receptors GPCRs, results in a rapid and transient increase in ERK1/2 phosphorylation via PKC and PI3kinases pathways (Liu et al. 2003; Van der Westhuizen et al. 2007). PTX pre-treatment completely abolishes ERK phosphorylation in all in vitro models tested highlighting the importance of $G\alpha_{i/0}$ subunit in the signalling pathway. Additionally, reporter gene

assays have allowed, in posterior studies, to elucidate the downstream genes upregulated after RXFP3 activation. These are; the Activator protein 1 (AP-1) transcription factor and the NF-ƙB transcription factor.(Van der Westhuizen et al. 2010).

## 1.4. Functions of Relaxin-3/RXFP3 system

Given the RLN3/RXFP3 broad spread innervation throughout the brain many behaviours were postulated to be modulated by this system. Pharmacological approach using both first and second generation RXFP3 agonists and antagonists have been used to study RLN3/RXFP3 system role on behaviour.

Intracerebroventricular infusion of RLN3 and R3/I5 agonists promotes food intake (McGowan et al. 2005; Ganella et al. 2013; de Ávila et al. 2018). It also displays an anxyolitic effect in in rats (Ryan et al. 2013b). In addition, RXFP3 antagonist infusion at the ST reduces alcohol seeking (Ryan et al. 2013b). Other studies conducted on both RXFP3 KO and RLN3 KO show hypoactivity on a running wheel (Smith et al. 2012; Hosken et al. 2015).

In spite being so strongly expressed in hippocampus, septum and amygdala, the role of RLN3/RXFP3 system regulating these areas dependent behaviours have not been carried out in deep. Traditionally spatial memory and social behaviour are hippocampus and amygdala –related behaviours respectively.

Theta rhythm is a rhythmical wave (7-12Hz) that takes place in CA1, CA3 fields and DG of the hippocampus (Buzsáki 2002). RLN3/GABA projections modulate the MS septohippocampal pathway an theta rhythm (Nuñez et al. 2006; Ma et al. 2009a; Ma et al. 2013; Martínez-Bellver et al. 2015; Martínez-Bellver et al. 2017) through its connections on PV and Cholinergic connections. GABAergic-PV positive neurons are fast-firing (Sotty et al. 2003; Yoder and Pang 2005; Vandecasteele et al. 2014) and inhibit hippocampal interneurons which in turn facilitates theta rhythm (Freund and Antal 1988; Toth et al. 1997; Freund and Gulyas 1997; Hangya et al. 2009). On the other hand slow-firing cholinergic positive neurons at the MS/DB also

project to the hippocampus and also promote theta rhythm (Sotty et al. 2003; Yoder and Pang 2005; Vandecasteele et al. 2014).

NI stimulation, in urethane anesthetized rats, evoked theta oscillations and lesions of NI abolished theta rhythm evoked by brainstem stimulation (Nuñez et al. 2006). Specifically, when using R3/I5 agonist injected directly into the MS promoted theta rhythm with a peak 5-10min from infusion which lasted up to 30 minutes.

### 1.4.1. Spatial memory

Hippocampal-dependent spatial memory was firstly described in the 1970s, electrophysiological experiments showed behavioural correlates between spatial location and neuronal firing (O'Keefe and Dostrovsky 1971; Ranck 1973). Spatial memory refers to memories that store information regarding the location of physical surroundings in space (Morellini 2013). A typical behavioural response that relies on spatial memory is navigation, which is the ability to travel from one place to another. Behavioural biologists use navigation as it is the observable and measurable parameter used to obtain insight into spatial memory (McNaughton et al. 1996; Thompson and Varela 2001; McNaughton et al. 2006; Morellini 2013). As any other memories, spatial memory, as an experience based, processes information gets encoded, stored and finally retrieved (Atkinson and Shiffrin 1968; Baddeley and Warrington 1970; Milner 1972). The duration that information gets stored determines if the spatial memory is short-term memory or long-term memory (Eysenck 1988). Most animal models which analyse spatial memory asses working memory using T, Y or radial mazes. Working spatial memory is a term used to refer to memory while is being used to plan and carry out a behaviour. Specifically, working memory is a cognitive process which includes attention, short-term memory and information processing (Baddeley 1992; Becker and Morris 1999). T, Y and radial mazes which analyse spatial working memory use spontaneous alternation, tendency in rodents which avoids them re-entering the same arm from a maze which they have already entered. The rationale behind is that if they do not re-enter an already visited arm is because they remember the have already been there and enter the next arm. Nonetheless, it is argued that the tendency to explore the last-visited arm declines due to habituation thus leading

to alternation. Under this hypothesis no manipulation of information takes place (Sanderson and Bannerman 2012). However, it is plausible that manipulation of information on these paradigms could be debatable and it could be argued that only short-term memory is being analysed. From this point onward on our T-maze paradigms, we interpret that we are assessing spatial short-term memory.

The hippocampal correlate to this behaviour was enlightened from the finding that certain neurons only fire on a specific location. These neurons were named *place cells* (O'Keefe and Dostrovsky 1971; Ranck 1973). Place cells spiking within the CA1 and CA3 fields are preceded and have a phase relationship with Theta rhythm cell spiking at the hippocampus (O'Keefe and Recce 1993). While place cells spiking correlates with animal location in an environment (O'Keefe and Dostrovsky 1971), theta rhythm correlates with a class of movement that changes the rats location in an environment (Taube et al. 1990; O'Keefe and Recce 1993; Hirase et al. 1999; Buzsáki 2005). Furthermore, hippocampal neurons which are modulated by theta rhythm "theta-modulated place-by-direction cells" (TPD) code for both the location and head direction of animals (Cacucci et al. 2004).

Modulation of spatial memory through the RLN3/RXFP3 system is thought to take place simultaneously through RLN3/GABA positive projections from the NI to the MS/DB and to the DG in the hippocampus (both ventral and dorsal) (Haidar et al. 2017).

Agonist R3/I5 infusions into the MS showed no effect on spatial working memory compared with vehicle group (aCSF infused, on a continuous spontaneous alternation test, when). However, antagonist ΔR3/I5 impaired spatial working memory which was returned to basal levels (vehicle levels) with R3/I5 agonist (Ma et al. 2009a).

GABAergic and cholinergic neurons from the MS/DB send projections to the DG hilus, CA1 and CA3 fields (Freund and Antal 1988; Dutar et al. 1995; Vertes and Kocsis 1997). Most GABAergic septal projections contact on DG hilus interneurons (Freund and Antal 1988; Amaral et al. 2007) participating in the control of theta rhythm (Vertes and Kocsis 1997; Vertes 2005) and the

processing of cognitive and spatial maps (O'Keefe and Recce 1993; Leutgeb et al. 2005; Schiller et al. 2015). Some recent work in mice, has focused on how the RLN3/RXFP3 system in the DG hilus modulates spatial working memory (Haidar et al. 2017). Endogenous RXFP3 silencing at DG hilus impair spatial working memory during the 1st minute (10 minute test) of a spontaneous continuous alternation task (SAT) but does not on the remaining 9 minutes (Haidar et al. 2017).

The role of RLN3/RXFP3 system in spatial memory has been studied. However, spatial working memory and/or short-term spatial memory can be further studied including new variants and untested critical times.

### 1.4.2. Social behaviours, social recognition memory.

Social recognition memory (SRM) can be defined as ability to recall a conspecific subject which has previously been encountered (Gheusi et al. 1994). In rodents, SRM is mediated by chemical cues perceived via the main (MOB) and accessory (AOB) olfactory bulbs (Dulac and Torello 2003) which then send information to the MeA (Ferguson et al. 2001; Lukas et al. 2013; Gur et al. 2014). MeA is crucial for social recognition memory as it receives direct projections from the social olfactory stimuli centres (Scalia and Winans 1975). This information is modulated by vasopressin and oxytocin (OT) and its receptors V1 and V2 for vasopressin and OXTR for oxytocin. OT/OXTR system is especially important as OT knockout mice do not display social recognition memory while local infusions into the MeA rescue the ability to form social memories (Everts and Koolhaas 1997; Winslow et al. 2000; Ferguson et al. 2001; Choleris et al. 2007; Veenema 2008). Furthermore, OT knockout mice show a decrease in C-Fos expression in MeA, ST and medial preoptic area (Ferguson et al. 2001) compared to vehicles after an social interaction and social memory test (Ferguson et al. 2001; Richter et al. 2005) (**Fig.1.7**).

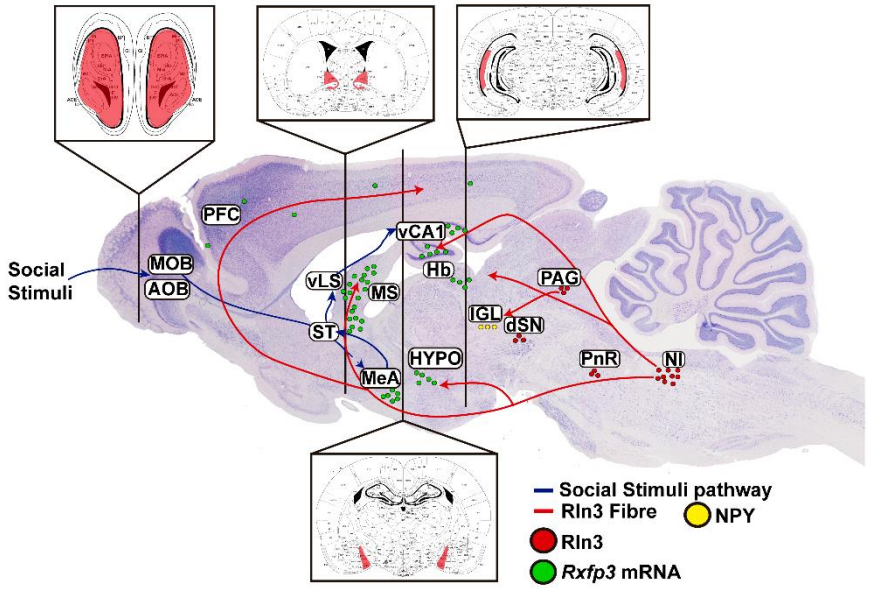


**Figure 1.7**. **Social recognition memory (SRM) pathway and RLN3/RXFP3 system**. Olfactory stimuli processed at the main olfactory bulb (MOB) and accessory olfactory bulb (AOB) which then gets transferred to the MeA. MeA is key in SRM processing through its OT/OXTR innervation which transfers social discrimination information to the ventral lateral septum (vLS) through the bed nucleus of the stria terminals (ST). Finally from lateral septum, in a vasopressin dependent mechanism social memory gets stored at the ventral CA1 from the hippocampus.

The role of RLN3/RXFP3 system in modulating social behaviours has not been studied. Although RLN3 fibres are very abundant in the MeA, from rostral to caudal levels, (Santos et al. 2016) and *Rxfp3* mRNA positive neurons are highly expressed on both MeA, ST and hippocampus (Sutton et al. 2004) **(Fig1.7).**

## 1.5. Hypothesis and Aims

Considering all evidence implicating RLN3/RXFP3 system on spatial short-term memory and social behaviour we considered two hypothesis:

**Hypothesis 1**: RLN3/RXFP3 System has an impact on spatial memory through its RLN3 projections and RXFP3 expression in the septal area.

- **Aim 1**: Study the impact of RXFP3 activation over the septal area using ERK1/2 phosphorylation as a marker
- **Aim 2:** Study the distribution in specific septal nuclei and phenotype of pERK1/2 positive neurons.
- **Aim 3:** Study if RXFP3 activation has an impact on spatial short-term memory.
- **Aim 4:** Study the distribution and phenotype of Rxfp3 mRNA positive neurons.

**Hypothesis 2**: RLN3/RXFP3 system has an impact on social behaviour through its RLN3 projections and RXFP3 expression in the amygdala.

- **Aim 1**: Study the impact of RXFP3 activation over the amygdala using ERK1/2 phosphorylation as a marker.
- **Aim 2**: Study if RXFP3 activation has an impact on social behaviour.
- **Aim 3**: Study the distribution and density of pERK1/2 positive neurons in specific medial amygdala and extended amygdala nuclei.
- **Aim 4:** Study if pERK1/2 positive neurons in specific amygdala and extended amygdala nuclei colocalize with Rxfp3 expressing neurons.
- **Aim 5**: Study the distribution and phenotype of Rxfp3 mRNA positive neurons at the medial amygdala and extended amygdala

# 2

## Central relaxin-3 receptor (RXFP3) activation increases ERK phosphorylation in septal cholinergic neurons and impairs spatial working memory

## 2.1. Introduction

There is a strong body of evidences that supports the involvement of the septal area in regulation of behavioural processes of arousal and attention, mostly through connections from the medial septum/diagonal band (MS/DB) to the dentate gyrus (DG) in the hippocampus (Vertes and Kocsis 1997). Arousal, attention and locomotion related to navigation and exploration and mnemonic processes in humans (Morales et al. 1971; Bannerman et al. 2004a) are functionally associated with hippocampal theta rhythm, a synchronous 4-12 Hz oscillation of primarily principal neurons and with place cell configuration (Kemp and Kaada 1975; O'Keefe 1976; Leung and Yim 1986; Raghavachari et al. 2001).

Hippocampal theta rhythm can be generated and modulated from the septum (Morales et al. 1971; Bannerman et al. 2004b), and different types of neurons within the MS/DB participate in this process (Sotty et al. 2003; Robinson et al. 2016). Septal cholinergic neurons are slow-firing neurons that promote hippocampal theta rhythm (Sotty et al. 2003; Yoder and Pang 2005; Vandecasteele et al. 2014) and are responsible for transient arousal states and hippocampal activation (Zhang et al. 2011). Septal GABAergic parvalbumin (PV)-positive neurons are fast-firing (Sotty et al. 2003; Yoder and Pang 2005; Vandecasteele et al. 2014) and inhibit inhibitory hippocampal interneurons (Freund and Antal 1988; Freund and Gulyas 1997; Hangya et al. 2009). Resultant disinhibition of hippocampal granular and pyramidal cells promotes and facilitates synchronicity in theta frequency (Freund and Antal 1988; Freund and Gulyas 1997; Hangya et al. 2009). In addition, the majority of septal glutamatergic neurons are also fast firing and have been reported to drive hippocampal pyramidal cells (Huh et al. 2010). Furthermore, septal glutamatergic neurons were recently reported to excite interneurons at the CA1 stratum oriens/alveus border in mouse hippocampus, which regulate feedforward inhibition of Schaffer collateral and perforant path input to CA1 pyramidal neurons in a locomotion-dependent manner (Fuhrmann et al. 2015; Robinson et al. 2016).

Various strategies have been used to study the role of the MS/DB in memory processes. Most studies have centred on activation or deactivation of specific cell types within this region. For instance, time-dependent increases in acetylcholine levels have been observed in the hippocampus in association with spatial memory tasks such as the T-maze spontaneous alternation task (Hepler et al. 1985; Ragozzino et al. 1996; Fadda et al. 1996), while lesion studies of the MS/DB have been reported to disrupt spatial working memory, but not non-spatial working memory (Kelsey and Vargas 1993).

MS lesions did not impair working memory in reference memory visual discrimination tasks or a simultaneous conditional discrimination task (Thomas and Gash 1986). In addition, non-electrolytic lesions with specific excitotoxins which target cholinergic neurons impair a variety of spatial working memory tasks (Johnson et al. 2002; Gibbs and Johnson 2007; Fitz et al. 2008). The MS/DB receives strong projections from mesencephalic areas, including the posterior hypothalamus and supramammillary nucleus (Pan and McNaughton 1997; Kirk 1998) and from the brainstem, particularly from the nucleus incertus (NI) (Goto et al. 2001; Olucha-Bordonau et al. 2003; Ryan et al. 2011; Olucha-Bordonau et al. 2012). Pre theta rhythm and locomotion. For example, in urethane anesthetized rats, electrical stimulation of the NI induces an increase in hippocampal theta rhythm and electrolytic lesion of the NI abolishes the hippocampal theta induced by stimulation of the reticularis pontis oralis (RPO) region (Nuñez et al. 2006). In addition, it has been proposed that the NI may relay a general stress response to the telencephalon centres involved in memory processes (Rajkumar et al. 2016) and feeding behaviour (Calvez et al. 2016).

The majority of NI neurons in the rat synthesize and release GABA (Ford et al. 1995; Olucha-Bordonau et al. 2003; Ma et al. 2007) and a significant population of these neurons express the neuropeptide, relaxin-3, a member of the insulin/relaxin superfamily (Bathgate et al. 2002; Burazin et al. 2002; Ma et al. 2007). The largest population of relaxin-3 neurons is located in the NI, but others are also present in the ventral periaqueductal grey, the pontine raphe nucleus and an area dorsal to the lateral substantia nigra (Tanaka et al. 2005; Ma et al. 2007).

Relaxin-3 is the cognate ligand of the $G_{i/o}$-protein-coupled receptor, RXFP3 (Liu et al. 2003), and RXFP3 mRNA and binding sites are strongly expressed in the brain in a topographical distribution that fits with that of relaxin-3 containing axons and nerve terminals in rat (Sutton et al. 2004; Ma et al. 2007) and mouse (Smith et al. 2010) brain. Notably, infusion of a specific RXFP3 agonist, R3/I5, into the medial septum promotes theta rhythm (Ma et al. 2009a). In vitro studies in various cell lines (Chinese hamster ovary (CHO) cells and human embryonic kidney (HEK) 293 cells) stably expressing human RXFP3 and SN56 cholinergic neuroblastoma cells, which endogenously express RXFP3, demonstrate that RXFP3 stimulation can consistently decrease forskolin-stimulated cAMP levels and activate the MAPK/ERK pathway, as reflected by changes in ERK1/2 phosphorylation and activation of immediate early gene/transcription factor expression (e.g. activator protein 1, AP-1, nuclear factor-ĸB, NF-ĸB and serum response element, SRE). However, while central relaxin-3 injections have been associated with increases in immediate early gene expression (McGowan et al. 2007; Otsubo et al. 2010), and there are preliminary reports of RXFP3 activation producing hyperpolarization of putative RXFP3-positive neurons in rat brain slices in vitro (Kania et al. 2014), which is more consistent with inhibition of cellular cAMP levels by Gi/o coupled receptors, there are no reports on the effect of central RXFP3 activation in vivo on relevant cell signaling pathways.

Therefore, in this study, we investigated the effect intracerebroventricular (icv) administration of the selective RXFP3 agonist, RXFP3-A2 (Shabanpoor et al. 2012) on MAPK/ERK pathway-related signaling in the MS/DB. Cerebellum, which lacks RXFP3 expression (Sutton et al. 2004), was used as a negative control tissue. Using immunoblotting, we quantified phosphorylated ERK (pERK) and total ERK levels, as described in earlier in vitro studies (Van der Westhuizen et al. 2007), to assess the impact of central RXFP3 activation on overall septal MAPK/ERK activation. Subsequently, we used immunofluorescence staining to characterize the neurochemical phenotype of pERK-positive neurons by co-localizing pERK immunoreactivity (IR) with choline acetyltransferase (ChAT) as a marker for cholinergic neurons and the calcium-binding proteins (CaBPs), parvalbumin, calretinin and calbindin for different populations of septal GABAergic neurons (Olucha-

Bordonau et al. 2012). In addition, we have assessed the neuronal targets of relaxin-3 by double immunofluorescence staining of putative RXFP3 protein and medial septal markers. Finally, we studied the behavioural effects of icv administration of RXFP3-A2 in a delayed spontaneous alternation T-maze test (a working spatial memory task). Our data demonstrate that central RXFP3 agonist infusion increased ERK phosphorylation in cholinergic neurons of the MS/DB and impaired performance in the spontaneous alternation task consistent with effects seen after cholinergic neuron lesioning (Fitz et al. 2008) and consistent with the detection of RXFP3-like IR in cholinergic neurons in the MS/DB. These results provide novel neurochemical and anatomical evidence for the importance of the NI and relaxin-3 related regulation of MS/DB and hippocampal function, with implications for better understanding the ascending control by these neural networks of attention/arousal, navigation/exploration and associated cognitive processes.

## 2.2. Material and Methods

### 2.2.1. Animals and storage conditions

Procedures were in line with directive 86/609/EEC of the European Community on the protection of animals used for experimental and other scientific purposes and approved by the Ethics Committee of the University Jaume I. Adult male Sprague–Dawley rats between 300 and 350 g were used. All rats were maintained on a 12 h light cycle and provided with food and water ad libitum. For surgical procedures rats were first deeply anesthetized with ketamine (Imalgene 55 mg/kg i.p.; Merial Laboratories SA, Barcelona, Spain) and medetomidine (Xilagesic 20 mg/kg i.p.; Lab Calier, Barcelona, Spain). Cannula and holding-screw holes were made in the skull using a surgical drill. Stereotaxic coordinates used to insert a cannula into the right lateral cerebral ventricle were AP 0.48 mm, ML 0.1 mm, DV 4 mm from bregma (Paxinos and Watson 2014).

### 2.2.2. Experimental groups

One week after surgery, rats were injected with a total volume of 1 µL of RXFP3-A2 peptide (5 µg/µL) or vehicle (aCSF) at a rate of 0.5 µL/min through

the implanted cannula by means of a Harvard syringe injector (Harvard PHD 2000 Syringe Pump; Harvard Apparatus, Holliston, MA, USA). The 'RXFP3-A2' agonist ([R3A(11–24, C15 → A)B]) was kindly supplied by Dr Mohammad Akhter Hossain (The Florey Institute of Neuroscience and Mental Health, Parkville, Australia). This agonist has high affinity for the cognate relaxin-3 receptor, RXFP3, with higher selectivity for RXFP3 c.f. the relaxin receptor, RXFP1; and has been shown to alter anxiety-like and other behaviours following central administration (Shabanpoor et al. 2012; Ryan et al. 2013a). In the current studies, multiple experimental groups of rats were used with one cohort (n = 6–9/treatment group) used for measurement of pERK and ERK levels in different brain areas by Western blotting; and a second cohort (n = 6–7/group) used to assess cellular levels of pERK immunoreactivity in different types of neurons in the MS/DB. 'RXFP3-A2' rats were injected with 5lg/lL (*1 nmol) of the peptide analogue; 'sham' rats were injected with artificial cerebral spinal fluid (aCSF) vehicle; and time-matched 'naïve' rats did not undergo any surgery **(Table 1).**

### 2.2.3. Delayed spontaneous alternation T-Maze test procedure

Rats from vehicle (sham) and RXFP3-A2 groups were handled daily during the week prior to the behavioural test after the surgeries. On the day of behavioural test and sacrifice, both groups were habituated for 30 min to the behavioural room before the infusions (vehicle or RXFP3-A2). Five min after the infusion rats were allowed to explore the T-maze with one of the short arms closed (familiarization phase) for 5 min.

Throughout the whole procedure the closed arm was balanced, alternating the closed arm every two cases (one vehicle, one RXFP3-A2) to avoid side bias. The closed arm is refereed as the novel arm and the open arm which was explored during familiarization is the familiar arm. After familiarization, rats were returned to their home cages for 95 min before being returned to the T-maze for 3 min with all arms open and the alternation between familiar and novel arms was evaluated.

**Table 2.1** Number of rats in each experimental group

| Method | Time (min) | NAÏVE | SHAM | RXFP3-A2 |
|---|---|---|---|---|
| **Western blots** | 20 | 7 | 7 | 8 |
| | 90 | 8 | 7 | 9 |
| **Immunofluorescence** | 90 | - | 7 | 6 |
| **T-maze** | 90 | - | 7 | 6 |

### 2.2.4. Immunoblotting

In Western blotting studies, pERK levels were assessed at 20 and 90 min after peptide injection. Rats were lightly anesthetized (Dolethal, 200 mg/Kg Vetoquinol S.A., Madrid, Spain) and then killed by decapitation. Brains were rapidly removed and frozen in cold isopentane (Sigma-Aldrich, St Louis, MO, USA). Brain areas of interest (septum and cerebellum) were dissected with 1 mm diameter disposable biopsy punches (Interna Miltex, Ratingen, Germany) from 20 µm brain slices cut using a cryostat at -15 ºC to preserve protein phosphorylation. For the immunoblot assays, we pooled tissues from 2-3 rats in each experimental group. Tissue was lysed in RIPA buffer containing protease and phosphatase inhibitors (Halt protease and phosphatase inhibitor, Thermo Scientific, Waltham, MA, USA). Mechanical cell lysis was achieved using a Sonicator (Hielsher Ultrasound Technology, Teltow, Germany). Forty (40) µg of total proteinwas subjected to SDS-PAGE, transferred to Immobilon-P membranes (MERCK Millipore, Darmstadt Germany), which were blocked for non-specific binding and incubated with primary antibodies: anti-phospho MAPK/ERK1/2 (Cell Signaling, Danvers,MA, USA 1:2,000); and anti-ERK (Santa Cruz Biotechnology, Santa Cruz, CA, USA; 1:1,000) overnight at 4 ºC. After several washes with washing buffer containing 0.1 % Triton X-100, membranes were incubated for 1 h at RT with peroxidase-conjugated secondary antibodies (anti-rabbit and anti-mouse, Jackson Immunoresearch, Suffolk, UK).Staining was developed using ECL (BioRad, Hercules CA, USA) and digital images were captured with a charge-coupled device (CCD) imager (IMAGEQUANT LASc 4000, GE Healthcare Little Chalfont, UK). Immunoreactive bands were quantified with ImageJ blots toolkit software

(National Institutes of Health, Baltimore, MD, USA). Data was analysed by one way-ANOVA, followed by Bonferroni post hoc test.

### 2.2.5. Immunofluorescence staining

Treated and naïve rats used for immunofluorescence (IF) assays were euthanized with an intraperitoneal (i.p.) injection of sodium pentobarbital (120 mg/Kg Eutanax, Fatro, Barcelona, Spain) 90 min after either RXFP3-A2 or vehicle icv infusions in the homecage. Rats were transcardially perfused with saline (0.9 % NaCl) followed by fixative (4 % paraformaldehyde in 0.1 M PB, pH 7.4) for 30 min (*600 mL per rat). After perfusion, brains were removed and immersed in the same fixative for 4 h at 4 ºC. After fixation, brains were cryoprotected in 30 % sucrose in 0.01 M phosphate buffered saline (PBS) pH 7.4 for 3 days.

Coronal sections (40 µm) were obtained using a freezing slide microtome (Leica SM2010R, Heidelberg, Germany). For each brain (n = 6-7 per group), 6 series of sections between Bregma +0.8 to +0.4 mm (Paxinos and Watson 2014) were collected in 30 % sucrose in 0.01 M PBS. The neurochemical phenotype of pERK-positive neurons was assessed by dual-labeling with a pERK1/2 antiserum and antisera against neuronal markers in MS/DB sections from rats sacrificed 90 min after agonist or vehicle (sham) infusion. Coronal brain sections were incubated in blocking solution (4% NDS, 2% BSA in 0.05M TBS, 0.3%TritonX-100, pH 8) followed by primary antibody incubation; rabbit antiphospho- MAPK/ERK (Cell Signaling), 1:200; goat anti-ChAT (MERCK Millipore, Darmstadt Germany) 1:700; mouse anti-calbindin (CB) (Swant, Marly, Switzerland) 1:2,000; mouse anti-calretinin (CR) (Swant) 1:2,000 and mouse anti-parvalbumin (PV) (Swant) 1:2,000 in 0.05 M TBS, 0.3% Triton X-100 (2% NDS, 2% BSA, pH 8) overnight at RT. After several rinses, sections were incubated for 2 h at RT with either goat anti-rabbit Cy3 and goat anti-mouse Alexa Fluor 488, or donkey anti-rabbit Cy3 and donkey anti-goat Alexa Fluor 488, secondary antibodies (Jackson

Immunoresearch). Following further rinsing sections were mounted on slides and coverslipped using glycerol.

### 2.2.6. Immunofluorescence imaging and analysis and statistics

Fluorescence images were taken with a confocal scan unit with a module TCS SP8 equipped with argon and helioneon laser beams attached to a Leica DMi8 inverted microscope (Leica Microsystems). Excitation and emission wavelengths for Cy3 were 433 and 560–618 nm respectively; Alexa488-labeled excitation wavelength was 488 nm and its emission at 510–570 nm. Serial 0.2 µm scans were obtained in the Z-plane and a maximal projection of 20 µm was generated with Image J. For quantification of dual-labeling we used a 209 lens.

Image J software combined with loci.tools plugin (BIOFORMATS, University of Wisconsin-Madison), was used to count the number of positively-labelled cells in 15–18 sections from 4 brains from the different experimental groups. Data were expressed as the percentage of double labeled neurons (neuronal marker + pERK), divided by the total number of marker-positive (ChAT, PV, CR or CB) neurons. All analyses were conducted by an observer blinded to the experimental conditions of the samples. Statistical analyses for significant differences in the pERK positive neurons comparing sham and RXFP3-A2 groups, employed the Student's t-test with probability set at $\alpha<0.05$ (GraphPad Prism V5 software, GraphPad, La Jolla, CA, USA).

## 2.3. Results

### 2.3.1. Icv administration of RXFP3-A2 increases ERK phosphorylation in MS/DB

ERK and pERK proteins were reliably detected by immunoblot in tissue extracts of septum and cerebellum from rats sacrificed 20 and 90 min after infusion of RXFP3-A2 or aCSF vehicle (sham) and from naïve untreated rats (**Fig. 2.1**).

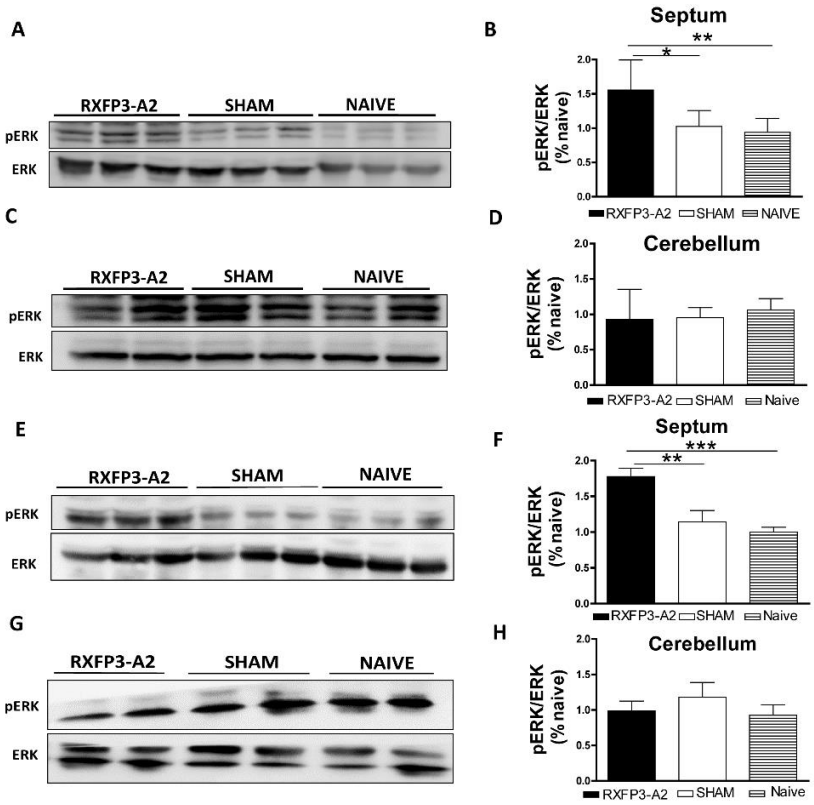


**Figure. 2.1 pERK/ERK detection by Western blot** (**A–D**) 20 and (**E–H**) 90 min after icv infusion of RXFP3-A2 (*1 nmol) (black bars), aCSF vehicle (white bars) and in time-matched naïve rats (stripped bars) (n = 7–9 rats per group). Rats sacrificed 20 min after agonist infusion displayed an increased ERK activation in the septal area compared to sham and naïve groups (**A, B**), but did not display any differences in the cerebellum (**C, D**). Similarly, rats sacrificed 90 min after RXFP3-A2 infusion displayed higher pERK levels than control (sham and naïve) in the septum (**E,F**) but not in cerebellum (**G,H**).*p<0.05; **p<0.01;***p<0.001

ERK activity was quantified by measuring the pERK and ERK band intensity and normalization to the ERK signal in each sample. In order to compare RXFP3-A2, sham and naïve samples within and between experiments, we expressed the data as a percentage of the naive group pERK/ERK ratio and all samples followed a normal distribution according to the Shapiro–Wilk test. Data from septal samples collected 20 min after agonist or vehicle infusion were analysed by one-way ANOVA followed by Bonferroni post-test ($F_{20,21} = 8.128$, $p = 0.0031$; **Fig. 2.1A and B**) and pERK/ERK levels

in the RXFP3-A2 group were significantly higher (1.5 ± 0.16, n = 8) than in the sham (1.0 ± 0.08, n = 7) and naïve (0.93 ± 0.07, n = 7) groups. In contrast, cerebellar levels of pERK/ERK from matched samples were not different from each other [one-way ANOVA followed by Bonferroni post-test ($F_{21,22}$ = 0.4348, p = 0.65; **Fig. 2.1C and D**)] RXFP3-A2 (0.93 ± 0.14), sham (0.95 ± 0.05) and naïve (1.0 ± 0.06; n = 7/group). Similarly, 90 min after agonist or vehicle infusion, normalized septal pERK levels in RXFP3-A2 treated rats (1.78 ± 0.16) were significantly higher than normalized pERK levels in sham (1.10 ± 0.15) and naïve (1.00 ± 0.06) rats [n = 7–9/group; one-way ANOVA followed by Bonferroni post-test ($F_{26,27}$ = 11.66, p = 0.0003; **Fig. 2.1E and F**)]. The pERK/ERK ratio in cerebellar samples from the same groups were similar [one-way ANOVA followed by Bonferroni post-test ($F_{26,27}$ = 0.6339, p = 0.5337; **Fig. 2.1G and H**)] RXFP3-A2 (0.99 ± 0.13), sham (1.18 ± 0.20) and naïve (0.92 ± 0.14) (n = 7 rats/group).

### 2.3.2. Icv administration of RXFP3-A2 increases pERK in cholinergic but not GABAergic neurons in MS/DB

pERK immunostaining was reliably detected within cells in different areas of the MS/DB. Relative levels of staining were assessed in coronal sections between 0.8 and 0.4 mm relative to Bregma (Paxinos and Watson 2014) in an area comprising MS and the vertical DB division (MS/vDB) and an adjacent area comprising the horizontal diagonal band (HDB) of the MS/DB complex. pERK labelling in these areas followed a normal distribution (Shapiro–Wilk test) and the density of pERK positive cells was increased in the HDB after RXFP3-A2 treatment (235 ± 28.8, n = 5) compared to sham vehicle treatment (111.9 ± 11.09, n = 5; **Fig. 2.2**; Student's t-test; p = 0.004).

The density of pERK-positive neurons in the MS/vDB was also increased by RXFP3-A2 (137.6 ± 5.78) compared to sham (76.3 ± 5.08, n = 4/group; Student's t-test, p = 0.001). In studies to characterize the neurochemical content of pERK-positive neurons in the MS/DB complex, we analysed dual immunofluorescence (IF) labelling in the MS/vDB (**Fig. 2.3**) and HBD (**Fig. 2.4**). The total numbers of pERK cells, marker-positive (ChAT, CR, PV and CB) cells and double-labelled cells were counted. The ratio of pERK + marker neurons divided by total number of marker-positive neurons was

compared between RXFP3-A2 treated and sham rat groups. In the MS/vDB, normalized pERK/ChAT double-staining increased significantly in RXFP3-A2 treated compared to sham (**Fig. 2.3C–H**) rats (69.1 ± 5.59 and 20.9 ± 5.69, n = 6–7/group; Student's t-test, p\0.0001; **Fig. 2.3B**).

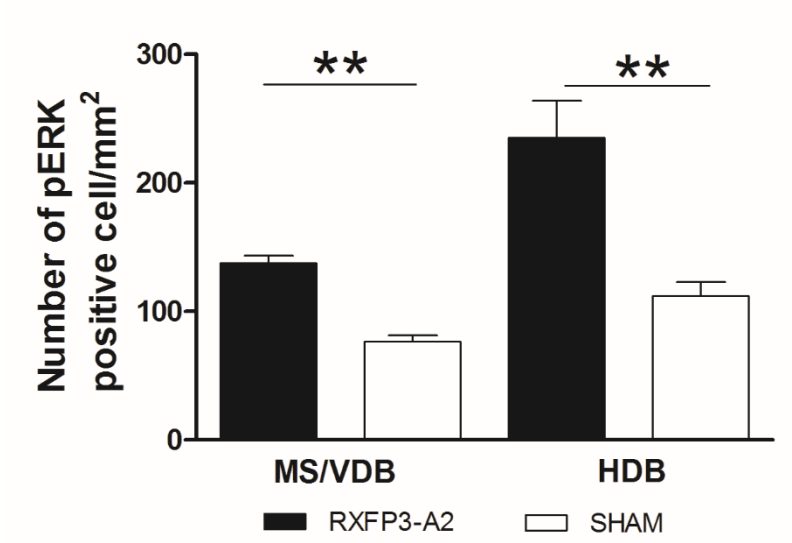


**Figure. 2.2 Density of pERK-positive neurons in septal MS/vDB and HDB regions** of brains from rats killed 90 min after RXFP3-A2 (black bars) or aCSF vehicle (sham, white bars) infusion. MS/vDB and HDB contain ≥2-fold higher pERK levels in RXFP3-A2 than sham rats. **p<0.01

Under the same conditions very few pERK neurons were double-labeled with GABAergic cellular marker proteins (CB, PV and CR) in sham rats and no increase in double-staining occurred after RXFP3-A2 infusion (**Fig. 2.3B**). Similarly, pERK was present in ChATpositive neurons of the HBD in sham rats (25.1 ± 5.93, n = 6–7/group; **Fig. 2.4C–E**), and the level of double-staining was increased significantly after RXFP3-A2 infusion (59.65 ± 4.37, n = 6–7; **Fig. 2.4F–H**; Student's t-test, p = 0.0008; **Fig. 2.4B**).

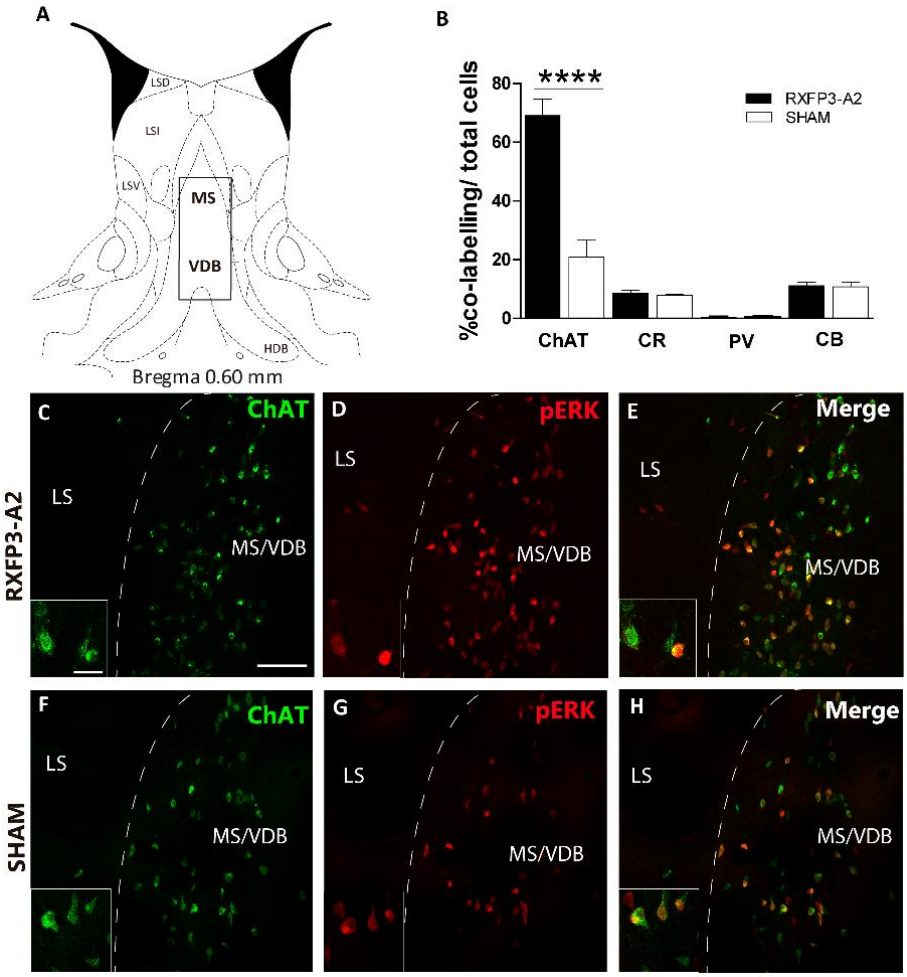


**Figure. 2.3 pERK/ChAT immunofluorescence in the MS/vDB**. **(A)** Schematic of MS/vDB region in which labeled cells were counted (adapted from Paxinos and Watson 2014), (**B)** levels of % dual-labeling in the MS/vDB of pERK and ChAT and different calciumbinding proteins, documenting a >3-fold increase in the % colocalization of pERK/ChAT in rats sacrificed 90 min after RXFP3-A2 (black bars) compared with aCSF (white bars) infusion. (**C–H)** Low- and high-power (insets) illustrations of ChAT and pERK staining and merged images from RXFP3-A2 treated (**C–E**) and aCSF treated (**F–H**) rats. Scale bar 100 µm, inset scale bar 25 µm. ****p<0.0001; ***p<0.001

In contrast, little or no co-labeling of pERK and PV, CB or CR was observed, similar to observations in the MS/vBD (**Table 2.2**), as illustrated by doublelabeling of pERK with CR (**Fig. 2.5A–C**), PV (**Fig. 2.5D–F**) and CB (**Fig.**

**2.5G–I**) in MS/VDB; and pERK with PV in HBD (**Fig. 2.5J–I**). The distribution of the different molecular markers within the MS/vDB was consistent with its 'onion-like' structure (Wei et al. 2012). CaBP-positive neurons were arranged in three bands, from the midline outward-PV, CR and CB. Increased pERK staining induced by icv administration of RXFP3-A2 was present lateral to PV neurons (**Fig. 2.5A–C**). Neurons containing increased pERK levels were detected in the same regions as CB (**Fig. 2.5D–E**) and CR (**Fig. 2.5G–H**) neurons, but there was no co-localization of pERK with CB (**Fig. 2.5C**) or CR (**Fig. 2.5I**).

The density of CR- and CB-positive-neurons in this area was low and dispersed and no colocalization with pERK was observed (data not shown).

**Table 2.2** Relative level of colocalization of pERK with different CaBP markers for GABAergic neurons in MS/DB

| Brain area | Dual-labeling | CabP cells/section | Sham | RXFP3-A2 | P value |
|---|---|---|---|---|---|
| MS/vDB | pERK + CR | 22 ± 3 | 7.91 ± 0.42 | 9.36 ± 1.19 | 0.37 |
| | pERK + CB | 27± 2 | 10.8 ± 1.63 | 11.19 ±1.04 | 0.85 |
| | pERK + PV | 28±2 | 0.40 ± 0.05 | 0.37 ± 0.03 | 0.95 |
| HDB | pERK + CR | 10± 2 | 0.33 ± 0.33 | 0.43 ± 0.28 | 0.83 |
| | pERK + CB | 4 ± 1 | 1± 0.58 | 1.33 ± 0.88 | 0.78 |
| | pERK + PV | 40 ± 4 | 2.23 ±1.47 | 0.88 ± 0.88 | 0.47 |

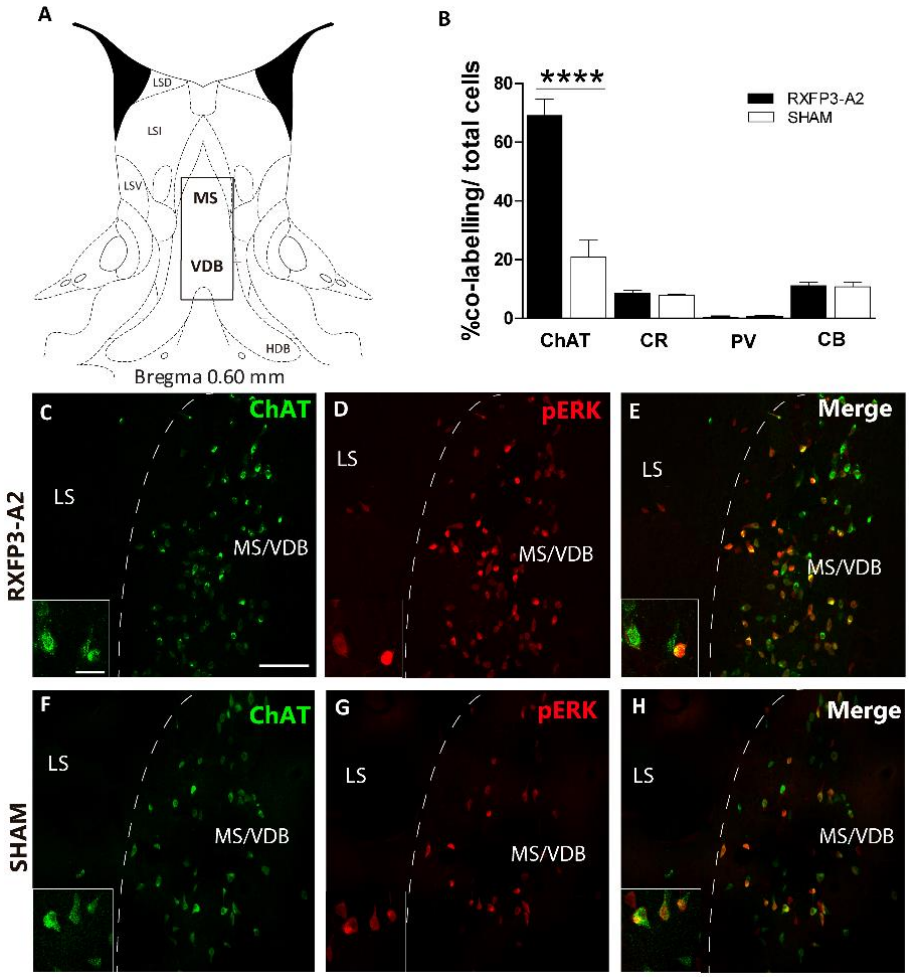


**Figure. 2.4** pERK/ChAT immunofluorescence in the septal HDB. (**A**) Schematic of HDB region in which labeled cells were counted (adapted from Paxinos and Watson 2014), (**B**) levels of % duallabeling in the HDB of pERK and ChAT and different calcium-binding proteins, documenting a[threefold increase in the % co-localization of pERK/ChAT in rats sacrificed 90 min after RXFP3-A2 (black bars) compared with aCSF (sham, white bars) infusion. (**C–H)** Low- and highpower (insets) illustrations of ChAT and pERK staining and merged images from RXFP3-A2 treated (**C–E**) and aCSF treated (**F–H**) rats. Scale bar 100 lm, inset scale bar 25 lm. *p<0.05

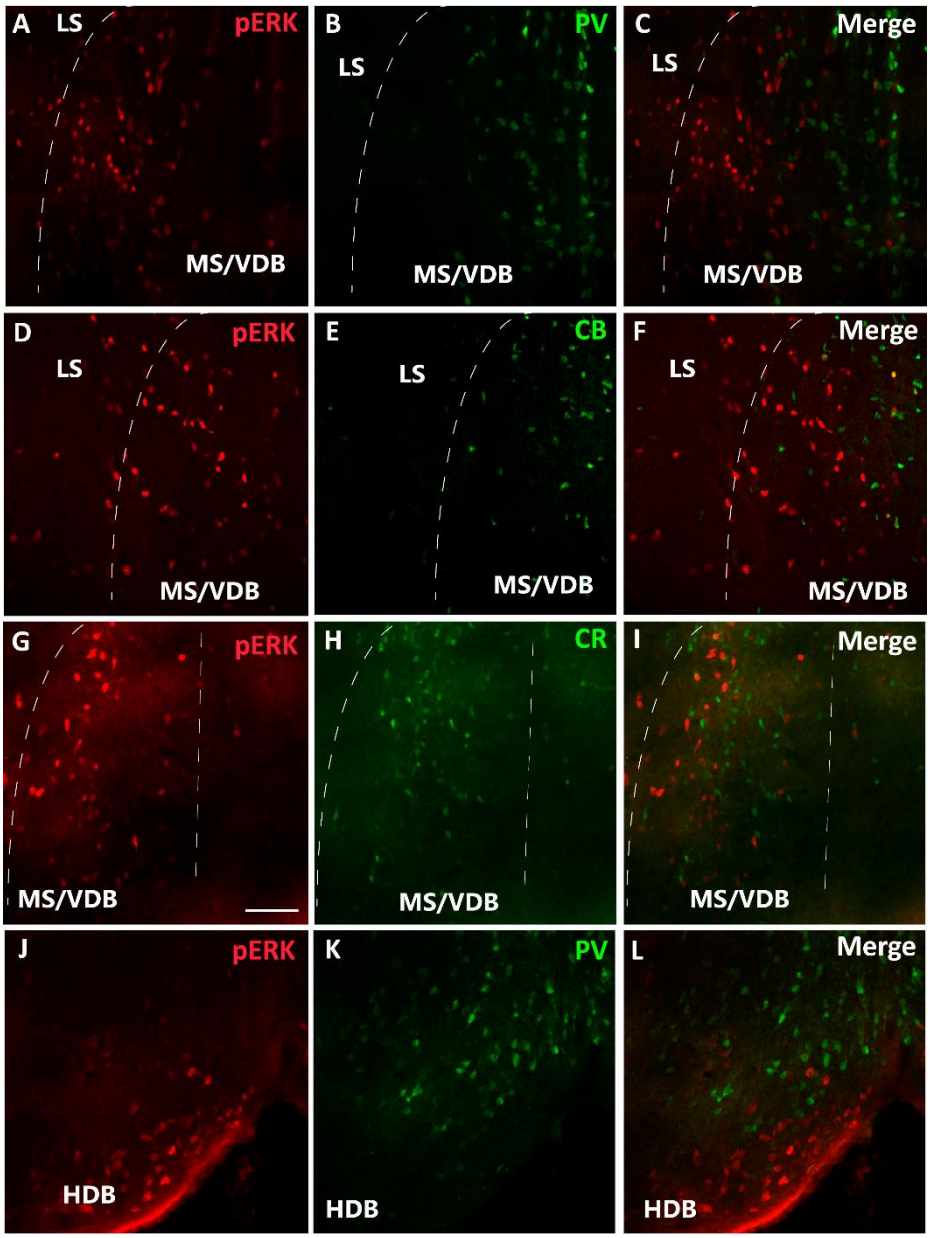


**Figure. 2.5 pERK and calciumbinding protein immunofluorescence in the MS/vDB and HDB**. (**A–C**) pERK and parvalbumin, (**D–F**) pERK and calbindin and (**G–I**) pERK and calretinin staining in the MS/vDB in RXFP3-A2 treated rats processed after 90 min. (**J–L**) pERK and parvalbumin staining within the HDB in RXFP3-A2 90 min rats. Scalebar 100 µm.

### 2.3.3. Icv administration of RXFP3-A2 impaired spatial working memory in a delayed spontaneous alternation T-maze test

RXFP3-A2 infused rats displayed disrupted performance compared to sham rats in the spontaneous alternation T-maze. The percentage of permanence time (%PT) in novel (52.2 ± 2.18) and familiar arm (47.8 ± 2.18) was similar in RXFP3-A2 subjects. In contrast, sham rats spent significantly more time in the novel arm (41.1 ± 3.28) than in the familiar arm (58.9 ± 3.28) (n = 6–7/group; Kruskal–Wallis test, p = 0.007) (**Fig. 3.6A**). Accordingly, when comparing the percentage of the number of entries to each arm, RXFP3-A2 rats did not display a significant difference between familiar (48.0 ± 2.06) and novel arm (52.0 ± 2.06); whereas the sham rats had significantly higher alternation, entering in the novel arm (58.9 ± 3.40) more often than in the familiar one (41.1 ± 3.40) (n = 6–7/group; Kruskal–Wallis test, p = 0.014) (**Fig. 3.6B**). In addition, the analysis of the total number of entries to any of the 3 arms in the T-maze (start + novel + familiar), indicated that the RXFP3-A2 rats were more active (27.2 ± 1.96), compared to sham rats (18.4 ± 1.46); data analysed by Student's t-test, p = 0.0031) (**Fig. 3.6C**).

## 2.4. Discussion

The current study has demonstrated that acute central activation of RXFP3 by icv infusion of the agonist peptide, RXFP3-A2 (Shabanpoor et al. 2012) results in specific changes in the levels of phosphorylated ERK (pERK) in the septal area, assessed in vivo using Western blotting of pERK and ERK and immunohistochemical detection of pERK. RXFP3 is a metabotropic receptor to routinely couple to Gi/o-proteins in mammalian cells based on extensive characterization in in vitro cell-based systems (Liu et al. 2003; Van der Westhuizen et al. 2005; Van der Westhuizen et al. 2007). It is thought to exert its actions on target cells via inhibition of adenylate cyclase and cellular cAMP levels and activation of phosphorylation of ERK (Liu et al. 2003; Van der Westhuizen et al. 2005; Van der Westhuizen et al. 2007).

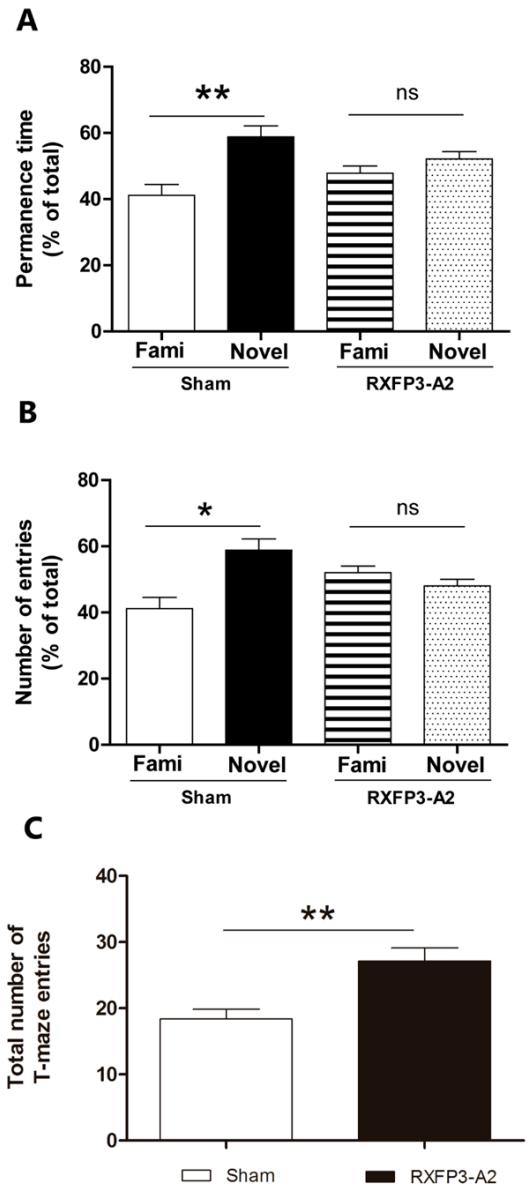


**Figure. 2.6** Effect of icv RXFP3-A2 administration on spontaneous alternation in a T-maze paradigm. Sham rats had a percentage permanence time significantly higher in the novel arm (white column) than in the familiar arm (black column), whereas RXFP3-A2 rats did not display a different percentage of permanence time in familiar arm (horizontal stripes) versus novel arm (dotted columns) (**A**). Sham rats showed an increased percentage number of entries in the novel arm compared to the familiar, while RXFP3-A2 rats explored both arms¡ equally **(B**). Total number of entries in all T-maze arms was higher in RXFP3-A2 than sham rats (**C**). *p <0.05; **p<0.01

In our in vivo studies and in line with these findings, we have observed a rapid and sustained RXFP3-related increase in pERK levels in septal tissue, with no effect in RXFP3-negative, cerebellar samples. This is consistent with the reported anatomical distribution of RXFP3 in rat brain in adult rats (Sutton et al. 2004; Ma et al. 2007; Smith et al. 2010). Human relaxin-3 (H3) activation of human RXFP3 heterologously expressed in CHO cell lines (Van der Westhuizen et al. 2005; Van der Westhuizen et al. 2007), induces ERK phosphorylation and a downstream up-regulation of AP1, NF-kB

and SRE (Van der Westhuizen et al. 2007; Kocan et al. 2014), which are involved in gene expression changes related to long-term synaptic plasticity (Impey et al. 1999; Cammarota et al. 2000; Davis et al. 2000; Sweatt 2001; Mattson and Camandola 2001; Ramanan et al. 2005; Ahn et al. 2008). Thus, similar such changes may contribute to some or all of the behavioural effects produced by acute central relaxin-3 or selective RXFP3 agonist administration in rats, such as altered anxiety-like behaviour (Ryan et al. 2013a), increased feeding (McGowan et al. 2005; McGowan et al. 2007; Shabanpoor et al. 2012), and altered memory (Ma et al. 2009a).

In the current study, we conducted cell signaling studies in rats maintained in their home cage throughout the experiment. Further investigations of the nature of the septal activation following RXFP3-A2 administration are warranted, and whether the time-related increase in pERK levels is related to the duration of the peptide action and/or behavioural changes produced by the peptide. The septal area plays a central role in controlling hippocampal function, and while the importance of the medial septum for ‘pacemaking’ of hippocampal theta rhythm was reported in very early studies (Stumpf et al. 1962), there is still a great deal to learn about the role of different septal neuron populations and their interactions (Wu et al. 2000; Sotty et al. 2003) (see ‘‘Introduction’’). Indeed, while there is both old and new evidence for the importance of septal glutamate, GABA and ACh neurons in regulating hippocampal activity and locomotion, navigation and exploration (Fuhrmann et al. 2015; Robinson et al. 2016), septal theta does not always precede hippocampal theta, suggesting that regulation of hippocampal theta activity is better viewed as occurring via a set of functionally interrelated components than via a single entity (Nerad and McNaughton 2006).

A better understanding of how septal systems integrate the complex brainstem and telencephalic inputs/functions can be obtained by documenting the cytoarchitectonics and related circuits of the septum. Different types of neurons are distributed in an organized onion-like pattern within the septum from the medial to the most lateral regions, with neurotransmitters (acetylcholine, GABA, glutamate, nitric oxide) and a number of protein markers of different neuronal populations (parvalbumin (PV), calretinin (CR) and

calbindin (CB) expressed across the area (Gritti et al. 2003; Sotty et al. 2003; Ujfalussy and Kiss 2006). These various types of neurons are involved in an intricate pattern of connections with telencephalic (Freund and Antal 1988) and brainstem areas (Leranth and Kiss 1996; Borhegyi and Freund 1998; Leranth et al. 1999; Olucha-Bordonau et al. 2012; Sánchez-Pérez et al. 2015) and also innervate each other and participate in the formation of the synchronous rhythmic output to the hippocampus (Mysin et al. 2015; Robinson et al. 2016). In the current study, we observed that the activity of a population of cholinergic neurons within the MS/DB is altered by central administration of a selective RXFP3 agonist. A comparison of pERK staining in the septum of RXFP3-A2 treated vs sham rats revealed a significantly higher number of pERK-positive neurons in the MS/vDB and HDB, where a topographic distribution of RXFP3 (GPCR135) mRNA and RXFP3 agonist (R3/I5) binding sites are present, particularly in the lateral part of MS/VDB (Sutton et al. 2004; Ma et al. 2007) and where relaxin-3-positive fibres make synapses with cholinergic, CB, CR and PV neurons (Ma et al. 2009b; Sanchez-Perez et al. 2012; Sánchez-Pérez et al. 2015). These data suggest that relaxin-3/RXFP3 signalling alters the activity of septal cholinergic neurons and provide a putative mechanism by which NI relaxin-3 projections regulate the septo-hippocampal system (Olucha-Bordonau et al. 2012). Moreover, putative pERK immuno-labelling displayed a similar pattern that of RXFP3 mRNA observed by in situ hybridization (Ma et al. 2007).

Recent studies in transgenic mice, identified cholinergic neurons in medial septum as key elements in the septo-hippocampal connections modulating the shifting behavioural states in the brain (Lee and Dan 2012; Tsanov 2015). Cholinergic neuron activation can trigger the septohippocampal system during inactive behavioural states, whereas non-cholinergic septal cell activation regulates hippocampal function during explorative behaviour (active states). Cholinergic neuron activity is, thus, necessary for the transition from inactive to active hippocampal-related behaviour, but is inefficient in inducing significant change in the activity of the hippocampal neurons during arousal states (Mamad et al. 2015). Moreover, optogenetic activation of septal cholinergic neurons increases hippocampal activity within the theta band (2–6 Hz) in anesthetized mice (Vandecasteele et al. 2014), and exploratory tasks

have been reported to increase ACh in hippocampus (Roland et al. 2014), which are related to changes in septal cell activity. Supporting a role for relaxin-3/RXFP3 signalling in the modulation of septo-hippocampal activity, direct infusion of an RXFP3 agonist peptide (R3/I5), (Liu et al. 2005) into the MS/DB enhanced hippocampal theta activity in urethane anesthetized rats and theta frequency in awake rats; while intra-septal RXFP3 antagonist injections impaired spatial working memory (Ma et al. 2009a). As mentioned, optogenetic activation of septal cholinergic neurons enhances hippocampal theta oscillations (Vandecasteele et al. 2014), supporting the need for activation of medial septal cholinergic neurons to increase theta. However, RXFP3 is thought to couple to inhibitory Gi/o-proteins and inhibition of cAMP (Liu et al. 2005; Van der Westhuizen et al. 2007), which would imply a likely acute inhibition of septal cholinergic neurons. Indeed, there is independent evidence of the acute and reversible hyperpolarisation by RXFP3-A2 of RXFP3-positive hypothalamic neurons in vitro (Kania et al. 2014). In the present study, we demonstrate pERK is expressed on cholinergic neurons. Whether this effect may be through RXFP3 direct or indirect action or may occur over a different time course still need to be clarified.

Alternation in a T-maze have long been considered a paradigm for testing septohippocampal function (Brito and Thomas 1981). Moreover, septal cholinergic neurons have been reported to contribute to working spatial memory (Kitabatake et al. 2003; Fitz et al. 2008). Therefore, we determined if icv RXFP3 A2 infusion could alter performance of the alternation task in a T-maze. We observed that RXFP3-A2 produced an impairment of the spontaneous alternation task, which suggests that RXFP3 activation may produce an inhibitory effect on the septal cholinergic projections to hippocampus. On the other hand, we observed that icv RXFP3-A2 injection produced a general increase in locomotor activity in the acute spatial memory task, whereas similar effects are not observed in anxiety tests (Ryan et al. 2013a). This effect may be associated with changes in the cholinergic and/or GABAergic septohippocampal pathways (Fuhrmann et al. 2015; Robinson et al. 2016); but further studies addressing the effect of RXFP3 signalling on specific cell types are required to elucidate the contribution of relaxin-3/RXFP3 in different rat brain circuits. Notably, these acute locomotor effects are in broad

agreement with the reported chronic hypoactivity observed in relaxin-3 and RXFP3 knockout mice (Smith et al. 2012; Hosken et al. 2015), but again the different tests and time courses involved in these effects, as well as species differences, suggest further studies are required to confirm their consistency.

In conclusion, this study provides biochemical, anatomical and behavioural evidence that relaxin-3/RXFP3 signalling regulates MS/DB activity. The MAPK/ERK pathway in cholinergic neurons is activated for a sustained period in vivo by ICV RXFP3 agonist administration, and the assays used provide a paradigm to further assess RXFP3 signalling pathways underlying the outcomes of related physiological and behavioural studies. These findings have implications for the acute and chronic regulation by relaxin-3/RXFP3 signalling of arousal and attention, exploration and navigation, and associated cognitive processes.

# 3

## GABAergic neurons in the rat medial septal complex express relaxin-3 receptor (RXFP3) mRNA

## 3.1. Introduction

Intrinsic neural circuits within, and projections from, the medial septum (MS) subserve various roles of this important brain area in different functions ranging from arousal, attention and spatial working memory (Givens and Olton 1990; Sweeney et al. 1992; Osborne 1994). Much research on the MS has centred on characterizing its projections to the hippocampus (see (Zaborszky et al. 2012; Zaborszky et al. 2014) for review), in addition to descending projections from the MS to the hypothalamus, raphe nuclei and the nucleus incertus (NI) (Borhegyi and Freund 1998; Leranth et al. 1999; Sánchez-Pérez et al. 2015). Modulation of septal function has been traditionally viewed to derive strongly from ascending projections from the posterior hypothalamus and brainstem, including the raphe nuclei, which have been described as modulators of hippocampal theta rhythm via activation of the septohippocampal projection system (Vertes and Kocsis 1997; Vertes 2005). In addition, descending projections from the somatostatin-positive GABA projection neurons of the hippocampus provide a descending feedback regulation of the MS (Toth et al. 1993; Gulyas et al. 2003; Yuan et al. 2017).

However, the less well-studied projection from the NI in the pontine tegmentum also strongly modulates the MS (Goto et al. 2001; Olucha-Bordonau et al. 2003; Olucha-Bordonau et al. 2012). Specifically, NI projections to the MS are associated with modulation of hippocampal theta rhythm. Electrical stimulation of the NI increased theta rhythm band power of the CA1 hippocampal field potential and NI lesions attenuated the increased hippocampal theta rhythm power induced by stimulation of the nucleus reticularis pontis oralis (RPO) in urethane-anesthetized rats (Nuñez et al. 2006).

A major population of GABA neurons in the NI co-express the neuropeptide, relaxin-3 (Ma et al. 2007) and NI projections and relaxin-3-positive fibres are in close contact with cholinergic and GABAergic neurons in the MS (Olucha-Bordonau et al. 2012). Moreover, infusion of a relaxin-3 analogue into the MS increased hippocampal theta rhythm, whereas infusion of a relaxin-3 receptor antagonist impaired the theta rhythm produced by novel

environment exploration or RPO stimulation (Ma et al. 2009a). Different approaches in recent years have confirmed and extended these observations regarding the role of the NI and its associated peptide relaxin-3 in subcortical modulation of hippocampal theta rhythm, with an observed synchrony between the firing of NI neurons and different phases of hippocampal theta rhythm (Ma et al. 2013; Martínez-Bellver et al. 2015; Martínez-Bellver et al. 2017).

The cognate receptor for relaxin-3 is the Gi/o-protein-coupled receptor, RXFP3. In in vitro studies in Chinese hamster ovary cells transfected with RXFP3, bath application of relaxin-3 results in inhibition of cAMP synthesis and increased ERK phosphorylation (Liu et al. 2003; Van der Westhuizen et al. 2005; Van der Westhuizen et al. 2007; Bathgate et al. 2013). In agreement with a potential inhibitory effect of neuronal RXFP3 activation, relaxin-3 and a selective RXFP3 agonist, RXFP3-A2 (Shabanpoor et al. 2012), hyperpolarized RXFP3-expressing magnocellular neurons in the rat paraventricular and supraoptic hypothalamic nuclei (Kania et al. 2017). Furthermore, following intracerebroventricular (icv) infusion of RXFP3-A2, we observed increased phospho-ERK levels in the MS and disruption of spatial working memory in a spatial alternation test (Albert-Gascó et al. 2017), although the precise relationship between these effects is not known.

The MS is composed of a heterogeneous population of neurons and each neuronal type participates in a different way in septo-hippocampal interactions (Sotty et al. 2003). For example, slow firing cholinergic neurons facilitate hippocampal activity (Sotty et al. 2003), while parvalbumin GABAergic projection neurons inhibit hippocampal interneurons (Toth et al. 1997). Somatostatin positive neurons are concentrated in the horizontal diagonal band (Köhler and Eriksson 1984), but to our knowledge, no functional role has been assigned to these neurons. Different types of calcium-binding protein-expressing neurons and neurons expressing choline acetyltransferase (ChAT) are targeted by nucleus incertus axons/terminals in the rat (Olucha-Bordonau et al. 2012), but it is not clear which of these neurons express RXFP3. Thus, we explored the distribution of Rxfp3 mRNA expression in different neuronal types of the rat septal area using multiplex in situ hybridization and specific

probes for Rxfp3, ChAT, vesicular GABA transporter (vGAT; slc32a1), parvalbumin (PV) and somatostatin (SOM) transcripts.

## 3.2. Material and methods

### 3.2.1. Animals

Experiments were conducted with approval from The Florey Institute of Neuroscience and Mental Health Animal Ethics Committee, in compliance with guidelines of the National Health and Medical Research Council of Australia. Adult male Sprague-Dawley rats weighing 300-320 g were maintained on a 12-12 h light-dark cycle with lights on at 0700 h. Rats were provided free access to food and water.

### 3.2.2. Multiplex in situ hybridization (ISH)

The distribution of septal Rxfp3 mRNA-positive neurons and their GABAergic or cholinergic phenotype was assessed using RNAscope multiplex in situ hybridization. RNAscope® is a commercial method provided by Advanced Cell Diagnostics (ACD, Newark, CA, USA), which involves the incubation of post-fixed, fresh-frozen brain sections with up to three custom probes. Standard probes contain 20 ZZ pairs (25 base pairs/Z) which cover a total of ~1000 base pairs of the target mRNA. In silico verification of the probes is performed and validated to select oligonucleotides with compatible melting temperature for optimal hybridization under RNAscope assay conditions and minimal cross-hybridization to off-target sequences. There is a verification procedure conducted following each major step during the probe design to guarantee accuracy, according to previously described rules (Wang et al. 2012).

Two naïve rats were deeply anesthetized with pentobarbitone (100 mg/kg, i.p.), decapitated, and brains were quickly extracted and rapidly frozen on dry ice. The fresh-frozen brains were embedded in OCT embedding gel (Tissue-Tek® OCT, Optimum Cutting Temperature, Sakura Finetek USA Inc., Torrance, CA, USA) and stored at -80ºC. Before cryo-sectioning, brains were warmed to -20ºC for 2 h and then mounted on a cryostat (Cryocut CM 1800, Leica Microsystems, North Ryde, NSW, Australia) using OCT embedding gel.

Coronal sections (16 µm) were cut and thaw-mounted on Superfrost-Plus Slides (Fisher Scientific, Hampton, NH, USA, Cat#12-550-15).

Sections were fixed in 4% paraformaldehyde (PFA) for 16 min at 4ºC, rinsed in PBS, and dehydrated in increasing ethanol concentrations (50%, 70% and 100%). Once dehydrated the sections were stored in 100% ethanol overnight at -20ºC. The next day, slides were air-dried and a hydrophobic barrier was drawn around the sections (ImmEdge hydrophobic PAP pen, Vector Laboratories, Burlingame, CA, USA; Cat #310018). Sections were incubated with protease pretreatment-4 (ACD, Cat #322340) for 16 min. After a PBS rinse, sections were incubated for 2 h at 40ºC with three different probe combinations targeting (i) Rxfp3 (ACD, #316181), ChAT (ACD, #430111) and vGAT (Slc32a1) (ACD, #424541) mRNA; (ii) Rxfp3, PV (pvalb, ACD, #407828) and SOM (Sst, ACD, #412181-C3) mRNA; (iii) Rxfp3, PV and vGAT mRNA. Sections were processed in two different trials. Following incubation, sections were rinsed with wash buffer (ACD, Cat#310091) and signals were amplified with ACD amplifier reagents according to manufacturer's protocol. After 2× rinses with wash buffer, sections were stained with DAPI (ACD, #320851), covered with fluorescent mounting medium (Fluoromount-G, Southern Biotech, Birmingham, AL, USA, Cat# 17985-10), coverslipped, and stored at -20ºC.

### 3.2.3. Imaging and quantification of co-expression of transcripts

Fluorescence images were taken with an LSM 780 Zeiss Axio Imager 2 confocal laser scanning microscope (Carl Zeiss AG, Jena, Germany).

**Table 3.1**. Semi-quantification of the number of neurons expressing *Rxfp3*, *vGAT* mRNA alone and in combination throughout the different regions of the rat septal area.

| Bregma | Area | 1.08 mm | | | | 0.6mm | | | | 0.48 mm |
|---|---|---|---|---|---|---|---|---|---|---|
| | | MS | | VDB | HDB | MS | | VDB | HDB | MS |
| | *Rxfp3* | 77 ± 28 | | 67 ± 14 | 62 | 107 ± 13 | | 54 ± 12 | 37 ± 6 | 172 ± 16 |
| | *vGAT* | 240 | - | 148 | - | 500 ±100 | | 89 | 162 | 1500 ± 30 |
| | *PV* | - | 116 | - | 16 | - | 179 | - | - | 126 |
| | *SOM* | - | 0 | - | 78 | - | - | - | - | - |
| | *ChAT* | 91 | - | 41 | - | 75 | - | 9 | 26 | - |
| | *Rxfp3/ vGAT* | 44 | - | 45 | - | 82 | 99 | 31 | 21 | 109 ± 8 |
| | *Rxfp3/PV/ vGAT* | - | 39 | - | 1 | 7 | - | - | - | 27 ± 8 |
| | *Rxfp3/Ch AT* | 0 | - | 3 | - | 0 | - | 0 | 0 | - |
| | *Rxfp3/-* | 5 | 66 | 5 | 53 | 14 | 12 | 34 | 10 | 22 ± 15 |

| | | VDB | HDB | LSI | SFi | MS | LSD | SFi | TS | LS V | SF O |
|---|---|---|---|---|---|---|---|---|---|---|---|
| 0.24 mm | | 50 | 41.5 ± 13 | 11 | 20 | 8 | 14 | 100 | 245 | 223 | 30 |
| | | 306 ±20 | 188 ± 16 | 37 | 97 | 86 | 61 | 314 | 800 | 307 | 4 |
| | | 83 ± | 23 ± | - | - | - | - | - | - | - | - |
| | | - | - | - | - | - | - | - | - | - | |
| | | - | - | 2 | 2 | 4 | 0 | 0 | 3 | 4 | 6 |
| -0.24 mm | | 24 | 23 ± 10 | 9 | 19 | 8 | 12 | 75 | 193 | 142 | 2 |
| | | 14 | 7 ± 2 | - | - | - | - | - | - | - | - |
| | | - | - | 0 | 0 | 0 | 0 | 0 | 0 | 1 | 0 |
| | | 12 | 12 ± 5 | 2 | 1 | 0 | 2 | 25 | 52 | 80 | 28 |

Note. – Mean ± SEM are indicated on cases where more than one subject was analysed. - indicates not determined probe combinations and split rows indicate each of different trials.

The system is equipped with a stitching stage, and Zen software (Carl Zeiss AG) was used to stitch tiled images taken with a 20× objective. Quantification of cellular colocalization of transcripts (one section/bregma level, rat and probe combination) was conducted manually using Fiji (Schindelin et al. 2012).

[Note: Results consistent with those observed in the sections assessed, were also observed in adjacent brain areas, and in other rat brains, for all probes]. The total number of positive neurons for each region was

counted separately, relative to DAPI-stained nuclei, to avoid bias. The percentage co-expression of transcripts was related to the total number of Rxfp3 mRNA-positive neurons in each of the septal areas. Higher-power, (inset) images to illustrate co-localization were taken using a 40× objective.

## 3.3. Results

In these experiments, we assessed the rostrocaudal distribution of Rxfp3 mRNA-positive neurons in the MS/diagonal band, lateral septum, triangular septal nucleus, and septofimbrial nucleus, and determined whether these Rxfp3 mRNA-positive neurons co-expressed ChAT or vGAT mRNA or PV and/or vGAT mRNA (or SOM and/or vGAT mRNA). All these neurotransmitter-related transcripts and their related proteins or peptides have been described as clear markers of the onion-like structure of the septum. According to Wei et al., (2012), the onion-like medial septum can be described as a five-layer structure with layers determined by their highest density marker (MS-1-MS-3, LSv and LSi). Layers are distributed from the midline to the LSi with MS-1 on the midline, rich in PV neurons; followed by MS-2, rich in ChAT neurons; followed by MS-3, rich in nNOS; followed by CR (LSV) and CB (LSi). The following results illustrate a high level of co-localization of Rxfp3 and vGAT mRNA in neurons in most septal regions. In contrast, in caudal septal regions and diagonal band, no co-localization of Rxfp3 with vGAT mRNA occurred, suggesting an alternative non-GABAergic phenotype **(Table 3.1)**.

### 3.3.1. Rxfp3 mRNA-positive neurons in MS co-express vGAT, but not ChAT mRNA

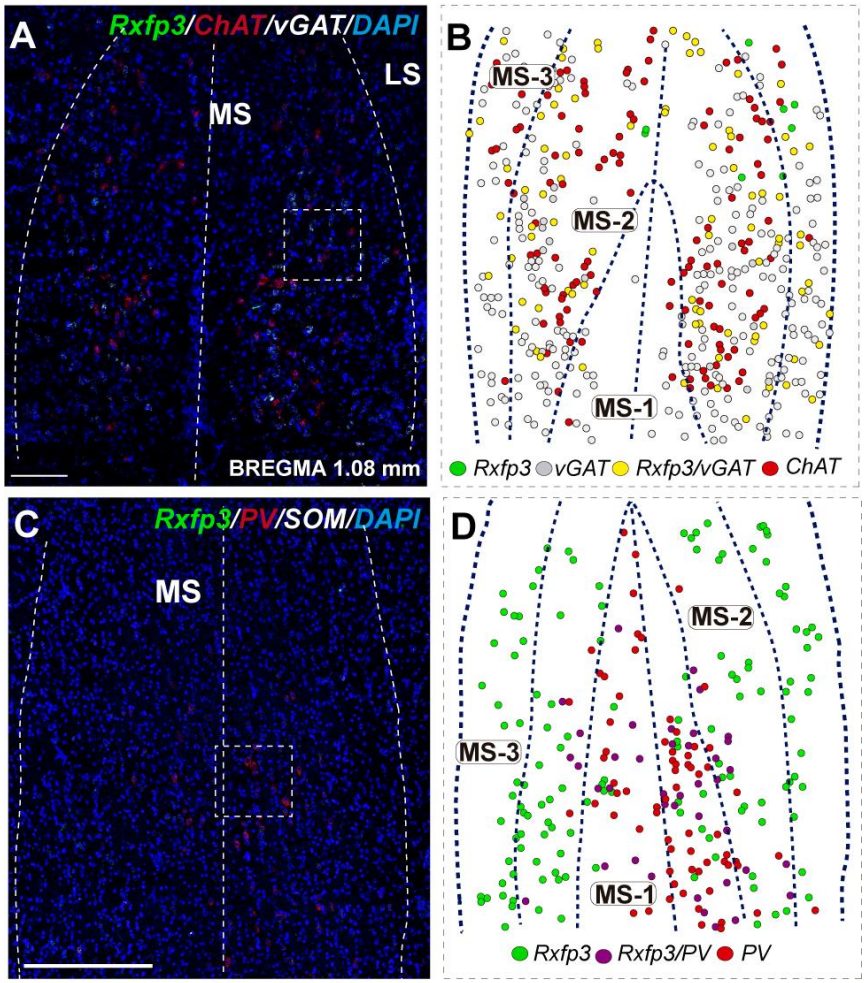


**Figure. 3.1 *Rxfp3*, *vGAT* and *ChAT* mRNA distribution relative to DAPI-stained nuclei, and *Rxfp3*, *SOM* and *PV* mRNA in the rat MS at bregma +1.08 mm (A and C)**; and a schematic map illustrating the different neuronal phenotypes based on mRNA co-expression, and their distribution (**B and D**). Thick dotted lines indicate the midline and the medial and lateral septal border and thin dotted lines, the layers within MS. L. Calibration bar in (**A**) 250 µm, (**C**) 250 µm.

At the most rostral level of the MS (bregma ~1.08 mm), Rxfp3 mRNA-expressing neurons were mainly located between the MS-1 and MS-3 layers (**Fig. 3.1A-D**). The majority of Rxfp3 mRNA-positive neurons in these layers

co-expressed vGAT mRNA (~90%; 44/49) of expressing neurons) while only ~10% (5/49 neurons) of Rxfp3 mRNA-positive neurons lacked vGAT and ChAT mRNA (**Fig. 3.1E-H and 3.2)**. Given the distribution of these neurons and the co-localization of Rxfp3 mRNA with vGAT and not ChAT mRNA, this labelling is consistent with expression of RXFP3 by GABA neurons (Ma et al. 2009a; Olucha-Bordonau et al. 2012; Ma et al. 2017). With a different combination of probes for Rxfp3/PV/SOM mRNA, ~37% of Rxfp3 mRNA-expressing-neurons in the MS (39/105 neurons), expressed PV mRNA, and were distributed within MS-1, while 63% (66/105) of Rxfp3 mRNA-positive neurons that did not co-express PV mRNA (**Fig. 3 1I-L**), were located within MS-2 and 3 (**Fig. 3 1D**).

In the mid-anterior dorsal part of the MS (bregma ~0.6 mm), Rxfp3 mRNA-expressing neurons were present mainly in the MS-1 layer, characterized as containing PV neurons, and in more lateral layers containing lower PV neuron densities (Kiss et al. 1990; Wei et al. 2012). The highest number of Rxfp3 mRNA-expressing neurons was located between MS-2 and MS-3. In the ventral part of this mid-MS level, Rxfp3 mRNA-positive neurons were limited to the MS-2 (**Fig. 3.3A-D**). At this level, the majority of Rxfp3 mRNA-expressing neurons co-expressed vGAT mRNA (~87% (82/94) of labelled neurons), while only ~13% (13/94 neurons) of labelled cells expressed Rxfp3 mRNA in the absence of vGAT and ChAT mRNA (**Fig. 3.3E-H**).

In sections labelled with the Rxfp3/PV/vGAT probe combination, some Rxfp3 mRNA-expressing-neurons co-expressed PV mRNA (~6%; 7/111 neurons), but most co-expressed vGAT mRNA, distributed within MS-2 (82% (91/111) of labelled neurons). Only 12% (14/111 neurons) of Rxfp3 mRNA-expressing neurons did not co-express either transcript (**Fig. 3.2 and 3.3I-L**). In the mid-posterior part of the septal area (bregma ~0.48 mm), the Rxfp3/PV/SOM probe combination revealed that Rxfp3 mRNA-expressing neurons were distributed across MS-1 to MS-3. Rxfp3 mRNA-positive neurons that co-expressed PV mRNA (17%; 27/157 neurons) were mostly located near the midline (**Fig 3.4A-D**). In the MS-2 and MS-3 layers, 69% (109/157 neurons)

of Rxfp3 mRNA-positive neurons co-expressed vGAT mRNA and 14% (22/172 neurons) did not co-express either transcript (**Fig 3.2 and 3.4E-L**).

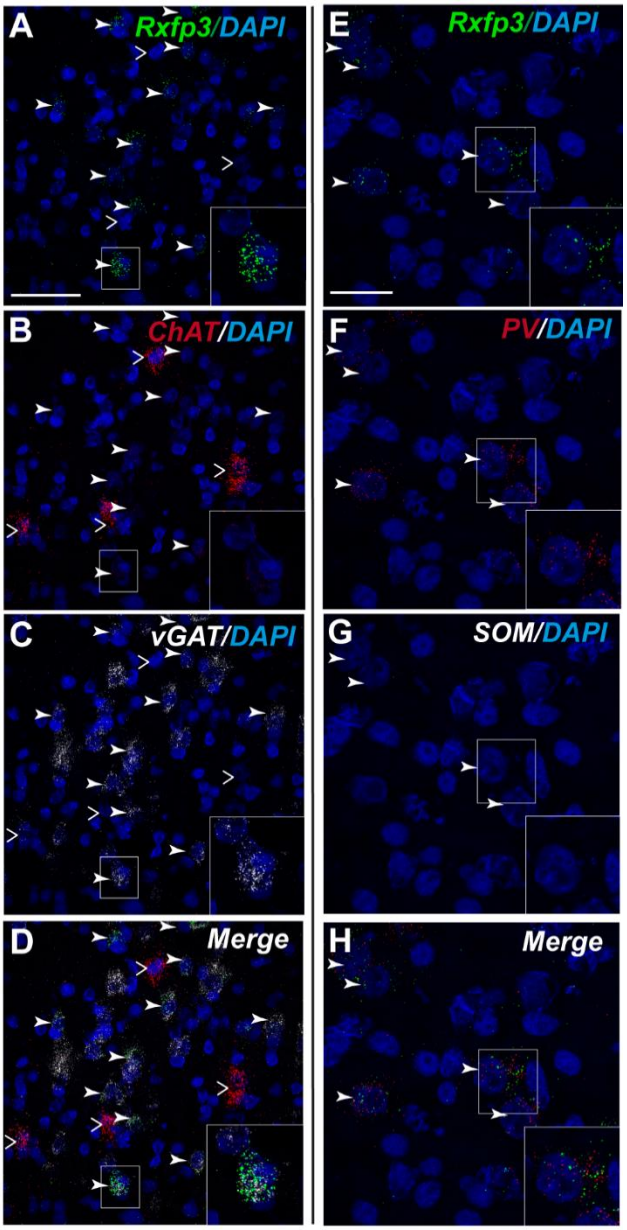


**Figure. 3.2** High-magnification images illustrating colocalization of Rxfp3 (**A**), ChAT (**B**), and vGAT (**C**) mRNA, and merged signals (**D**). and of Rxfp3 (**E**), PV (**F**), and SOM (**G**) mRNA and merged signals (**L**) in the rat MS at bregma +1.08mm. Arrowheads indicate neurons double-labelled for Rxfp3 and vGAT mRNA (A-D) and Rxfp3, vGAT and PV mRNA (E-H). open arrowheads indicate no cololocalization. Calibration bar in (A) 50 µm and 20 µm (I-L).

In the posterior septum (bregma ~0.24 mm), Rxfp3 mRNA-positive neurons were present in the MS and were more dense in the septofimbrial nucleus (SFi) and the intermediate lateral septum (LSI) (**Fig. 3.5A-B**). In the MS, Rxfp3 mRNA-positive neurons co-expressed vGAT mRNA in ~100% of cases (8/8 neurons), but did not express ChAT mRNA (**Fig. 3.2**

**and 3.5C-F**). In the SFi ~95% (19/20 neurons) of Rxfp3 mRNA-positive neurons co-expressed vGAT mRNA, and ~5% (1/20 neurons) of Rxfp3

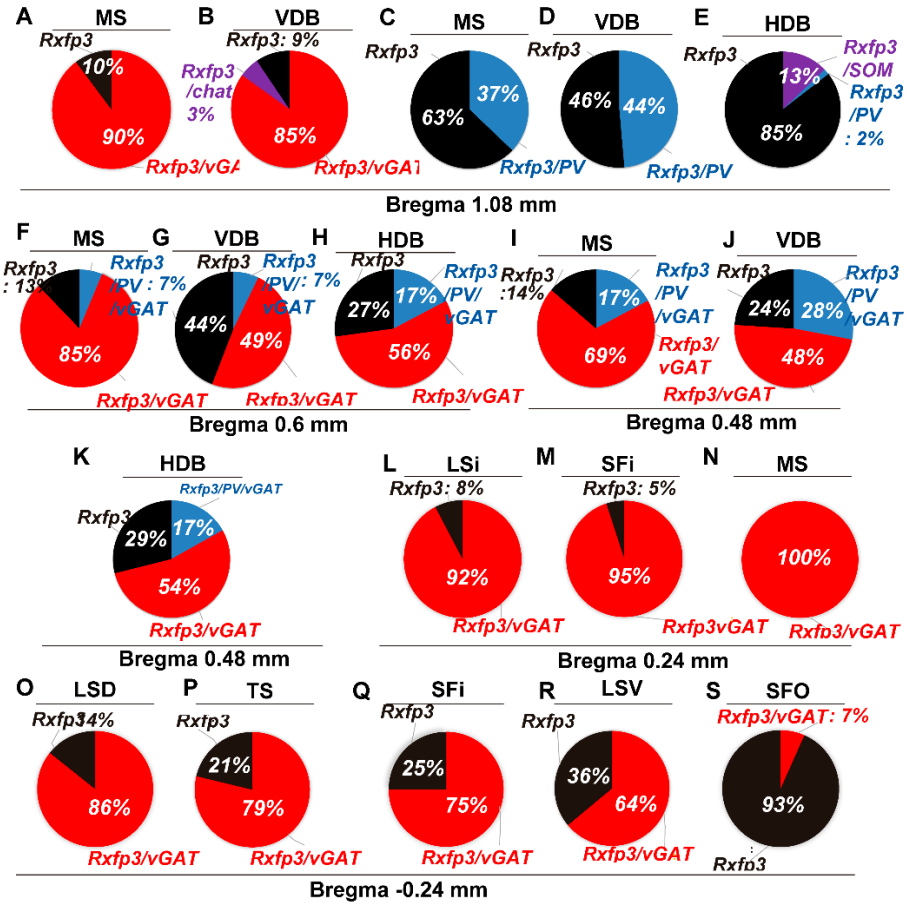


**Figure. 3.3 Percentage co-localization of *Rxfp3*, *vGAT, PV* and *SOM* mRNA throughout the septal complex**. Rostral to caudal levels of MS (**A and C**), VDB (**B and D**) and HDB (**E**) at +1.08 mm from bregma; MS (**F**), VDB (**G**) and HDB (**H**) at +0.6 mm from bregma; MS (**I**), VDB (**J**) and HDB (**K**) at +0.48 mm from bregma; LSi (**F**), SFi (**G**) and MS (**H**) at +0.24 mm from bregma; and LSD (**I**), TS (**J**), SFi (**K**), LSV(**L**) and SFO (**M**) at -0.24 mm from bregma.

mRNA-positive neurons lacked vGAT and ChAT mRNAs (**Fig. 3.2 and 3.5G-J**). Finally, in the LSI ~92% (24/26 neurons) of detected neurons co-expressed Rxfp3 and vGAT mRNAs whereas only ~8% (2/26 neurons) of Rxfp3 mRNA-positive neurons lacked vGAT and ChAT mRNA (**Fig. 3.2 and 3.5K-N**).

### 3.3.2. Diagonal band neurons co-express Rxfp3 and vGAT (slc32a1) mRNAs

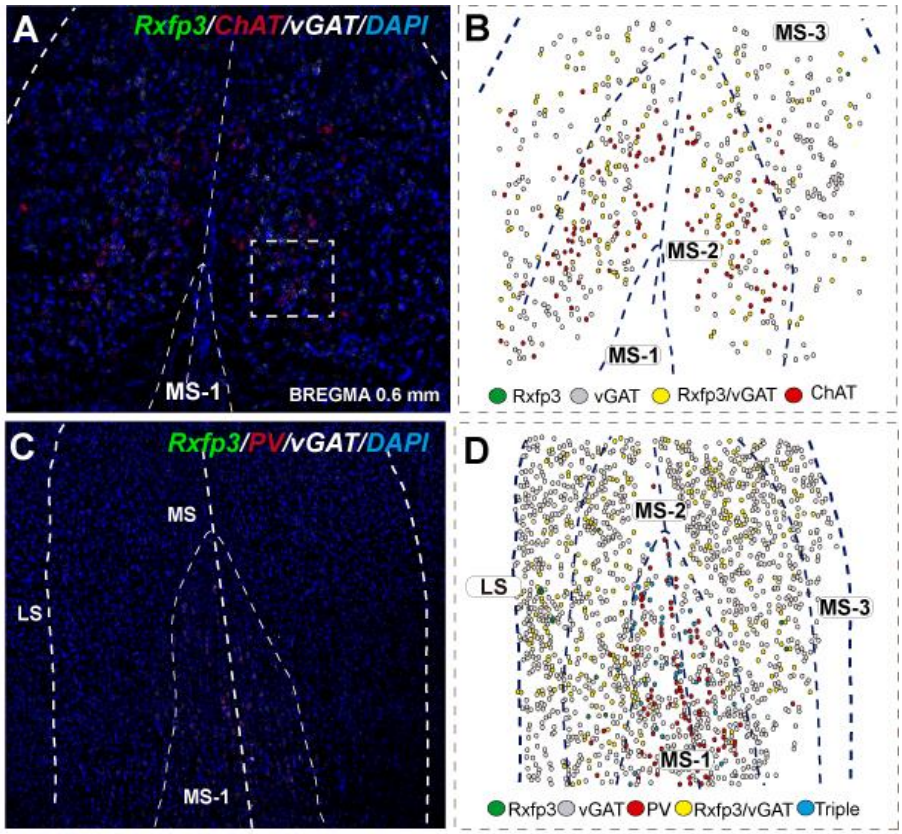


**Figure.3.4** –Rxfp3, vGAT, ChAT and PV mRNA distribution relative to DAPI-stained nuclei in the rat MS at bregma +0.60 mm (**A and C**), and a schematic map illustrating the different neuronal phenotypes based on mRNA co-expression, and their distribution (**B and D**). Thick dotted lines indicate the midline and the medial and lateral septal border and thin dotted lines, the layers within MS. Calibration bar in (A) 250 µm, (C) 250 µm.

In the anterior vertical diagonal band (VDB; bregma ~1.08 mm), Rxfp3 mRNA-positive neurons were evenly distributed laterally at a similar distance from the midline (**Fig. 3.6A-D'**). Rxfp3 mRNA-positive neurons were present in the vicinity of ChAT mRNA-expressing neurons, but Rxfp3 and ChAT mRNA were sparsely co-expressed in ~6% (3/53 neurons) of total Rxfp3 mRNA-positive cells, while ~85% (45/53 neurons) co-expressed Rxfp3 and vGAT

mRNA, and Rxfp3 transcripts were present in the absence of the other markers in only ~9% (5/53 neurons) of identified neurons (**Fig. 3.2 and 3.6E-H**).

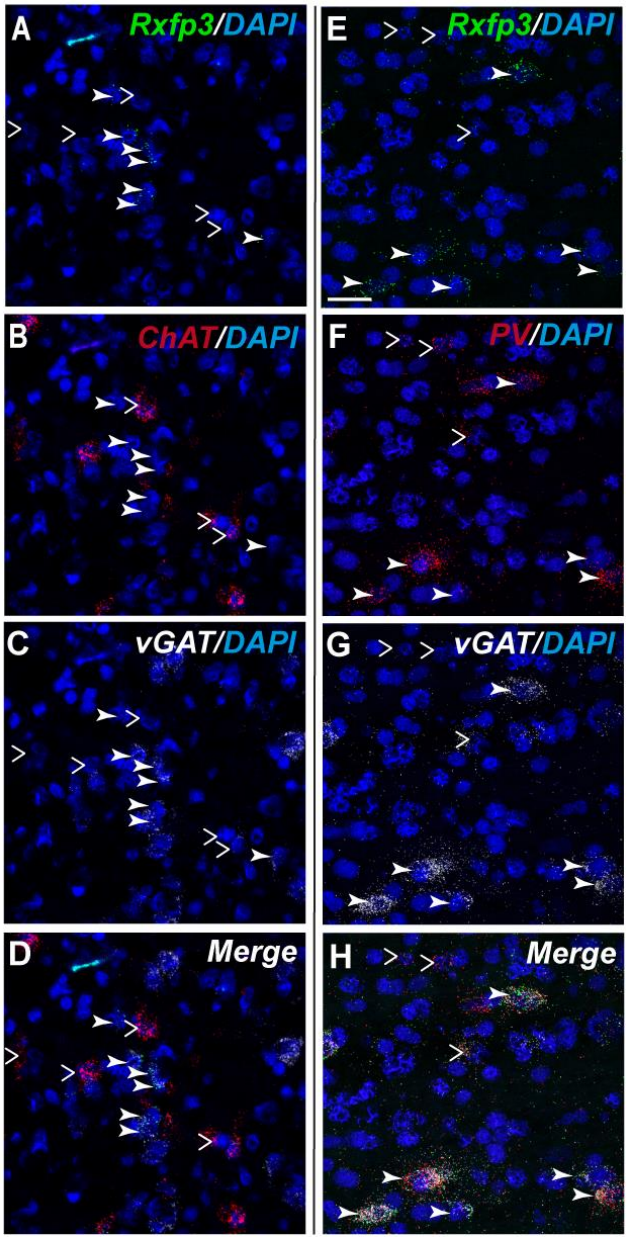


**Figure. 3.5** High-magnification images illustrating colocalization of Rxfp3 (**A**), ChAT (**B**), and vGAT (**C**) mRNA, and merged signals (**D**). and of Rxfp3 (**E**), PV (**F**), and vGAT (**G**) mRNA and merged signals (**H**) in the rat MS at bregma +0.60mm. Arrowheads indicate neurons double-labelled for Rxfp3 and vGAT mRNA (E-H) and Rxfp3, vGAT and PV mRNA (I-L). open arrowheads indicate no cololocalization

In sections incubated in a different combination of probes, Rxfp3 mRNA-expressing neurons in the VDB co-localized with PV mRNA (44%; 35/80 neurons) and did not co-localize with any marker in 46% (37/80) of neurons (**Fig. 3.2 and 3.6I-L**) In contrast, in the HDB, some Rxfp3 mRNA-expressing neurons co-expressed SOM (13%; 8/62) and PV (2% 1/62) mRNA, but most did not co-

express either of these transcripts (85%; 53/62 neurons) (**Fig. 3.2, 3.7A -B and 3.7E - H**).

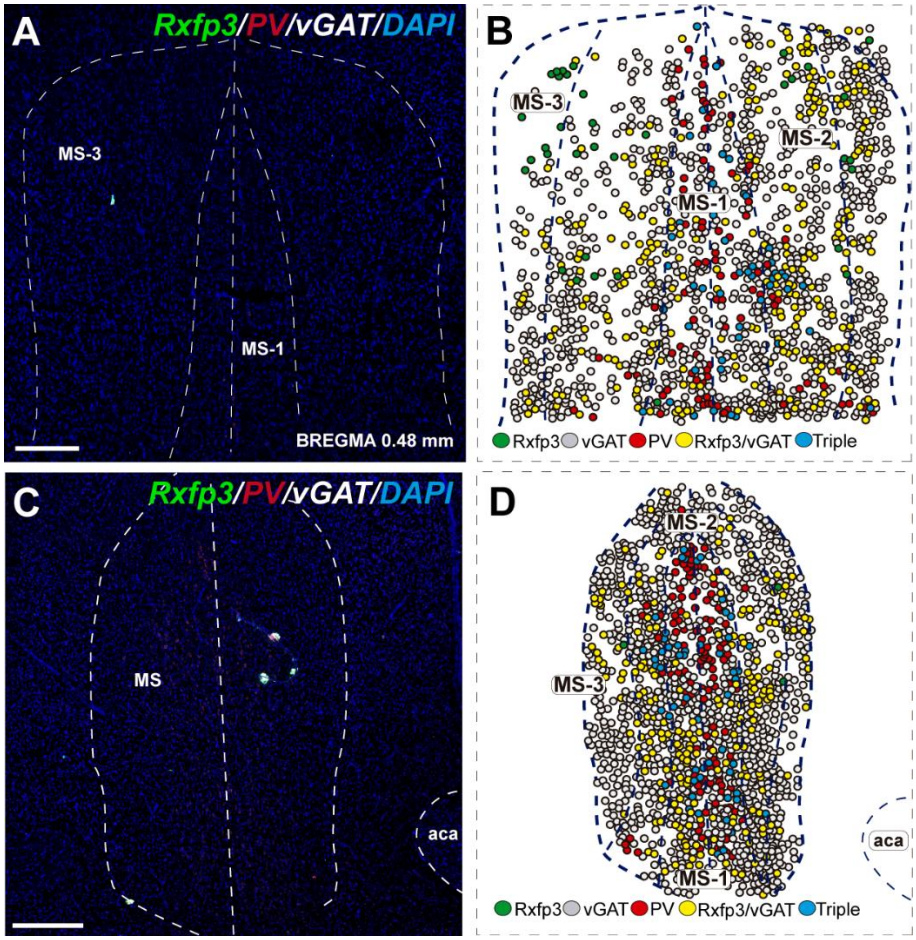


**Figure.3.6** –Rxfp3, vGAT and PV mRNA distribution relative to DAPI-stained nuclei in the rat MS at bregma +0.48 mm (**A and C**), and a schematic map illustrating the different neuronal phenotypes based on mRNA co-expression, and their distribution (**B and D**). Thick dotted lines indicate the midline and the medial and lateral septal border and thin dotted lines, the layers within MS. Calibration bar in (A) 250 µm, (C) 250 µm.

At more posterior levels (bregma ~0.6 mm), Rxfp3 mRNA-positive neurons were present in the VDB and the horizontal diagonal band (HDB) (**Fig. 3.6C-C′ and 2.7C-D).** In the VDB, Rxfp3 mRNA-expressing neurons were present in two clusters. From the total amount of Rxfp3 mRNA positive neurons ~48% (31/65) of them co-expressed vGAT mRNA. A second cluster/population

of Rxfp3 mRNA-positive neurons, ~52%; 34/65 neurons, did not co-express vGAT or ChAT mRNA.

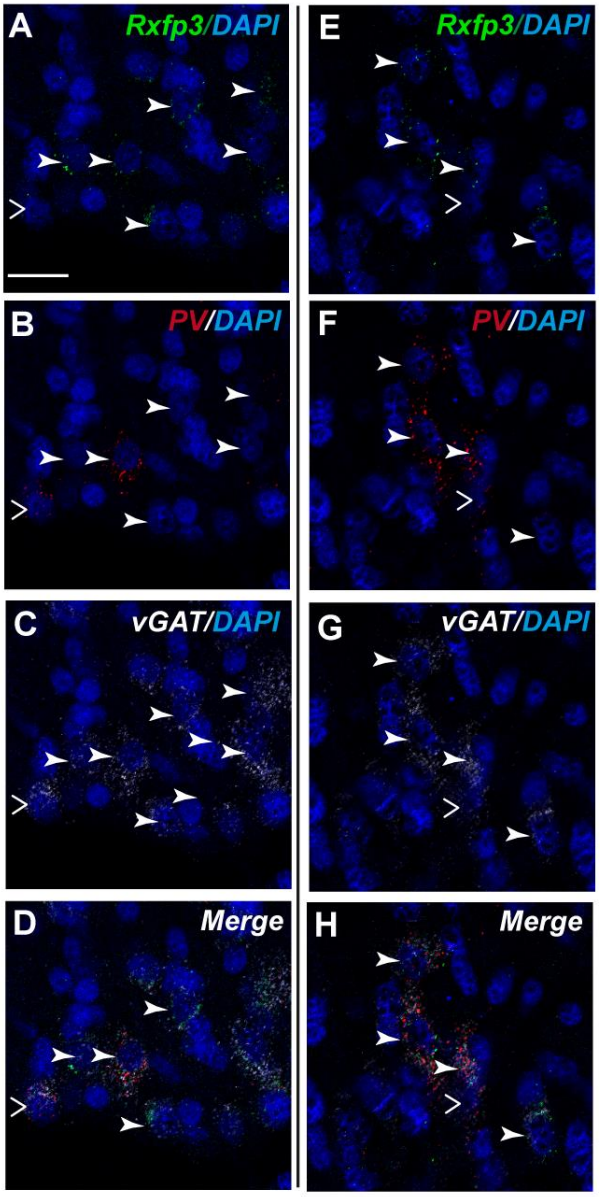


**Figure. 3.7** High-magnification images illustrating colocalization of Rxfp3 (**A and E**), PV (**B and F**) and vGAT (**C and G**) mRNA, and merged signals (**D and H)** in the rat MS at bregma +0.48mm. Arrowheads indicate neurons double-labelled for Rxfp3 and vGAT mRNA (**E-H**) and Rxfp3, vGAT and PV mRNA (**I-L**). open arrowheads indicate no cololocalization

In sections labelled for Rxfp3/PV/vGAT mRNA some Rxfp3 mRNA-expressing neurons expressed PV mRNA (7%; 4/56), while 49% (27/56) expressed vGAT mRNA and 44% (25/56) did not express either of the other transcripts (**Fig. 3.2 and 3.6M-P**).

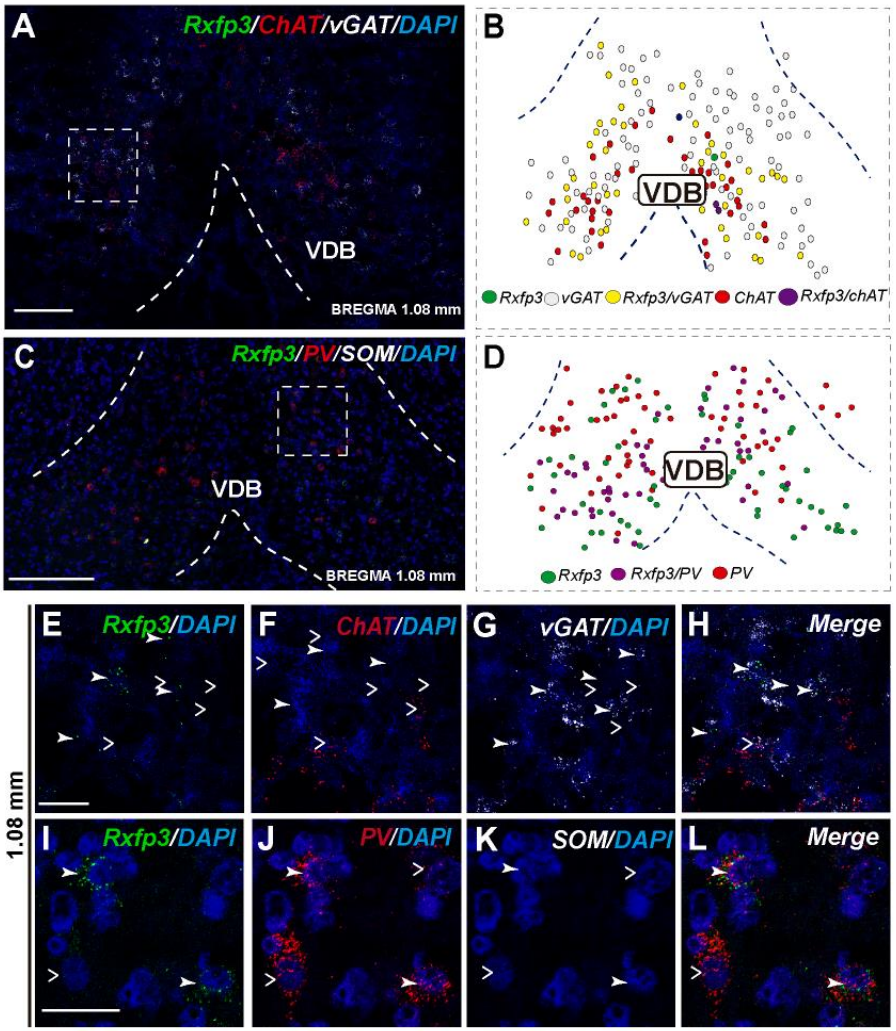


**Figure. 3.8** – Distribution of neurons expressing Rxfp3, vGAT, ChAT and PV mRNAs relative to DAPI-stained nuclei in the vertical limb of the diagonal band at bregma +1.08 mm (A and C) and schematic map illustrating different colocalization neuronal phenotypes and their distribution (B and D). Dotted lines indicate the midline and the vertical diagonal band border. Higher magnification images illustrate colocalization of Rxfp3 (E), ChAT (F), vGAT mRNA (G) and merged signals (H). High-magnification images illustrate co-localization of Rxfp3 (I), PV (J,), SOM (K) vGAT (O) mRNA and merged signals (L). Arrowheads indicate neurons double-labelled for Rxfp3 and vGAT (E-H) or Rxfp3, vGAT and PV (I-L) mRNA and open arrowheads indicate ChAT or PV mRNA-positive neurons that do not express Rxfp3 mRNA. Calibration bar in (A) 100 µm, (C) 125 µm, (E) 50 µm and (I) 20 µm.

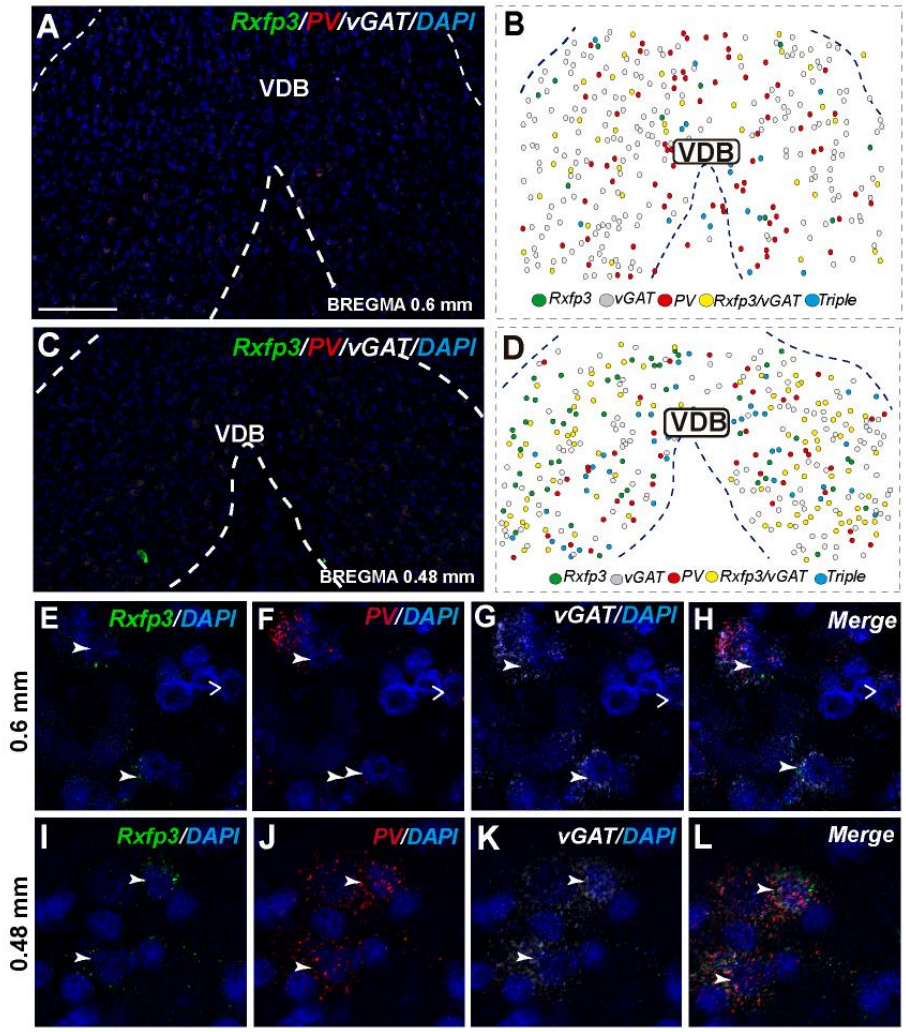


**Figure. 3.9** – Distribution of neurons expressing Rxfp3, vGAT, and PV mRNAs relative to DAPI-stained nuclei in the vertical limb of the diagonal band at bregma +0.6 and 0.48 mm (A and C) and schematic map illustrating different colocalization neuronal phenotypes and their distribution (B and D). Dotted lines indicate the midline and the vertical diagonal band border. Higher magnification images illustrate colocalization of Rxfp3 (E), ChAT (F), vGAT mRNA (G) and merged signals (H). High-magnification images illustrate co-localization of Rxfp3 (I), PV (J,), SOM (K) vGAT (O) mRNA and merged signals (L). Arrowheads indicate neurons double-labelled for Rxfp3 and vGAT (E-H) or Rxfp3, vGAT and PV (I-L) mRNA and open arrowheads indicate ChAT or PV mRNA-positive neurons that do not express Rxfp3 mRNA. Calibration bar in (A) 100 µm, (C) 125 µm, (E) 50 µm and (I) 20 µm.

The number of Rxfp3 mRNA-positive neurons in the HDB was lower than in the VDB (**Fig. 3.6B and B'**). In contrast to the VDB, in the HDB the

majority (~68%; 21/31 neurons) of Rxfp3 mRNA-positive neurons expressed vGAT mRNA, while the remaining were vGAT mRNA and ChAT mRNA negative (~32%; 10/31 neurons) (**Fig. 3.2 and 3.6I-L**). Rxfp3 mRNA colocalized with vGAT mRNA (56%; 23/41 neurons), and with PV/vGAT mRNA (17%; 7/41 neurons) and was also expressed in the absence of either transcript (27%; 11/41) (**Fig. 3.2, 3.8A-B and E-H**).

In the mid-posterior part of the septal area (bregma ~0.48 mm) sections labelled with Rxfp3/PV/vGAT probes displayed Rxfp3 mRNA expressing neurons in the VDB (**Fig. 3.8C and D**) that co-expressed PV/vGAT mRNA (28%; 14/50 neurons), and vGAT mRNA (48%; 24/50 neurons), but some Rxfp3 mRNA-positive neurons did not express either transcript (24%; 12/50 neurons). Likewise, analysis of the HDB, revealed that the majority of Rxfp3 mRNA-positive neurons expressed vGAT mRNA (54%; 23/42 neurons) and a small proportion expressed PV/vGAT mRNA (17%; 7/42 neurons) or neither of the other transcripts (29%; 12/42 neurons) (**Fig. 3.2 and 3.8I-L**).

### 3.3.3. Triangular septal area, and septofimbrial and dorsolateral septal area contain heterogeneous populations of Rxfp3 mRNA-positive neurons

In the most caudal region of the septum analyzed (bregma -0.24 mm), the distribution and phenotype of Rxfp3 mRNA-positive neurons varied within the different nuclei. In the dorsolateral septum (LSD), Rxfp3 mRNA-positive neurons were widely and evenly distributed (**Fig. 3.9A and B**) and were mainly vGAT mRNA positive (~86%; 12/14 neurons), with a small number of neurons located near the SFi that were vGAT mRNA negative (~14%; 2/14 neurons; **Fig. 3.2 and 3.9K-N**).

Rxfp3 mRNA-positive neurons in the SFi were mainly distributed in the most dorsal part of the nucleus near the corpus callosum (cc). In the ventral SFi, Rxfp3 mRNA-positive neurons were lower in number (**Fig. 3.9A and B**). Throughout the dorsal and ventral SFi, the majority of Rxfp3 mRNA-positive neurons co-expressed vGAT mRNA (~75%; 75/100 neurons; **Fig. 3.2 and 3.9L-O**).

The triangular septal area (TS) contained three Rxfp3 mRNA-positive neuron populations based on their differential phenotype and distribution. Dispersed Rxfp3 mRNA-positive neurons were present in the most dorsal portion near the midline, while in the most ventral TS, a large, densely packed population of Rxfp3 mRNA-positive neurons were distributed alongside the border with the subfornical organ (SFO) (**Fig. 3.9A and B**). The ventral TS area was rich in vGAT mRNA-expressing neurons, while the dorsal TS was not. Rxfp3 mRNA-positive neurons in the dorsal TS were generally vGAT mRNA-negative, while in the ventral TS, Rxfp3 mRNA-positive neurons were generally vGAT mRNA-positive. In the lateral part of the ventral TS, there was a population of Rxfp3 mRNA-positive neurons which were vGAT mRNA-negative. Overall, ~79% of Rxfp3 mRNA-positive neurons in TS co-expressed vGAT mRNA (193/245 neurons), while the remainder were negative (~21%; 52/245 neurons; **Fig. 3.2 and 3.9C-K**).

Similar to ventral TS, the LSV contained a large population of vGAT mRNA-positive neurons and most were Rxfp3/vGAT mRNA-positive (64%; 142/223 neurons). In addition to these GABAergic neurons, this area also contained a large non-GABAergic population (36%; 80/223 neurons; **Fig 3.2 and 3.9G-H**). Finally, we noted that within the SFO, a vast majority of Rxfp3 mRNA-positive neurons were vGAT mRNA-negative (93%; 28/30 cells; **Fig 3.2 and 3.9O-R**).

## 3.4. Discussion

These studies employed RNAscope multiplex in situ hybridization (Wang et al. 2014; Wang et al. 2015; Li and Kim 2015) to characterize the neurochemical phenotype of Rxfp3 mRNA-positive neurons in the rat septal area. The highly specific nature of the method means that these data represent a more accurate estimation of the distribution of RXFP3 over studies using putative antisera against the receptor protein (Meadows and Byrnes 2015), although this powerful approach does not provide information about the subcellular location of RXFP3, which might be available with alternative protein detection methods.

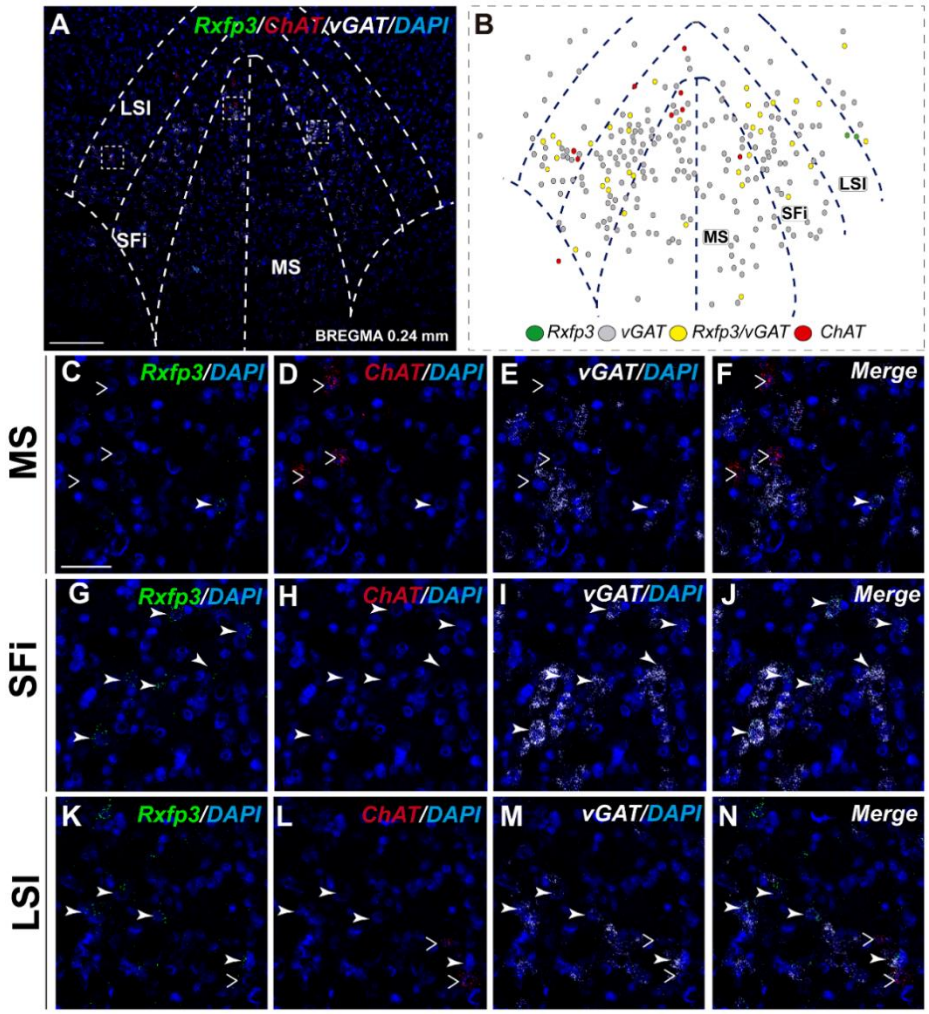


**Figure. 3.10** Rxfp3, vGAT and ChAT mRNA distribution, relative to DAPI-stained nuclei in the rat MS, SFi and LSI at bregma +0.24 mm (**A**) and a schematic map illustrating different neuronal phenotypes based on mRNA co-expression, and their distribution (**B**). Dotted lines indicate the midline and the medial and lateral septal and septofimbrial borders. High-magnification images illustrate co-localization of Rxfp3 (**C, G and K**), ChAT (**D, H and** L), vGAT (**E, I and M**) mRNA and merged signals (**F, J and N**) in the MS, SFi and LSI, respectively. No co-localization of Rxfp3 and ChAT mRNA was observed (open arrowheads). Calibration bar in (A) 125 µm, and (C-N) 50 µm.

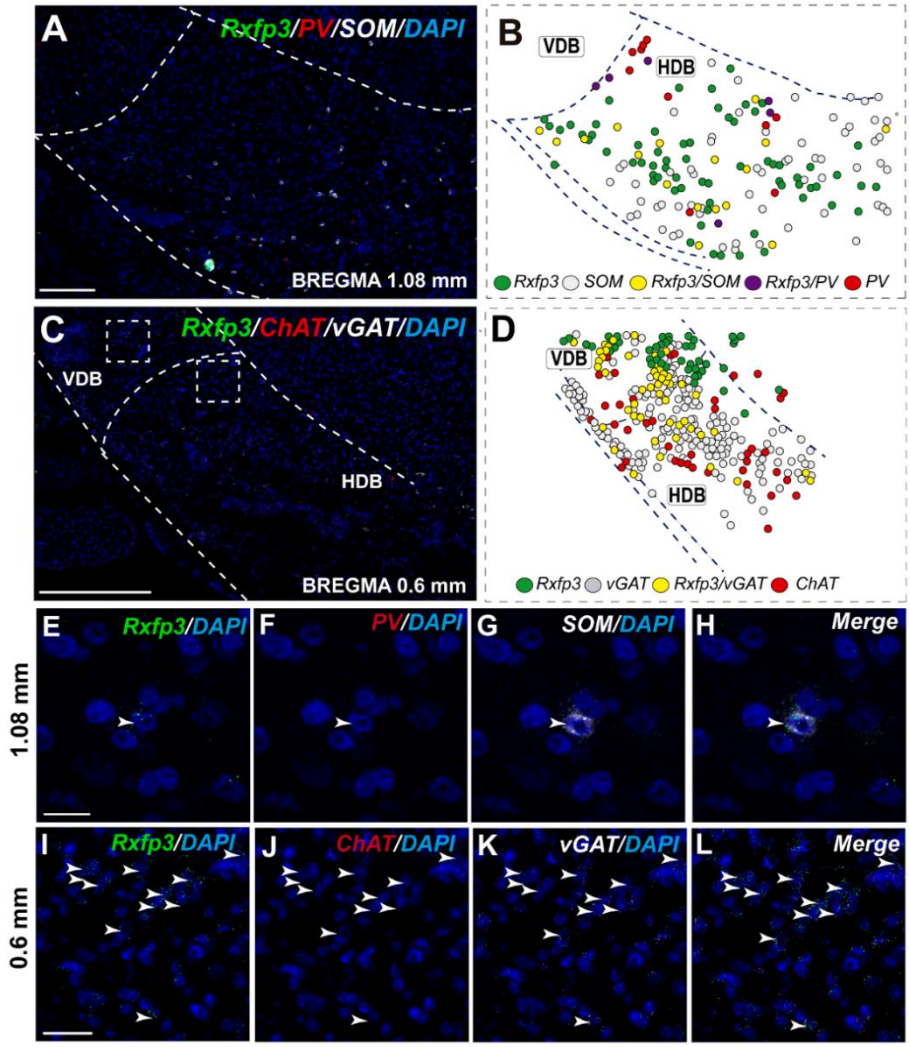


**Figure. 3.11** Distribution of neurons expressing *Rxfp3*, *vGAT*, *ChAT* and *PV* mRNAs relative to DAPI-stained nuclei in the HDB at bregma +1.08 mm (**A**) +0.60 mm (**C)** and schematic map illustrating different colocalization neuronal phenotypes and their distribution **(B and D)**. Dotted lines indicate the vertical and horizontal limbs of the diagonal band border. Higher magnification images illustrate colocalization of *Rxfp3* **(E)**, *PV* **(F)**, *SOM* mRNA **(G)** and merged signals **(H);** *Rxfp3* **(I)**, *ChAT* **(J)**, *vGAT* mRNA **(K)** and merged signals **(L)** in the HDB respectively. Arrowheads indicate neurons double-labelled for *Rxfp3*, *SOM* and *PV* **(E-H)** or *Rxfp3* and *vGAT* **(I-L)**. Calibration bar in (**A**) 125 µm, (**C**) 200 µm, (**E-H**) 20 µm and (**I-L**) 50 µm.

In the septal area, neurons expressing Rxfp3 transcripts were concentrated in the MS complex, including the diagonal band nuclei, and in the posterior septum, including the SFi and TS nuclei. Some Rxfp3 mRNA-positive neurons were also detected in LS divisions. Our findings are consistent with previous studies of the presence and distribution of Rxfp3 mRNA in the rat septal area detected using radioactive oligonucleotide probes. Specifically, MS and HDB displayed moderate to high levels of Rxfp3 mRNA, while in LSI and VDB, expression was moderate (Sutton et al. 2004; Ma et al. 2007). These findings are consistent with concurrent studies of these and other transcripts in rat hippocampus (Ma S, Gundlach AL, unpublished data).

Therefore, in light of the strong innervation of the rat septal region by relaxin-3-positive nerve fibres, the presence of septal RXFP3 binding sites, and functional studies (Ma et al. 2007; Ma et al. 2009a), we conclude that the detection of Rxfp3 mRNA reflects the expression of functional RXFP3 protein by these neurons.

In the MS, VBD and HDB, the vast majority of Rxfp3 mRNA-positive neurons co-expressed vGAT mRNA. Furthermore, a population of these presumed GABAergic Rxfp3 mRNA-positive neurons are PV mRNA-positive (Wei et al. 2012). Septal PV/GABA neurons are the main source of the GABAergic projections to the hippocampus and specifically target hippocampal interneurons (Freund and Antal 1988; Freund and Gulyas 1997). A number of studies have demonstrated that PV/GABA neuron activity is crucial for hippocampal theta rhythm (Borhegyi et al. 2004; Bassant et al. 2005; Simon et al. 2006). The modulation of the GABAergic inter-neuronal inhibition of hippocampal pyramidal neurons has been reported to be a source for hippocampal theta rhythm synchronization (Toth et al. 1997). In addition, septal PV/GABA neurons expressing cyclic nucleotide activated, non-selective cation channels play a role in driving hippocampal theta rhythm (Varga et al. 2008; Hangya et al. 2009). Notably, RXFP3 activation results in inhibition of cellular cAMP synthesis in cell-based assays in vitro (Liu et al. 2003; Van der Westhuizen et al. 2007; Van der Westhuizen et al. 2010), consistent with a similar interaction in vivo (see further discussion below).

In contrast to the strong association with GABAergic neurons, only a small number of cholinergic (ChAT mRNA-positive) neurons co-expressed Rxfp3 mRNA. However, anterograde neural tract-tracing and immunohistochemical studies suggest that cholinergic (ChAT-positive) septal neurons receive a robust innervation from the relaxin-3 rich NI (Olucha-Bordonau et al. 2012). Thus, the influence of NI neurons on the septal cholinergic system might be mediated by NI neurons that contain GABA only or other peptides, such as cholecystokinin, which is expressed in the NI (Kubota et al. 1983; Olucha-Bordonau et al. 2003) (Ma S, Gundlach AL, unpublished data).

The discovery that Rxfp3 mRNA is absent from MS cholinergic neurons provides new insights into the nature of the coordinated neural actions that result in the generation and modulation of hippocampal theta rhythm, and since RXFP3 activation often produces neuronal inhibition in vitro (Blasiak et al. 2013; Kania et al. 2017), it is possible that pERK activation in MS cholinergic neurons occurs via RXFP3-mediated inhibition of non-PV, GABAergic interneurons (Leranth and Frotscher 1989).

In this regard, optogenetic activation of cholinergic septohippocampal neurons suppressed ripple sharp waves and enhance theta rhythm oscillations (Vandecasteele et al. 2014) and local circuit inhibitory actions on cholinergic neurons are a primary process in the generation of septal rhythmicity (Leão et al. 2015). Furthermore, icv infusion of an RXFP3 agonist (RXFP3-A2;(Shabanpoor et al. 2012)) resulted in increased phosphorylation of ERK in the MS, mainly in ChAT-immunoreactive neurons (Albert-Gascó et al. 2017).

Given the observed absence of Rxfp3- and ChAT mRNA-positive neurons in the MS in the present study, and the observation that RXFP3 activation routinely induces neuronal inhibition (Kania et al. 2017),

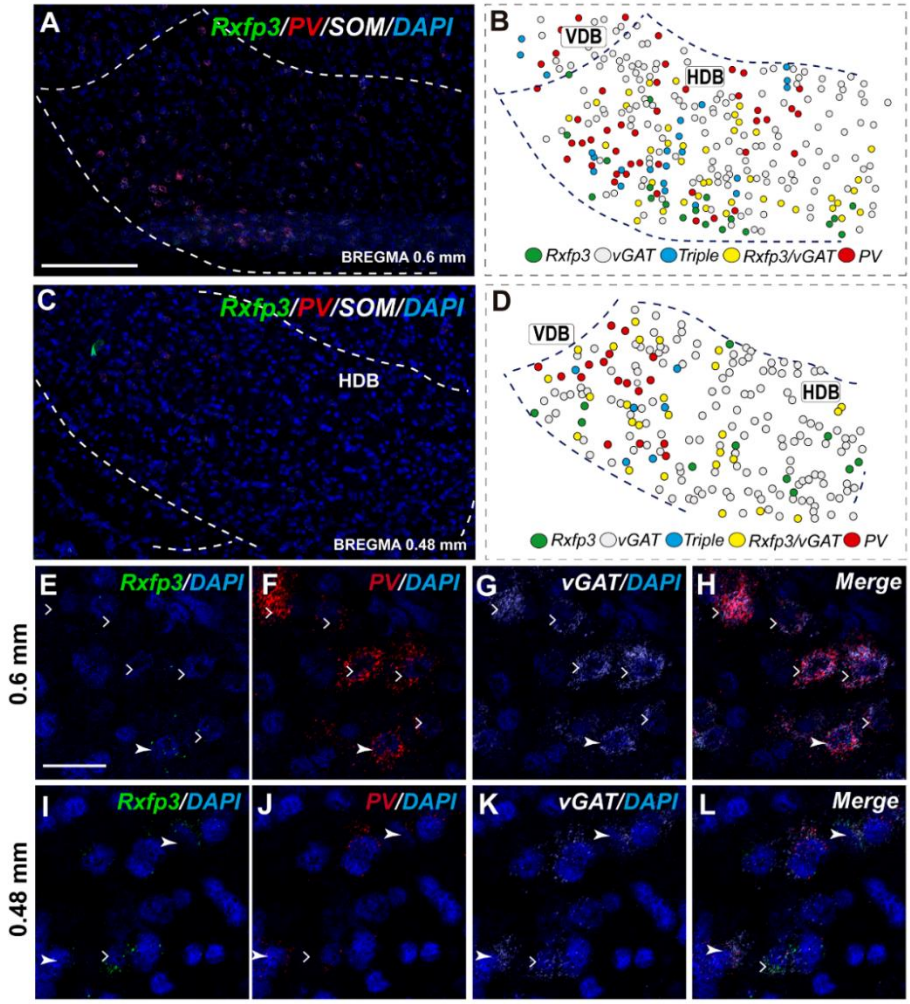


**Figure. 3.12** Distribution of neurons expressing *Rxfp3*, *vGAT*, *ChAT* and *PV* mRNAs relative to DAPI-stained nuclei in the HDB at bregma +0.6 mm **(A)** +0.48 mm **(C)** and schematic map illustrating different colocalization neuronal phenotypes and their distribution **(B and D)**. Dotted lines indicate the vertical and horizontal limbs of the diagonal band border. Higher magnification images illustrate colocalization of *Rxfp3* **(E)**, *PV* **(F)**, *vGAT* mRNA **(G)** and merged signals **(H)**; *Rxfp3* **(I)**, *PV* **(J)**, *vGAT* mRNA **(K)** and merged signals **(L)** in the HDB respectively. Arrowheads indicate neurons double-labelled for *Rxfp3*, *vGAT* and *PV* **(E-H)** or *Rxfp3* and *vGAT* **(I-L)**. Lack of colocalization of *Rxfp3* and *PV* mRNA indicated with open arrowheads. Calibration bar in (**A and C**) 125 µm, (**E-L**) 20 µm.

there is a possibility that the pERK activation within the cholinergic neurons occurs via a reduction in local circuit inhibition within the MS.

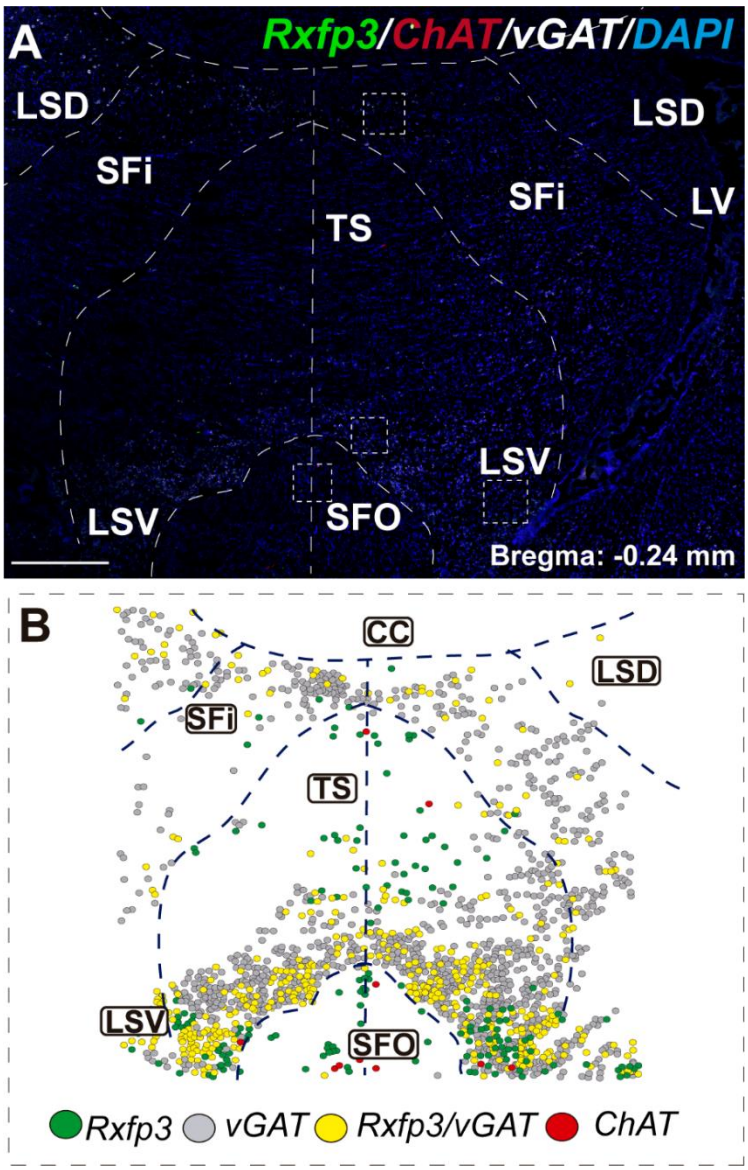


**Figure 3.13**. Distribution of neurons expressing *Rxfp3*, *vGAT* and *ChAT* mRNA, relative to DAPI-stained nuclei in LSD, SFi, TS, LSV and SFO at bregma -0.24 mm (**A**), and a schematic map illustrating the different neuronal phenotypes and their distribution **(B)**. Dotted lines indicate the midline and borders between the different regions. Calibration bar in (**A**) 500 µm.

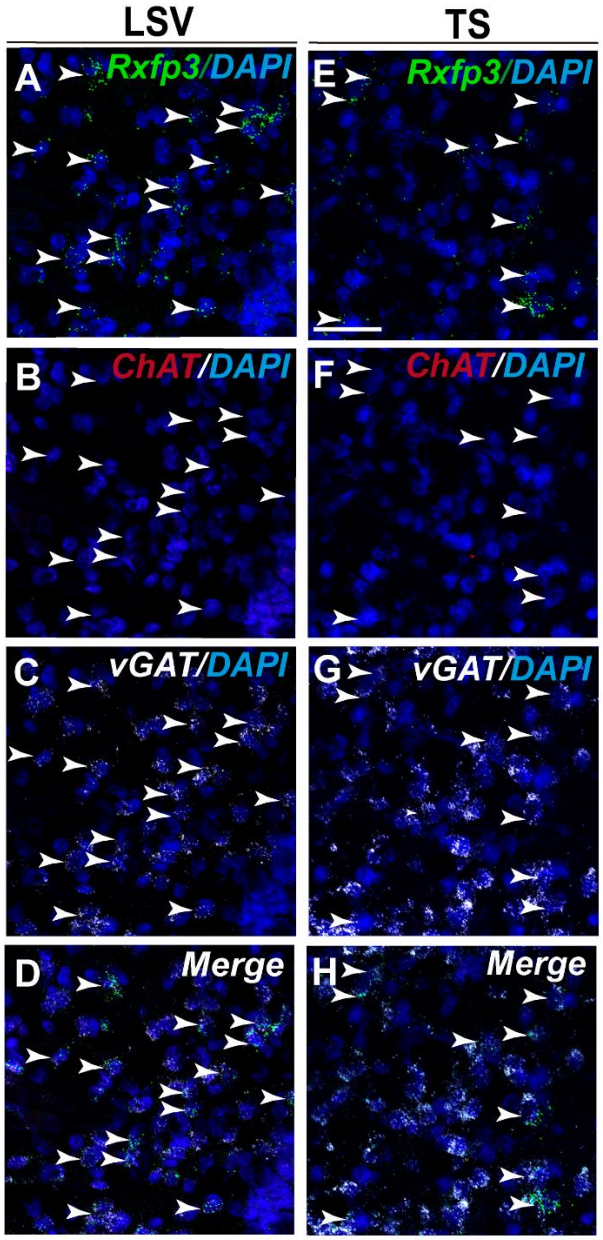


**Figure 3.14**. High-magnification images illustrate the co-localization of *Rxfp3* **(A and E)**, *ChAT* **(B and F)**, *vGAT* **(C and G)** mRNA and merged signals **(D and F) in rat LSV and TS at bregma -0.24mm**. Arrowheads indicate neurons double-labelled for *Rxfp3* and *vGAT* mRNA. No co-localization of *Rxfp3* and *ChAT* mRNA was observed (open arrowheads). Calibration bar in (**E**) 50 µm.

In addition, ~25% of the Rxfp3 mRNA-positive neurons in the MS were non-GABAergic, non-cholinergic in nature. Although further studies are required to better identify the phenotype of these neurons, it is presumed that some or many are glutamatergic neurons, since they constitute ~25% of the total MS neuron population (Colom et al. 2005; Gritti et al. 2006). Glutamatergic neurons provide both local and septohippocampal projections (Manseau et al.

2005; Henderson et al. 2010; Huh et al. 2010) and interestingly, optogenetic activation of MS glutamatergic neurons produces strong theta rhythm synchronization, mainly mediated by local septal circuits (Robinson et al. 2016).

Considerable data suggest a strong link between RXFP3 activation in the MS and modulation of hippocampal theta rhythm. Hippocampal theta rhythm has been traditionally associated with arousal mechanisms which are directly involved in attentional mechanisms of memory (Vinogradova 1995). The NI, along with other brainstem areas, the hypothalamus and the basal forebrain, promote arousal and fast electroencephalographic (EEG) rhythms (Brown and McKenna 2015; Korotkova et al. 2017). Moreover, stimulation of the NI promotes arousal and is associated with cortical EEG desynchronization, increased locomotor activity, and head-scanning vigilance behaviour during fear recall (Ma et al. 2017). In addition, ipsilateral NI stimulation induces locomotion and rotation at latencies consistent with a role in the modulation of premotor areas like the basal forebrain (Farooq et al. 2016). Furthermore, relaxin-3 and Rxfp3 gene knockout mice display reduced voluntary running wheel activity during the dark, active phase (Smith et al. 2012; Hosken et al. 2015) providing further evidence for a likely role for this signalling system in sustained arousal and related locomotor and exploratory activity.

Indeed, the MS controls exploratory behaviour (Köhler and Srebro 1980; Poucet 1989; Mamad et al. 2015; Gangadharan et al. 2016a). Different forms of memory, including spatial working memory and object recognition can be affected by manipulations of the MS (Givens and Olton 1994; Fitz et al. 2008; Roland et al. 2014; Okada et al. 2015; Gangadharan et al. 2016b). Interestingly, interference with global or septal relaxin-3/RXFP3 signalling in the rat results in disruption of spatial working memory in the spontaneous alternation test (Ma et al. 2009b; Albert-Gascó et al. 2017).

In conclusion, the strong expression of Rxfp3 mRNA by GABAergic neurons in the rat MS and adjacent nuclei, is consistent with the central role of these neurons in the control of hippocampal theta rhythm by actions on local septal circuits. In turn, these actions may indirectly influence septal cholinergic

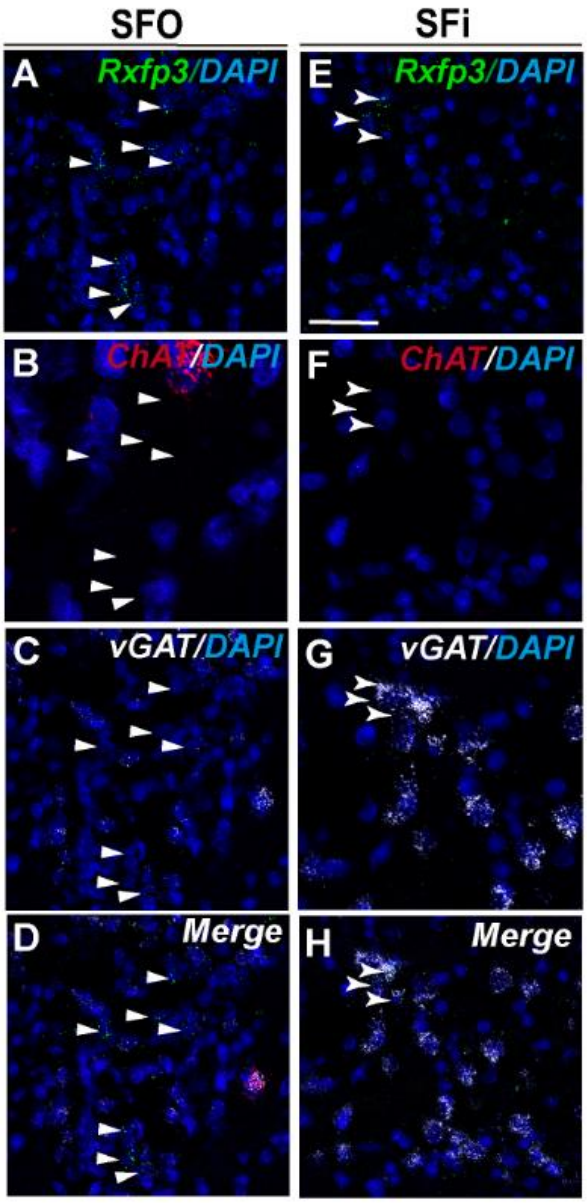


**Figure 3.15**. High-magnification images illustrate the co-localization of *Rxfp3* **(A and E)**, *ChAT* **(B and F)**, *vGAT* **(C and G)** mRNA and merged signals **(D and F) in SFO and SFI at bregma -0.24mm**. Arrowheads indicate neurons double-labelled for *Rxfp3* and *vGAT* mRNA. No co-localization of *Rxfp3* and *ChAT* mRNA was observed (open arrowheads). Calibration bar in (**E**) 50 µm.

neurons/circuits and hippocampal interneurons via septohippocampal projections. Notably, independent studies have revealed a strong relaxin-3 innervation of the hippocampus and identified Rxfp3 mRNA expression by hippocampal GABA neurons in the rat (Ma S, Gundlach AL, unpublished data), consistent with direct actions of relaxin-3/RXFP3 signalling on these circuits. Therefore, further studies of the neurotransmitter and neurochemical phenotype of septal and hippocampal neurons that express Rxfp3 mRNA and

their precise functional roles are warranted in both normal adult rats and mice, and in models of neuropathology and cognitive and psychiatric disorders.

# 4

## Relaxin-3 agonist alters conspecific social recognition memory and increases ERK activation in specific amygdala nuclei.

## 4.1. Introduction

The capacity to identify and recall familiar conspecifics is crucial for appropriate social interaction and its absence is associated with impaired social abilities ranging from borderline personality disorder (Servan et al. 2017), schizophrenia (Davis et al. 2014; Green et al. 2015) and autism spectrum disorders (Happé and Conway 2016). Social identification of conspecifics is intimately related to social recognition memory (SRM), a key process underlying long-term, socially-related behaviours, including pair bonding, aggression and mating (Dantzer et al. 1987; Gheusi et al. 1994; Williams et al. 2006; Maski et al. 2015). The amygdala is responsible for recognition of emotional facial expressions in humans (Baxter and Murray 2002; Seymour and Dolan 2008; Vuilleumier and Sander 2008; Gupta et al. 2011; Bonnet et al. 2015; Benarroch 2015) and social relationship pair-bonding in humans and rodents (Gobrogge et al. 2009; Hurlemann et al. 2010).

In rodents, conspecifics are recognized by olfactory information entering the amygdala from the main and accessory olfactory bulbs (Scalia and Winans 1975; Ferguson et al. 2001; Pro-Sistiaga et al. 2007; Trainor et al. 2010). Within the amygdala, the medial (MeA) nuclei and the bed nucleus of the stria terminalis (ST)[1], process social cues (Alheid et al. 1998; Rasia-Filho et al. 2000; Alheid 2006; Pereira et al. 2013; Fox et al. 2015). and, in turn, send projections to the hypothalamus (Hatalski et al. 1998; Smith and Vale 2006; Veenema 2008) and hippocampus (Hitti and Siegelbaum 2014; Okuyama et al. 2016). Ascending monoaminergic projections from neuros located in the brainstem also modulate several aspects of social behaviour (Korzan et al. 2001; Arakawa 2017).

In a similar fashion, neurons at the nucleus incertus (NI), located in the pontine tegmentum innervates the amygdala and other regions involved in

[1] The bed nucleus of the stria terminalis has been previously abbreviated as BNST, BST or ST. However, when describing subdivisions of the area, the abbreviations become long and less useful. Thus, in the 7th Edition of The Rat Brain in Stereotaxic Coordinates, the whole bed nucleus of the stria terminalis was abbreviated as ST (Olucha-Bordonau et al. 2014; Paxinos and Watson 2014).

social behaviour (Olucha-Bordonau et al. 2003; Ryan et al. 2011; Santos et al. 2016). The NI is characterised by GABA neurons which coexpress relaxin-3 (RLN3), a member of the insulin/relaxin superfamily (Bathgate et al. 2002; Burazin et al. 2002; Ma et al. 2007; Ma et al. 2017). The impact of NI GABA/ RLN3 systems on amygdala and extended amygdala-related behaviours has been described in different behavioural paradigms such as fear acquisition (Lee et al. 2014), extinction (Pereira et al. 2013), anxiety (Ryan et al. 2013a), feeding (Lenglos et al. 2014) and alcohol-seeking (Ryan et al. 2013b).

RLN3 is the cognate ligand of relaxin family peptide receptor 3 (RXFP3), which is a $G_{i/o}$-protein-coupled receptor (Bathgate et al. 2002; Liu et al. 2003). Recent studies indicate that RXFP3 activation predominantly produces hyperpolarization of RXFP3 mRNA-positive neurons in rat brain slices, including magnocellular and parvocellular oxytocin neurons (Blasiak et al. 2013; Kania et al. 2017) consistent with the inhibition of adenylate cyclase and reduced cellular cAMP levels associated with $G_{i/o}$-coupled receptor activation in cell-based systems (Liu et al. 2003; Halls et al. 2007). RXFP3 activation rapidly activates cellular externally-regulated kinases (ERKs) *in vitro* (Van der Westhuizen et al. 2007; Van der Westhuizen et al. 2010; Kocan et al. 2014); and in vivo, intracerebroventricular (icv) RXFP3 agonist injection produced increased levels of phosphorylated ERK (pERK) in the rat medial septal cholinergic neurons (Albert-Gascó et al. 2017). However, this specific effect is thought to be indirect, as septal and diagonal band cholinergic neurons have been confirmed to be RXFP3 mRNA-negative (Albert-Gascó et al. 2018). Nonetheless, altered pERK levels in the amygdala have been associated with social interaction behaviour (Richter et al. 2005; Peng et al. 2010; Giese and Mizuno 2013) and changes in pERK levels have been used to assess brain activity changes underlying behavioural social deficits (Faridar et al. 2014).

We hypothesized that RXFP3 activation might modulate social recognition and/or recall of social recognition memory. Thus, we have examined the effects of icv infusion of the RXFP3 agonist, RXFP3-A2 (Shabanpoor et al. 2012; Zhang et al. 2015), on social discrimination performance in the 3-chamber paradigm and levels of pERK in the extended amygdala. Subsequently, we studied the relationship between behavioural responses and the occurrence of

pERK immunoreactivity in RXFP3 mRNA-expressing neurons. In addition, we investigated the anatomical association of RLN3-positive nerve fibres with activated neurons in the amygdala, reflected by neuronal pERK immunostaining. Finally, we assessed the neurochemical phenotype of RXFP3 mRNA-positive neurons in the extended amygdala by assessing relative co-expression of RXFP3 mRNA with vesicular GABA-transporter (SlC32a1) and oxytocin receptor (Oxtr) mRNA. Overall, our findings suggest a role for RLN3/RXFP3 signalling in modulating social memory, which might occur via rapid alterations in pERK and related signalling in GABAergic and Oxtr-positive neurons within specific regions of the extended amygdala.

## 4.2. Material and Methods

### 4.2.1. Animals and surgical procedures

The Ethics Committee of the University Jaume I approved all procedures (#2015/VSC/PEA/00091). Male Wistar rats (300-380g) were maintained on a 12-12 h light-dark cycle with lights on at 0700h GMT and behavioural procedures conducted between 10.00 and 12.00h GMT.

For surgical procedures, rats were anesthetised with ketamine (Imalgene 25 mg/kg i.p., Merial-Laboratories-SA, Barcelona, Spain) and xylazine (10 mg/kg i.p., X1251 Sigma-Aldrich, St Louis, MO, USA). Then, a cannula was implanted at stereotaxic coordinates AP 0.48mm, ML 0.1mm, DV -4mm from bregma (Paxinos and Watson 2014) and assessed with a screw attached to the skull.

### 4.2.2. Experimental groups

In this study, six experimental treatment groups were used. Except for rats in the naïve group, all subjects had a cannula targeting the right lateral cerebral ventricle implanted. One week after surgery, 1 µl of either artificial cerebrospinal fluid (aCSF; add molarity of constituents) or 5 µg/µl of RXFP3-A2 agonist solution (Shabanpoor et al. 2012) was infused at a rate of 0.5 µl/min, using a Harvard syringe injector (Harvard PHD2000 Syringe Pump; Harvard Apparatus, Holliston, MA, USA). [RXFP3-A2 agonist [R3A(11–24, C15 → A)B]

was kindly supplied by Dr M Akhter Hossain (The Florey Institute of Neuroscience and Mental Health, Parkville, Australia).

The agonist infused groups include: the RXFP3-A2-20 (*A2-20*) and RXFP3-A2-90 (*A2-90*) that were sacrificed 20 and 90 min respectively after peptide infusion for immunoblots and did not undergo behavioural test. The RXFP3-A2-Pref (*A2-Pref*) and RXFP3-A2-Soc (*A2-Soc*) groups underwent the 3-chamber social interaction behavioural test, and were sacrificed 20 and 90 min after peptide infusion, respectively (**Fig 4.1a**).

### 4.2.3. Three Chamber social interaction and memory test task

All rats were handled daily during the week after surgery. On the day of the behavioural test, rats habituated to the behavioural room for 30 before the vehicle or peptide infusions 20 min prior to each trial. The behavioural test was conducted in a three-chamber apparatus. Each chamber measured 22 × 39 × 40 cm. On the first trial, following a 5 min habituation, each rat was allowed to explore either a conspecific or an inanimate object for 10 min ('Sociability Test'). After a 1h inter-trial period, the 'Preference Test' was conducted in which rats could choose to explore a familiar conspecific (from the sociability test) or a novel one, for 10 min. Chambers in which the novel (stranger) rats or objects were placed were balanced in all experiments**.** Behavioural was analysed using video tracking (**Fig 4.2A and B)**. Rats were sacrificed immediately after the preference test. Data were expressed as either "sociability index", which was calculated as the time sniffing the subject minus the time sniffing the object (*sociability test*), or the "preference index", time sniffing the novel conspecific minus the time sniffing the familiar conspecific (*preference test*). Data were analysed by one way-ANOVA followed by a Bonferroni *post-hoc* test.

### 4.2.4. Immunoblotting

In western blot studies, pERK levels were assessed (as previously described (Albert-Gascó et al. 2017). Briefly, after sacrifice, brains were removed and deep frozen The amygdala was dissected using 1 mm diameter disposable biopsy punches (Interna Miltex, Ratingen, Germany) from 20 µm brain slices cut using a cryostat at -15ºC Tissue was lysed and equal amounts of protein were loaded onto a PAGE andtransferred to Immobilon-P membranes (MERCK

Millipore, Darmstadt Germany).primary antibodies: anti-pERK antibody (E-4) (Santa Cruz Biotechnology sc-7383, Santa Cruz, CA, USA; 1:500) and anti-ERK (Santa Cruz Biotechnology, Santa Cruz, CA, USA; 1:1,000), used.. Bands were developed using enhanced chemiluminescence (BioRad, Hercules CA, USA) and digital images were captured with a charge-coupled device imager (IMAGEQUANT LASc 4000, GE Healthcare Little Chalfont, UK and quantified with ImageJ blots toolkit software (National Institutes of Health, Baltimore, MD, USA). Data were expressed as the pERK/ERK ratio for each treatment relative to that of the naïve rat group and analysed by one way-ANOVA followed by Bonferroni *post-hoc* test.

### 4.2.5. Immunohistochemistry and Immunofluorescence stainings

Immunohistochemistry and immunofluorescence analysis were performed as descibried (Albert-Gascó et al. 2017). Briefly, RXFP3-A2 and naïve groups (n = 6-8/group) were euthanized with sodium pentobarbital (120 mg/kg, Eutanax, Fatro, Barcelona, Spain) and transcardially perfused for 30 min. Brains were then removed and immersed in fixative for 4 h at 4ºC, Subsequently, brains were cryoprotected in 30% sucrose in 0.01 M phosphate-buffered saline p H7.4 for 3 days.

Coronal sections (40 µm) from bregma 0.36 mm to -3.6 mm(Paxinos and Watson 2014) were obtained using a freezing slide microtome (Leica SM2010R, Heidelberg, Germany) and stored in sucrose-PBS. After incubation in blocking solution (10% NGS, in 0.1 M PBS, 0.3% Triton X-100, pH 7.6) primary antibody rabbit anti-phospho-MAPK/ERK (#9101 Cell Signalling, Danvers, MA, USA; 1:200) and mouse anti-RLN3 RLN3 (Tanaka et al. 2005; 1:5) in blocking solution was incubated overnight at room temperature.

For immunochemistry of pERK, after several rinses in PBS, sections were incubated for 1 h in 1:200 biotinylated goat anti-rabbit secondary antibody (Jackson Immunoresearch, 111-065-003), rinsed and transferred to avidin-biotin complex (Vectastain-Elite, Cat No. PK-6100; Vector Laboratories, Burlingame, CA, USA). Labelling was visualised with 0.025% DAB, 0.0024% $H_2O_2$ in Tris-HCl buffer, pH 7.6. After final washes, sections were mounted, air-dried, dehydrated and coverslipped with DPX (Sigma-Aldrich). The quantification of pERK-positive neurons was conducted using ImageJ (National

Institutes of Health). Data are expressed as the number of pERK-positive neurons/area and normalised to values observed in vehicle rats.

Double-staining immunofluorescence, was completed as described (Albert-Gascó et al. 2017). Briefly, sections were incubated with primary antisera and then with goat anti-rabbit Cy3 and goat anti-mouse Alexa Fluor 488 (Jackson Immunoresearch; #111-165-003+115-545-003). Following further rinsing, sections were mounted on slides and coverslipped using Fluoromount-G (#0100-01, Southern Biotech, Birmingham, AL, USA).

### 4.2.6. Multiplex in situ hybridization

In studies to evaluate ERK activation in RXFP3 mRNA-positive neurons, we combined detection of pERK immunofluorescence with *in situ* hybridization (ISH) detection of *Rxfp3* mRNA-positive neurons, using multiplex ISH (RNAscope™; Advanced Cell Diagnostics (ACD); Newark, CA, USA). After behavioural testing, rats were transcardially perfused, as described (Albert-Gascó et al. 2017).

After 18 h post-fixation at 4ºC, brain sections (30 µm) were collected using a vibratome (Leica VT 1200S, Wetzlar Germany) and transferred to a cryprotectant medium (30% ethylene glycol, 30% glycerol in phosphate buffer, pH 7.4) and stored at -20ºC.

For the detection of *Rxfp3* mRNA, standard probes covered ~1000 bp of the target mRNA. Sections were mounted onto Superfrost Plus Slides (Fisher Thermo Scientific, Hampton, NH, USA, Cat#12-550-15) and air dried. The next day, sections were fixed in 4% paraformaldehyde for 10 min at 4ºC, and rinsed in PBS. Once dry, a hydrophobic barrier was drawn around the sections (ImmEdge hydrophobic PAP pen, Vector Laboratories, #310018). Sections were incubated with protease pretreatment-4 (ACD, Cat #322340) for 30 min at 40ºC. After a distilled water rinse, sections were incubated for 2 h at 40ºC with *Rxfp3* mRNA probe (ACD, #316181). Following incubation, sections were rinsed with wash buffer (ACD, #310091) and the signal was amplified with ACD amplifier reagents. After several rinses in wash buffer and PBS, sections were incubated for immunofluorescence against pERK as above, with anti-phospho-

MAPK/ERK (Cell Signaling 1:50) for 90 min at room temperature and Cy3 goat anti-rabbit IgG for 30 min.

The neurochemical phenotype of *Rxfp3* mRNA-expressing neurons was assessed using multiplex ISH (RNAscope, ACD) using probes targeting *Rxfp3* (ACD, #316181), *Oxtr* (#483671), *Slc32a1* (#415681) mRNAs as described (Albert-Gascó et al. 2018).

### 4.2.7. Confocal analysis

Confocal analysis was performed as described (Albert-Gascó et al. 2017). Briefly, immunofluorescence images were captured with a Leica DMi8 inverted microscope (Leica Microsystems) at 0.3 µm interval stacks. Immunofluorescent neurons were counted using ImageJ software (National Institutes of Health). Percentages of co-expression in brains from the A2-pref group were compared to the vehicle-treatment group, using a Mann-Whitney test (n= 4).

Similarly, ISH images were obtained using an LSM 780 Zeiss Axio Imager 2 confocal laser-scanning microscope (Carl Zeiss AG, Jena, Germany). This system is equipped with a stitching stage, and Zen software (Carl Zeiss AG) was used to stitch tiled images taken with a 20× objective or 40× objective. Quantification of co-expression (1 section per level and per rat) was conducted manually using Fiji (Schindelin et al. 2012) with labelling with each probe counted separately, relative to DAPI-stained nuclei, to avoid bias.

## 4.3. Results

### 4.3.1. Icv RXFP3-A2 infusion impaired social recognition memory.

Previous studies have described robust effects of icv infusion of RXFP3 agonist within 20 min post–infusion (Ryan et al. 2013a; Albert-Gascó et al. 2017; de Ávila et al. 2018). Thus, we designed a schedule in which icv infusion of the agonist or vehicle was administered 20 min prior to the social or preference tests.

RXFP3 agonist treatment did not alter responses in the *sociability test*, as all groups of rats spent 78.4% ± 2.6% min sniffing the conspecific rat **(Fig 4.2C)**.

Sociability index was not significantly different across all groups ($F_{2,23}$ = 0.30; p = 0.74, **Fig 4.1B)**].

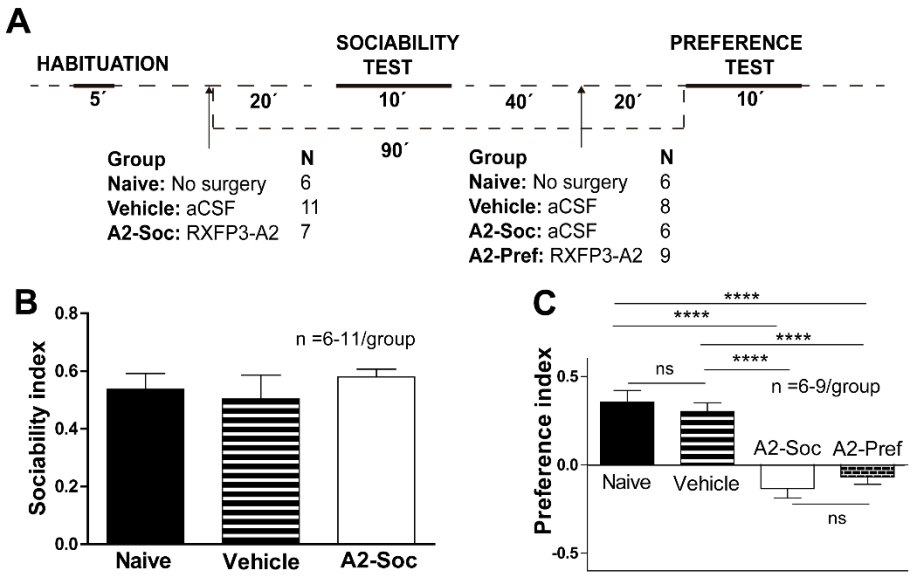


**Figure 4.1. Social recognition memory is impaired after Rxfp3-A2 infusion**. The 3-chamber social interaction and memory test scheme with Sociability test **(A)** Time scheme on the behavioural protocol indicating tests (solid lines), infusion points (red arrows) and time between tests (doted lines) **(B)** Preference index for sociability test; **(C)** Preference index for preference test. ns; non-significant *p < 0.05; ***p < 0.001; ****p<0.0001.

However, RXFP3 agonist infusion before the sociability test (A2-Soc) or the preference test (A2-Pref) significantly altered preference index, which was was positive for control groups (naïve: 0.35 ± 0.06, n = 6; vehicle: 0.33 ± 0.07, n = 5), whereas in A2-Pref (-0.14 ± 0.05, n = 5) and A2-Soc (-0.13 ± 0.06, n= 6) groups it was negative ($F_{3,21}$ = 19.14, p <0.0001; **Fig 4.1C**), indicating that agonist-treated rats had nor preference for novelty. This behaviour can be interpreted as a deficit in recalling the familiar rat. Control groups spent >60% duration exploring the novel conspecific, which is indicative of social memory of the familiar rat and preference to explore the novel rat. In contrast, rats with agonist treatment spent a significantly longer time exploring the familiar rat **(Fig 4.1C and 4.2D)**. However, the time exploring the familiar rat was not longer than 60%, of total therefore a particular bonding to the familiar was ruled out.

RXFP3-A2-treated rats did not display increased locomotor activity compared to control groups (data not shown).

### 4.3.2. Icv RXFP3 agonist (RXFP3-A2) infusion rapidly increased ERK phosphorylation in amygdala.

Using western immunoblotting, we quantified ERK and pERK levels in amygdala tissue extracts from rats sacrificed 20 and 90 min after RXFP3-A2 or aCSF infusions, and from naïve, untreated rats (**Fig 4.3)**. All data followed a normal distribution according to a Shapiro-Wilk normality test. When compared to naïve rats (1.00 ± 0.07, n = 8), rats receiving an aCSF infusion 20 min before perfusion did not display a significant increase in pERK (1.20 ± 0.08, n = 8). In contrast, rats that received RXFP3 agonist infusion (A2-20) displayed a significant increase of pERK levels (1.79 ± 0.2, n = 7) compared to naïve and aCSF-treated rats ($F_{2, 22}$ =10.29, p = 0.0008; **Fig 4.3A and B**). However, rats treated with the agonist 90 min prior to perfusion (A2-90) displayed a similar pERK/ERK ratio to naïve and aCSF-treated rats (0.9 ± 0.02, n = 5; $F_{2,14}$ = 1.00, p = 0.39; **Fig 4.3C and D**).

### 4.3.3. RXFP3-A2 infusion icv increased ERK activation in discrete amygdaloid nuclei after the three-chamber social interaction and memory test.

We assessed the effect of icv RXFP3-A2 infusion on pERK levels in specific amygdaloid nuclei after the three-chamber social interaction test (**Table 4.1**).

For analysis purposes, we considered the amygdala in two parts: the rostral extension containing the bed nucleus of the stria terminalis (ST), and the temporal extension containing the medial amygdala (MeA) (Olucha-Bordonau et al. 2014). Within the MeA (**Fig 4.4A)**, significantly increased pERK **(Fig 4.4B)** was observed in the anterior dorsal part (MeAD) of the A2-Pref group (190 ± 28.0%, n = 6) compared to the vehicle-treated (100 ±

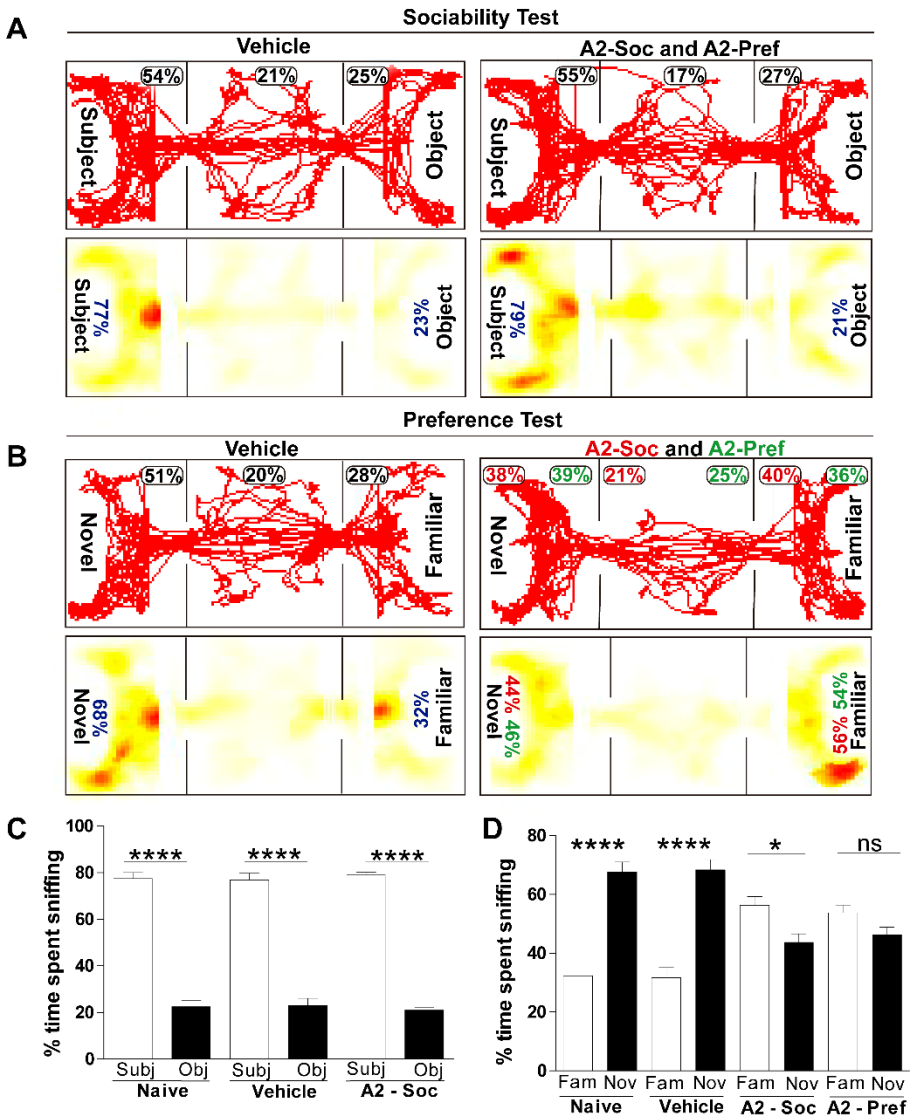


**Figure 4.2**. (**A**) Sociability Test Three-room chamber social interaction paradigm tracking (up) and activity map (down, white: low activity; red: high activity) for all experimental groups. (**B**) Preference Test Three-room chamber social interaction paradigm tracking (up) and activity map (down) for all experimental groups. (**C**) Percentage time sniffing the conspecific subject (white bars) and inanimate object (black bars). (**C**) Percentage time sniffing familiar subjects (whiter bars) and the novel subject (black). * p<0.05, **** p<0.0001, ns: non-significant.

15.4%, n = 6) and A2-Soc (101 ± 21.5%, n = 5) groups ($F_{2,16} = 5.49$, p = 0.017; **Fig 4.4C-E**). Similarly, significantly increased pERK was observed in the posterior ventral part (MePV) of the A2-Pref group (177.3 ± 18.9%, n = 8)

compared to the vehicle-treated ($F_{2,18}$ = 4.07, p =0.037) relative to vehicle (100 ± 19.4%, n = 6) and A2-Soc (133.4 ± 22.29%, n = 6) groups (**Fig 4.4F-H).** All other regions did not exhibit significant differences in pERK across groups (**Table 4.1**).

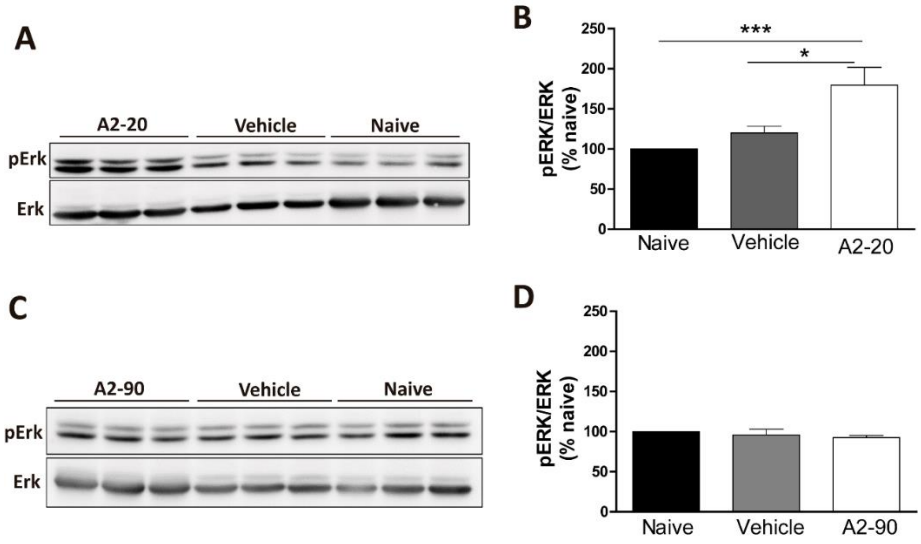


**Figure 4.3** pERK is increased in amygdala after agonist infusion. pERK/ERK detection by Western blot 20 min (**A, B**) and 90 min (**C, D**) after icv infusion of RXFP3-A2 (~1 nmol) (white bars), aCSF vehicle (grey bars) and in time matched naïve rats (black bars). Rats sacrificed 20 min after agonist infusion displayed an increased ERK activation in the amygdala area compared to vehicle and naïve rats (**A, B**). Conversely, rats sacrificed 90 min after infusion did not display an increase ERK activation when compared between the groups (**C, D**). *p < 0.05; ***p < 0.001.

In the ST (**Fig 4.5A)**, the A2-Pref group had significantly higher density of pERK-positive neurons in the ventral part (STMV) (275 ± 27.2, n = 8; **Fig 4.5B)** compared to A2-Soc (196 ± 49.0, n = 5) and vehicle (100 ± 21.9, n = 6) groups ($F_{2,18}$ = 8.10, p = 0.04; **Fig 4.5C-E**). The A2-Pref group also displayed a significantly increased density of pERK- neurons in the oval nucleus (STOV) (198 ± 29.0, n = 5) compared to the vehicle (100 ± 10.7, n = 5) and A2-Pref (118.5 ± 8.50, n = 5) groups ($F_{2,11}$ = 6.10, p = 0.02; **Fig 4.5F-H**).

Using dual immunofluorescence to pERK and RLN3 we demostrated close contacts between RLN3 fibres and pERK positive cells in the A2-Pref group in the MeAD, MePV (**Fig 4.4I-J'**) and in the STMV (**Fig 4.5J--J')**.

Densities of pERK-immunopositive neurons followed a normal distribution according to a Shapiro-Wilk normality test.

**Table 4.1** pERK density in the different areas analysed relative to vehicle

| Brain area | bregma (mm) | Vehicle | RXFP3-A2-Pref | RXFP3-A2-Soc | P value |
|---|---|---|---|---|---|
| STMA | 0.84 to -0.12 | 100 ± 18.45 | 136 ± 13.08 | 101 ± 7.9 | 0.078 |
| STMV | 0.36 to -0.36 | 100 ± 21.93 | 275 ± 27.21 | 196 ± 48.99 | **0.0037** |
| OV | 0.24 to -0.24 | 100 ± 10.67 | 198.8 ± 28.96 | 118.5 ± 8.5 | **0.0212** |
| MeAV | -1.8 to -2.52 | 100 ± 23.64 | 85.1 ± 11.21 | 161 ± 44.55 | 0.2066 |
| MeAD | -1.8 to -2.4 | 100 ± 15.39 | 190 ± 27.98 | 100.6 ± 21.53 | **0.0174** |
| MePV | -2.64 to-3.6 | 100 ± 19.41 | 177.3 ± 18.87 | 133.4 ± 22.3 | **0.0372** |
| MePD | -2.52 to -3.48 | 100 ± 13.02 | 146 ± 20.66 | 122 ± 17.36 | 0.2039 |
| CeA | -1.56 to -3.36 | 100 ± 13.26 | 197 ± 22.47 | 110 ± 17.09 | **0.0031** |
| BLA | -1.72 to -3.12 | 100 ± 13.98 | 89.29 ± 12.11 | 75 ± 2.8 | 0.3785 |

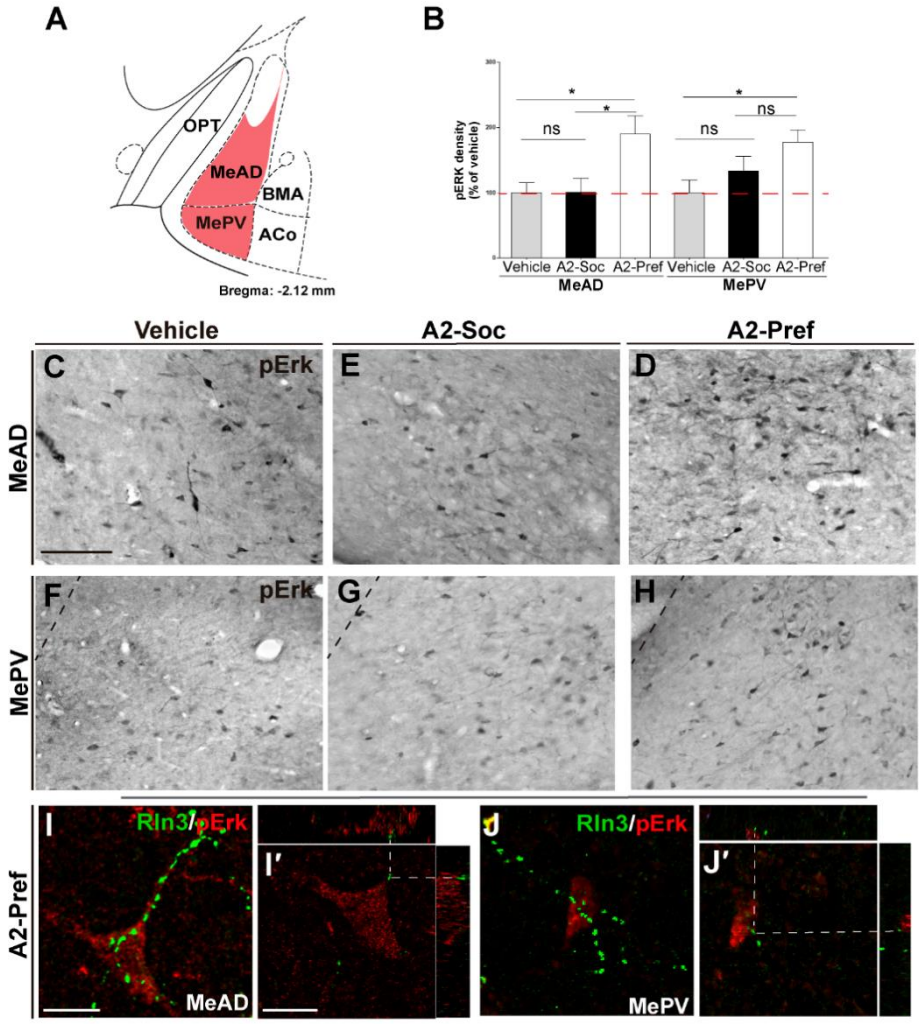


**Figure 4.4.** p**ERK in MeA after social encounters**. **(A)** Amygdala subunclei analyzed. (**B**) pERK positive cells were increased significantly in A2-Pref rats compared to vehicle (red line). Representative images of pERK in MeAD **(C);** vehicle **(D)** A2-Pref and (E) A2-Soc**.** pERK in MePV **(F)** vehicle **(G)** A2-Pref and (H) A2-Soc. RLN3 fibers contacting pERK positive neurons in A2-Pref in (I) MeAD and (I´) Single plane contact. (J) MePV and (J´) single plane contact. *p < 0.05; **p < 0.01. Scale bar: 10 μm (I′,J′).

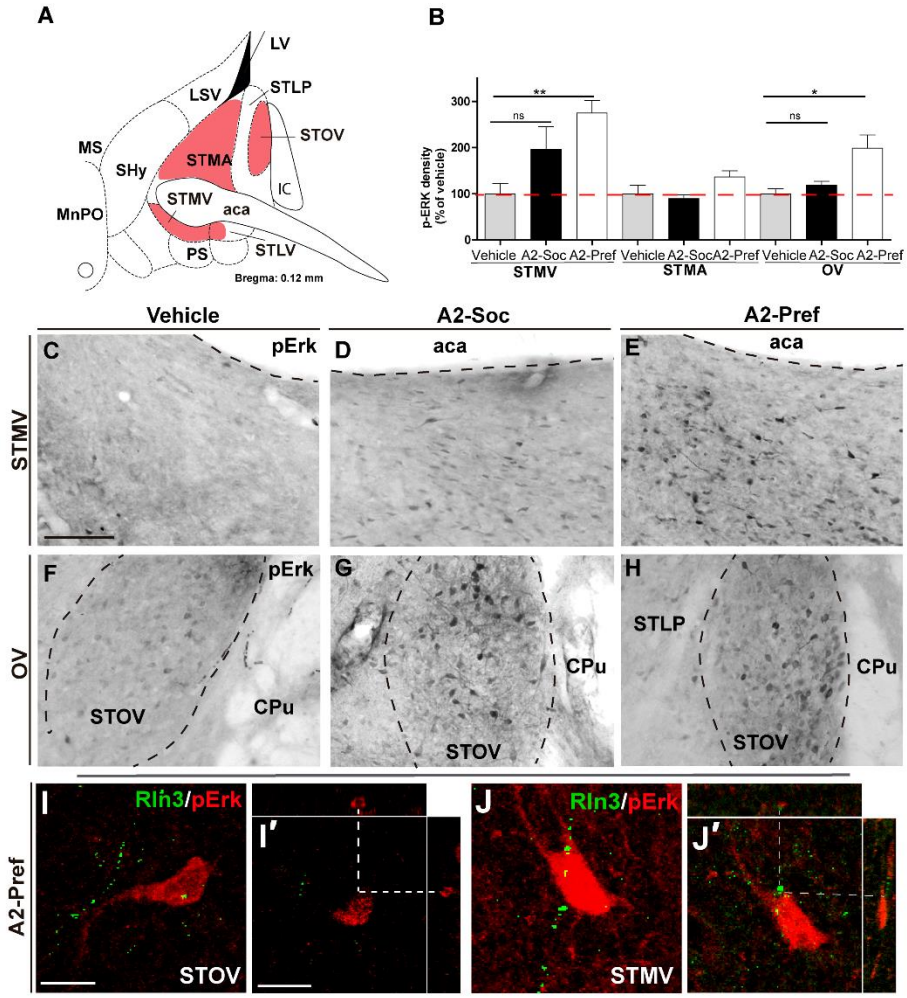


**Figure 4.5 pERK in extended amygdala after social encounters**. **(A)** Amygdala subunclei analyzed. (**B**) pERK positive cells were increased significantly in A2-Pref rats compared to vehicle (red line). Representative images of pERK in STMV **(C);** vehicle **(D)** A2-Pref and (E) A2-Soc**.** pERK in OV **(F)** vehicle **(G)** A2-Pref and (H) A2-Soc. RLN3 fibers contacting pERK positive neurons in A2-Pref in (I) STMV and (I´) Single plane contact. (J) OV and (J´) single plane contact. *p < 0.05; **p < 0.01. Scale bar: 10 µm (I′,J′).

### 4.3.4. Rxfp3 mRNA-positive neurons in the amygdala display increased pERK immunoreactivity after three-chamber social interaction testing

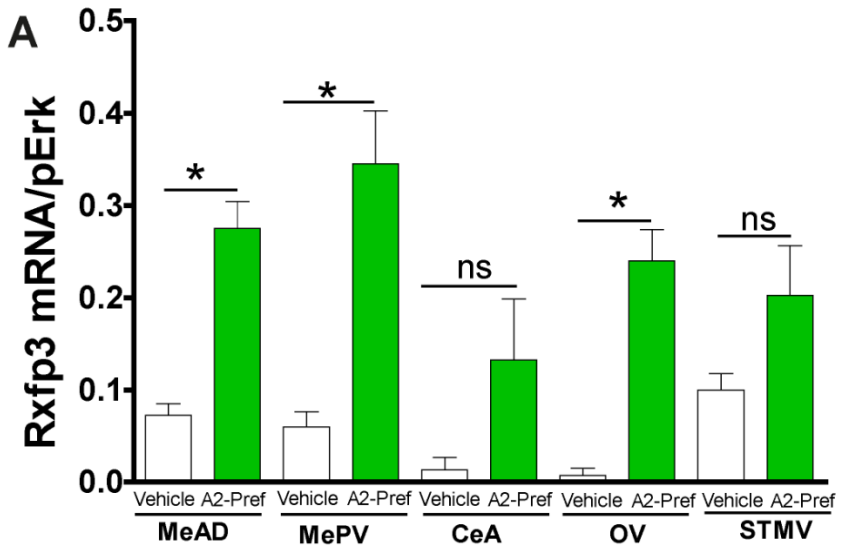


**Figure 4.6.** Ratio colocalization of Rxfp3 mRNA positive neurons with pERK positive neurons after a three chamber social interaction behavioural test in MeAD, MePV, CeA, OV and STMV. *p < 0.05; ns: non-significant.

We conducted the three-chamber social interaction test in a separate cohort of rats and assessed co-expression of of *Rxfp3* mRNA and pERK immunofluorescence. In the MeA the density of *Rxfp3* mRNA- and pERK immuno-positive neurons, was significantly higher in the A2-pref group than in the vehicle group, in both the MeAD (27.5 ± 2.91% A2-pref versus 7.25 ± 1.25% vehicle; n = 4; p < 0.05; **Fig. 4.6 and 4.7A –B´´)**, and the MePV (34.5 ± 5.7% A2-pref versus 6.75 ± 1.8% vehicle; n = 4; p < 0.05**; Fig. 4.6 and 4.8 A –B´´**).

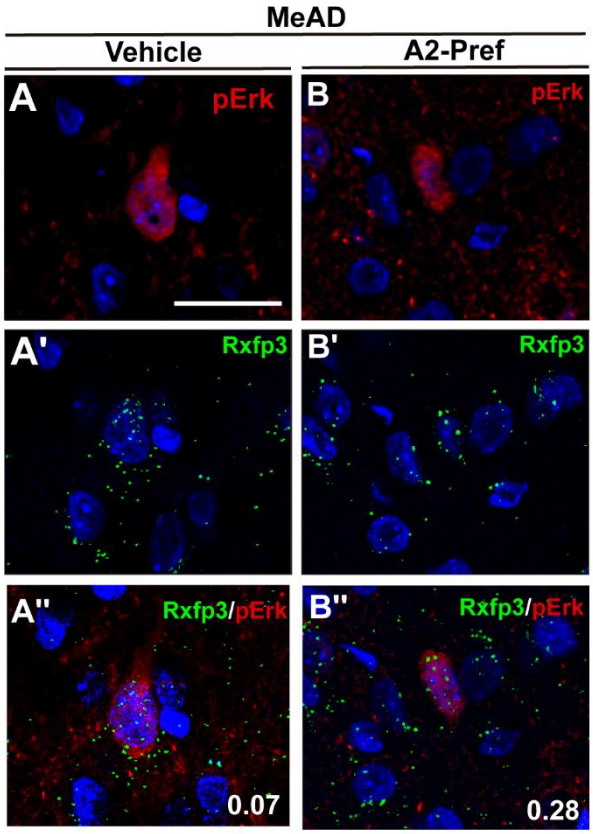


**Figure 4.7**.Colocalization with separated channels showing pERK **(A and B)**, Rxfp3 **(A´ and B´)** and the merge signal **(A´ and B´)** with DAPI for A2-pref and vehicle groups at MeAD. On the merge signal colocalization percentage are shown for each experimental group.Scale bar at (A) 25µm

Analysis of co-expression of *Rxfp3* mRNA and pERK immunolabelling in the OV detected a significant increase in the A2-pref group compared to the vehicle group (29.5 ± 0.96% versus 1.5 ± 1.5%; n = 4; p < 0.05;**Fig 4.6 and 4.8A-B´´)**. ). In contrast, although an increased density of pERK immunopositive neurons was observed in the STMV, co-expression of pERK and *Rxfp3* mRNA was not significantly different between these groups (A2-pref, 20.25 ± 5.41%; vehicle, 10 ± 1.8%; n = 4; p = 0.25; **Fig 4.6 and 4.8C-D´´**).

### 4.3.5. Characterisation of *Rxfp3* mRNA-expressing neurons in amygdala

Multiplex ISH was used to characterize key aspects of the neurochemical phenotype of *Rxfp3* mRNA-expressing neurons. In the temporal extended amygdala, expression of *Rxfp3*, *Oxtr* and *Slc32a1* mRNA was examined (**Table** 4.**2**). In the MeAD, ~78% of the *Rxfp3* mRNA-expressing neurons were *Slc32a1* mRNA-positive (GABAergic) (**Fig 4.10A-D and E)** 5% were *Oxtr* mRNA positive and ~12% were positive for *Oxtr* and *Slc32a1* mRNA

(**Fig 4.10F).** Only ~5% of *Rxfp3* mRNA-expressing neurons were negative for the other mRNA species. **(Fig 4.10B)**.

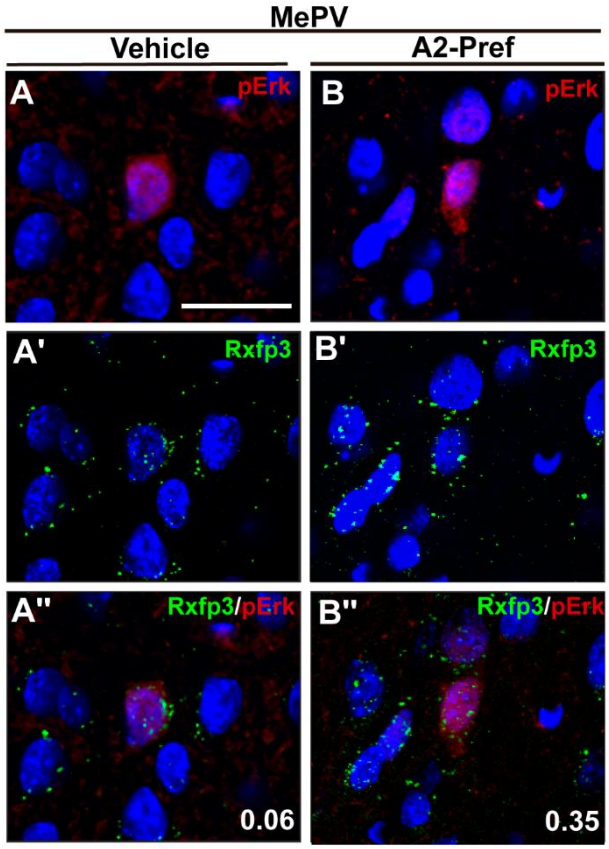


**Figure 4.8**.Colocalization with separated channels showing pERK **(A and B)**, Rxfp3 **(A´ and B´)** and the merge signal **(A´ and B´)** with DAPI for A2-pref and vehicle groups at MePV. On the merge signal colocalization ratio are shown for each experimental group. Scale bar at (A) 25µm

In the MePV, 36% of *Rxfp3* mRNA-expressing neurons were *Slc32a1* mRNA-positive (GABAergic) (**Fig 4.11A-D and E**), ~20% were *Oxtr* mRNA-positive (**Fig 4.11C)**, and 11% expressed all three mRNA species (**Fig 4.11F**). Furthermore, ~44% of *Rxfp3* mRNA-positive neurons expressed *Oxtr* mRNA **(Fig 4.12A-D and C)** (**Table 4.2**)

These data indicate that although a small proportion of *Rxfp3*-expressing neurons in the MeAD express *Oxtr*, this population is larger in the MePV, where ~31-44% of the *Rxfp3*-expressing neurons express *Oxtr*. Conversely, almost half the *Oxtr* expressing neurons in the MeAD expressed *Rxfp3*. Similarly, the percentage of *Oxtr*-expressing neurons that co-expressed *Rxfp3* in the MePV ranged from 42-69%, probably due to variation in the total number of *Rxfp3* expressing neurons (**Table 4.3**).

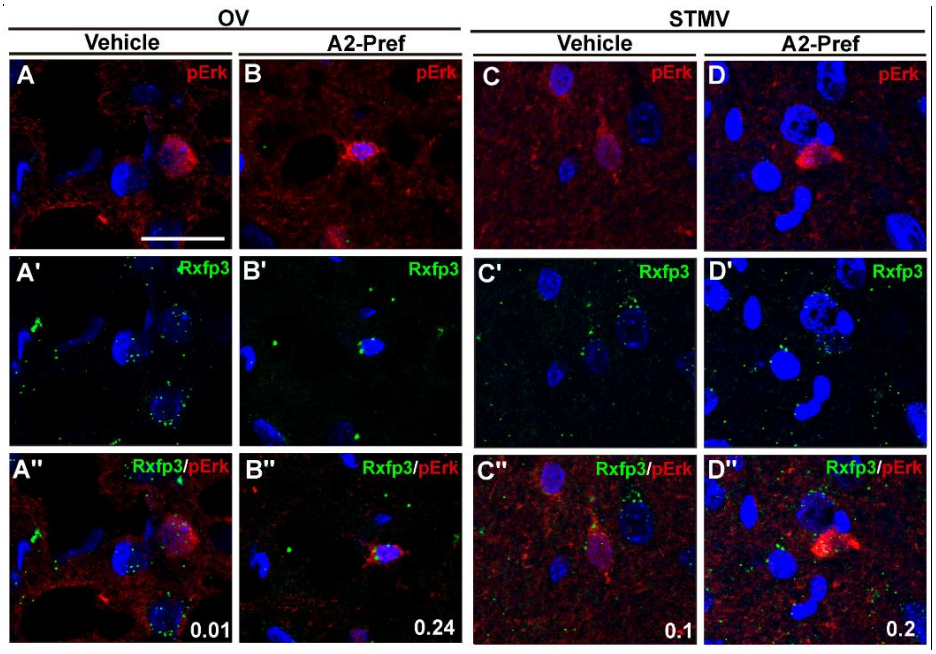


**Figure 4.9**.Colocalization with separated channels showing pERK **(A - D)**, Rxfp3 **(A´ - D´)** and the merge signal **(A´´ - D´´)** with DAPI for A2-pref and vehicle groups at OV and STMV. On the merge signal colocalization ratio are shown for each

In the OV, ~38% of *Rxfp3* mRNA-expressing neurons expressed *Oxtr* mRNA, (**Fig 4.13A-F**). Furthermore, ~95% of *Rxfp3* mRNA-positive neurons expressed Scl32a1 mRNA (i.e. GABAergic; **Table 2 and Supplementary Fig 9.1).**

In the STMV, ~43% of neurons co-expressed *Rxfp3* and *Oxtr* mRNA (**Fig 4.14A-F** and ~91% of these *Rxfp3* mRNA-positive neurons were *Slc32a1* mRNA-positive (**Table 2 and Supplementary Fig 9.1**). These data indicate a significant proportion of *Rxfp3* mRNA-positive neurons express *Oxtr* mRNA (38-43%), and ~89% of *Oxtr* mRNA-positive neurons in the OV and ~39% in the STMV express *Rxfp3* mRNA (**Table 4.3**).

**Table 4.2**. Proportion of Rxfp3 neurons that co-express different mRNA

| **MeAD** | | | | | |
|---|---|---|---|---|---|
| *Rxfp3-Oxtr-Slc32a1* | **Rxfp3/Oxtr** | **Rxfp3/Slc32a1** | **Triple** | **Rxfp3/-** | **Total Rxfp3** |
| | 5 | 85 | 13 | 6 | 111 |
| **MePV** | | | | | |
| *Rxfp3-Oxtr-Slc32a1* | **Rxfp3/Oxtr** | **Rxfp3/Slc32a1** | **Triple** | **Rxfp3/-** | **Total Rxfp3** |
| | 18 | 32 | 10 | 29 | 89 |
| *Rxfp3-Oxtr 1* | **Rxfp3/Oxtr** | | | **Rxfp3/-** | **Total Rxfp3** |
| | 44 | | | 55 | 99 |
| *Rxfp3-Oxtr 2* | **Rxfp3/Oxtr** | | | **Rxfp3/-** | **Total Rxfp3** |
| | 27 | | | 37 | 64 |
| **OV** | | | | | |
| Rxfp3-Oxtr | **Rxfp3/Oxtr** | | | **Rxfp3/-** | **Total Rxfp3** |
| | 29 | | | 29 | 76 |
| Rxfp3-Slc32a1 | **Rxfp3/Slc32a1** | | | **Rxfp3/-** | **Total Rxfp3** |
| | 118 | | | 6 | 124 |
| **STMV** | | | | | |
| Rxfp3-Oxtr | **Rxfp3/Oxtr** | | | **Rxfp3/-** | **Total Rxfp3** |
| | 17 | | | 13 | 30 |
| Rxfp3-Slc32a1 | **Rxfp3/Slc32a1** | | | **Rxfp3/-** | **Total Rxfp3** |
| | 30 | | | 3 | 33 |

## 4.4. Discussion

Social behaviour is characterised by a number of traits including social recognition, motivation and reward, and is governed by complex brain processes (Trezza et al. 2011; Pellissier et al. 2017). In this study, we demonstrate that activation of relaxin-3 receptor (RXFP3) signalling broadly throughout the forebrain impaired SRM of a familiar conspecific in adult male rats. We employed the truncated RXFP3 agonist, RXFP3-A2, which is selective for RXFP3 (Shabanpoor et al. 2012; Zhang et al. 2015); and has previously been administered icv to demonstrate RXFP3 influences on various modalities, including food intake (de Ávila et al. 2018), anxiety-like behaviour (Ryan et al. 2013b; Ma et al. 2017) and hippocampal-dependent spatial memory (Albert-Gascó et al. 2017).

Global RXFP3 activation decreased discrimination between novel and familiar conspecific rats, but did not alter social discrimination between subject and objects, as all experimental groups exhibited a similar preference to explore a conspecific rat rather than an inanimate object. Interestingly, RXFP3-A2 infusion prior to the sociability test also impaired social recognition memory at both 20 and 90 min post-infusion. A likely explanation for these findings is that RXPF3 signalling can inhibit memory formation when the agonist is present during the sociability test, and it can interfere with memory recall when present prior to and during the preference test. In both cases, RXFP3 agonist-treated rats were impaired during memory retrieval of familiar conspecifics, due to impaired memory formation and/or recall.

Complex brain circuitries are involved in SRM processes (Landgraf et al. 1995), and it is thought that the ventral CA1 is the primary repository or store for social-related memories (Okuyama et al. 2016). Amygdala nuclei and regions of ST are centrally involved in memory formation and in particular,

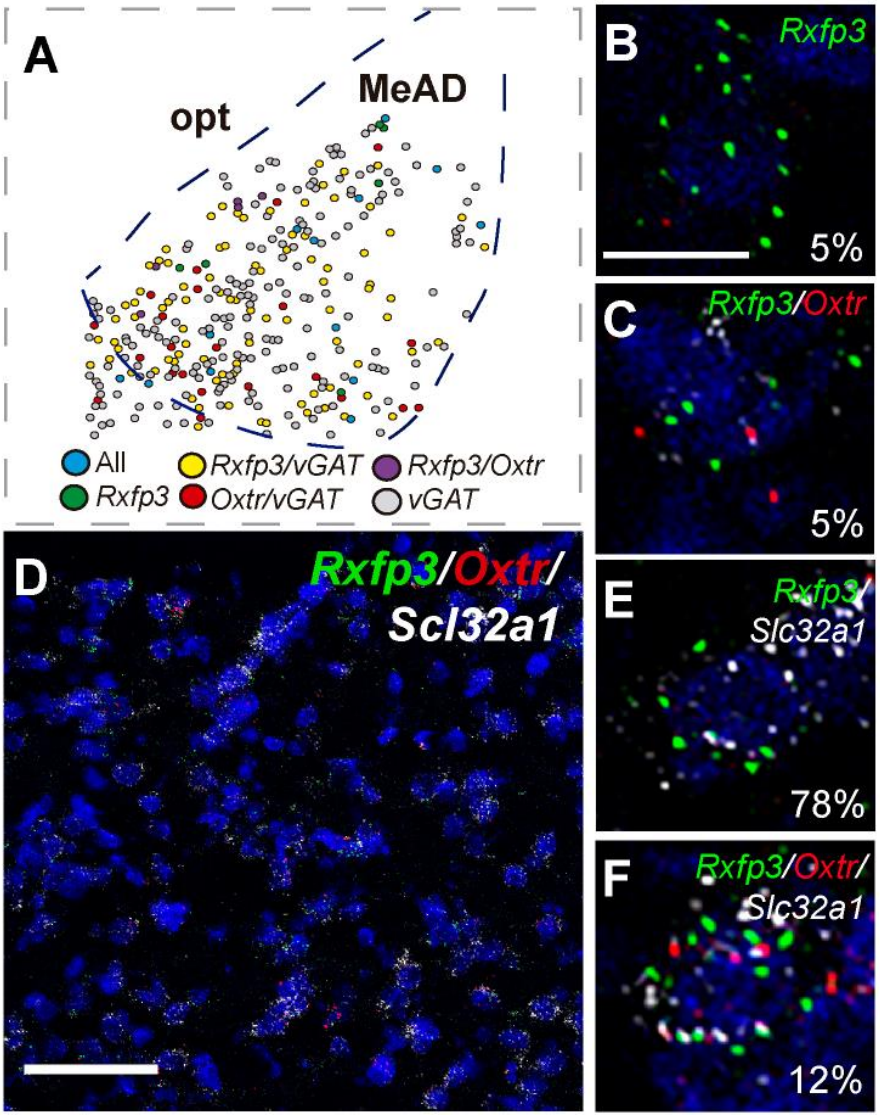


**Figure 4.10**. **Characterization and distribution of the *Rxfp3* mRNA positive neurons phenotype at the MeAD** (**A**) Schematic showing *Rxfp3* distribution and colocalization with *Oxtr and Slc32a1* mRNA in MeAD. (**D**) and representative images with quantification percentage of colocalization (**B**, **C, E and F**). Scale bar: 10µm (B), 100 µm (D).

the MeA has been strongly associated with SRM regulation (Ferguson et al. 2001; Lukas et al. 2013; Gur et al. 2014), as it receives direct projections from centers involved in social processing. The MeA is crucial for SRM as it receives direct projections from centres involved in social processing (Scalia and Winans 1975). Notably, this information is powerfully modulated by

vasopressin (Everts and Koolhaas 1997; Veenema 2008; Gobrogge et al. 2009) and oxytocin (OT) systems.

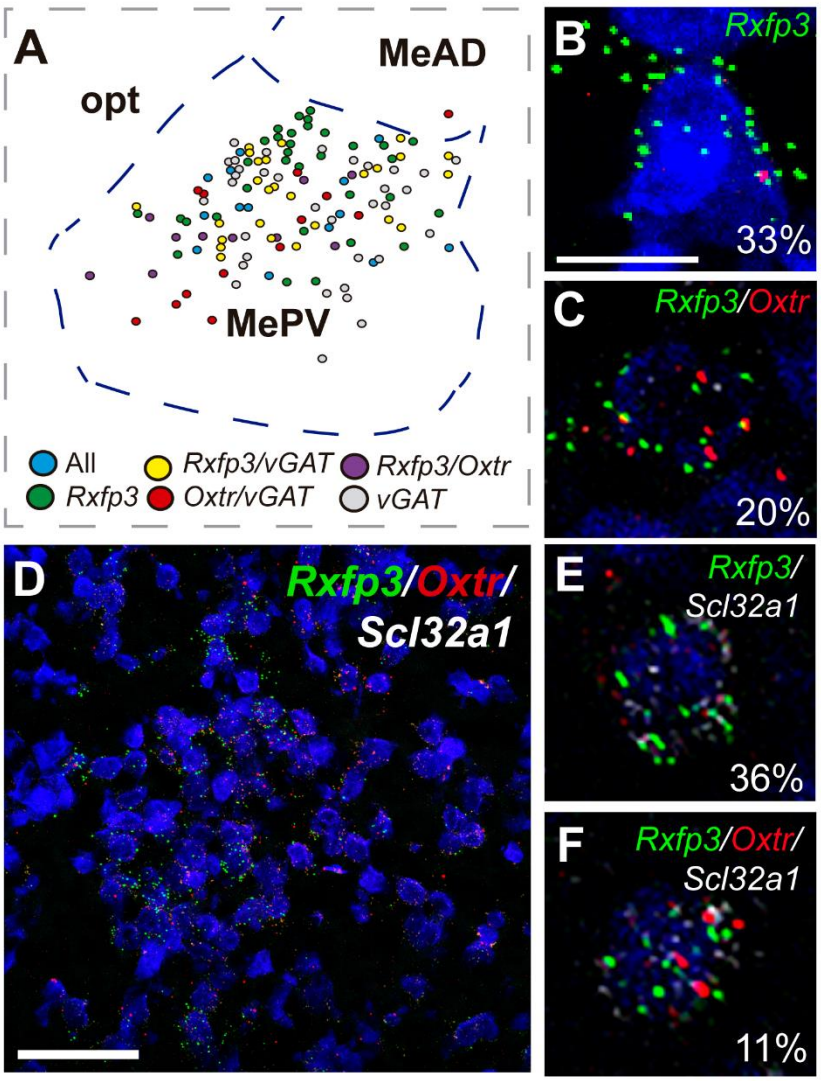


**Figure 4.11**. **Characterization and distribution of the *Rxfp3* mRNA positive neurons phenotype at the MePV** (**A**) Schematic showing *Rxfp3* distribution and colocalization with *Oxtr and Slc32a1* mRNA in MePV. (**D**) and representative images with quantification percentage of colocalization (**B**, **C, E and F**). Scale bar: 10µm (B), 100 µm (D).

For example, OT gene knockout mice exhibit impaired SRM, and local infusions of OT into the MeA rescued this social behaviour (Everts and Koolhaas 1997; Winslow et al. 2000; Ferguson et al. 2001; Choleris et al. 2007; Veenema 2008). Furthermore, OT gene knockout mice exhibit decreased c-

Fos expression in MeA, ST and medial preoptic area after a social interaction and memory test (Ferguson et al. 2001).

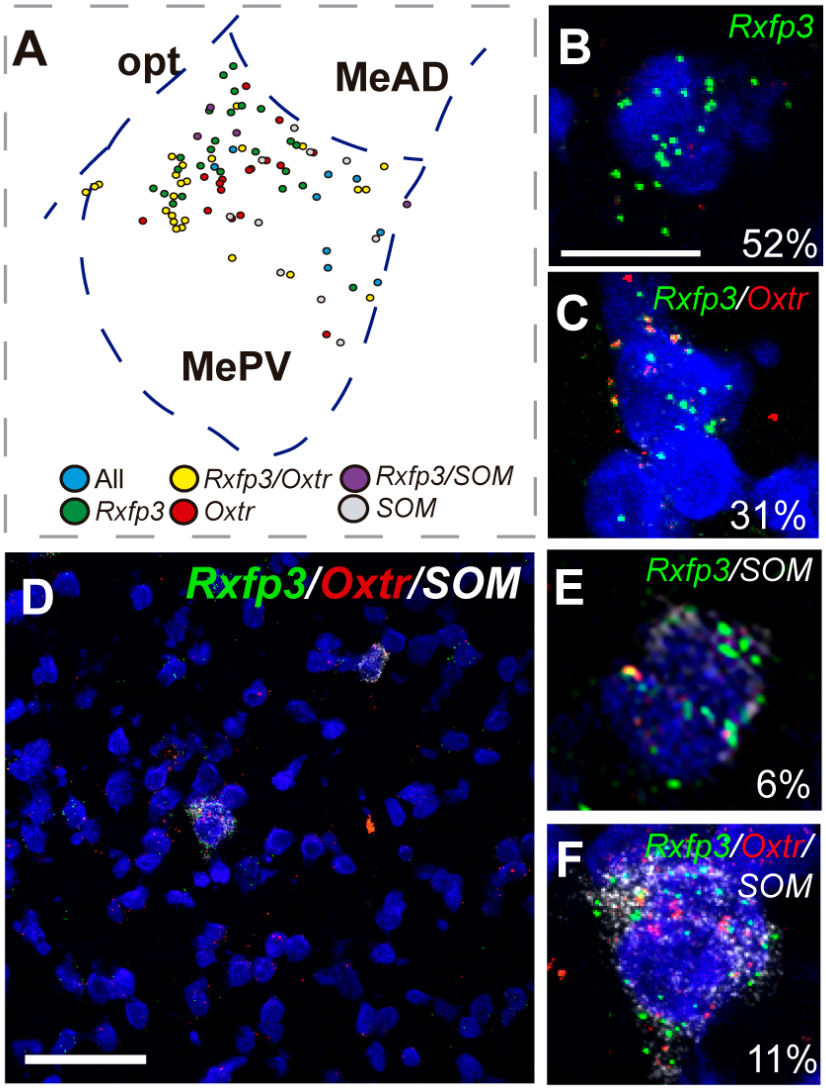


**Figure 4.12**. **Characterization and distribution of the *Rxfp3* mRNA positive neurons phenotype at the MePV** (**A**) Schematic showing *Rxfp3* distribution and colocalization with *oxtr and SOM* mRNA in MePV. (**D**) and representative images with quantification percentage of colocalization (**B**, **C, E and F**). Scale bar: 10µm (B), 100 µm (D).

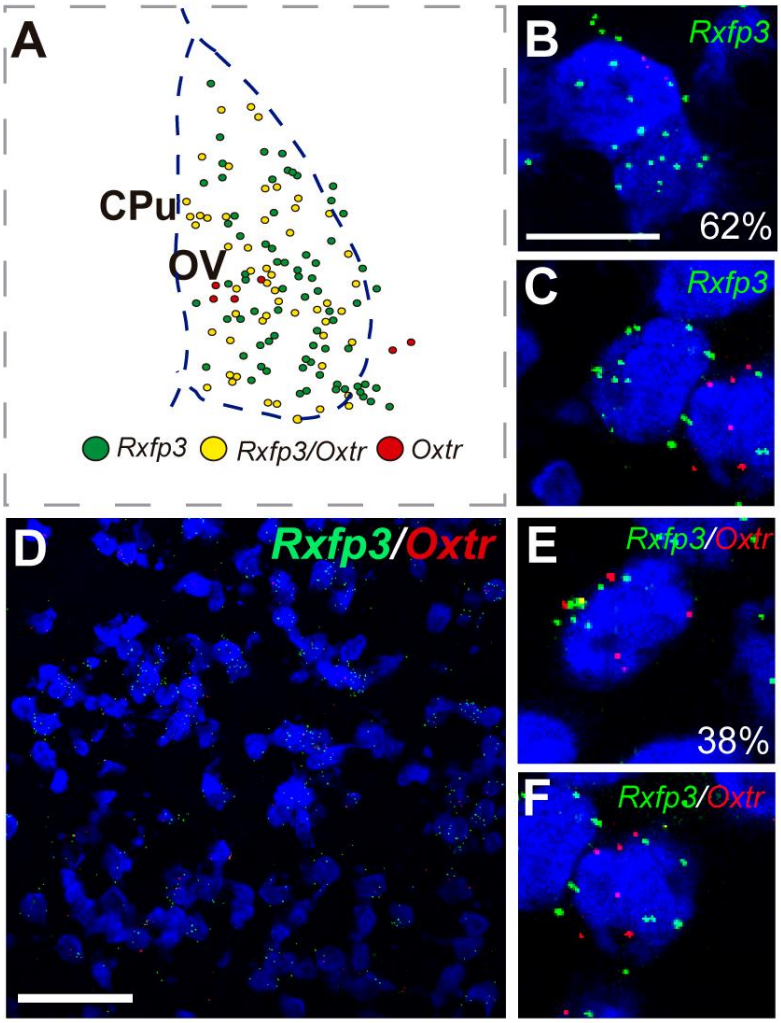


**Figure 4.13**. **Characterization and distribution of the *Rxfp3* mRNA positive neurons phenotype at the OV** (**A**) Schematic showing *Rxfp3* distribution and colocalization with *oxtr* mRNA in OV. (**D**) and representative images with quantification percentage of colocalization (**B**, **C, E and F**). Scale bar: 10µm (B), 100 µm (D).

In an effort to determine whether RLN3/RXFP3 signalling affected neural activity in the amygdala, we examined ERK activation. Western blot analysis revealed increased pERK immunoreactivity in amygdala extracts 20 min post-agonist infusion, compared to levels in vehicle-treated and naïve, untreated rats. At 90 min post-agonist infusion, pERK immunoreactivity levels were equivalent to basal levels in these control rats. Thus, the peak in ERK phosphorylation in the amygdala was reached during social recognition and

preference encounters and highlights the relevance of ERK activation in social learning and memory (Peng et al. 2010; Giese and Mizuno 2013) , as well as the consistent influence of the RLN3/RXFP3 system on the amygdala (Ma et al. 2007; Pereira et al. 2013; Santos et al. 2016).

Notably, in subsequent immunohistochemical studies, we detected an increase in pERK-positive neurons in the MeA. In line with this, pERK was increased in the MeA of mice with social deficits compared to controls, after a sociability and preference test (Faridar et al. 2014; Seese et al. 2014). Furthermore, in this model, oxytocin administration, improved social memory and reduced pERK levels in MeA, revealing a correlation between behavioural impairment and elevated pERK in MeA (Winslow et al. 2000; Winslow and Insel 2004). The observation that the RXFP3 agonist treatment increased pERK levels in MeA and induced an impairment of SRM further supports the importance of this MeA signalling in social behaviour regulation. In other anatomical studies we confirmed the nature of the RLN3 innervation pattern within the amygdala (Santos et al. 2016) and noted several RLN3-positive nerve fibres made close contacts with pERK-immunopositive neurons in MeAD and MePV after the SRM task.

In assessing the co-expression of RXFP3 mRNA and mRNA encoding other relevant neural markers, in the MeAD we observed that most *Rxfp3* mRNA-positive neurons were GABAergic (90% *Slc32a1* mRNA-positive), and 17% also expressed *Oxtr* mRNA. Furthermore, 46% of the *Oxtr* mRNA-expressing neurons in MeAD co-expressed *Rxfp3* mRNA. In contrast, in the MePV only 47% of *Rxfp3* mRNA-positive neurons expressed *Slc32a1* mRNA, while >60% of *Oxtr* mRNA-positive neurons co-expressed *Rxfp3* mRNA. Activation of the OXTR, which is coupled to excitatory Gq/11α class GTP binding proteins that stimulate together with Gβγ the activity of phospholipase C-β isoforms-proteins (Shojo and Kaneko 2000) has been shown to produce neuronal excitation in the MeA (Terenzi and Ingram 2005), and presynaptic OXTR activation promoted glutamate release (Mairesse et al. 2015). In contrast, RXFP3 is coupled to inhibitory $G\alpha_{i/o}$-proteins (Liu et al. 2003; Van der Westhuizen et al. 2007; Van der Westhuizen et al. 2010) and has been reported to hyperpolarise OT (and vasopressin) neurons *in vitro* (Kania et al. 2017). Thus, OXTR and RXFP3 likely have directly opposing effects on the activity of

some populations of amygdala neurons, and bidirectional regulatory mechanisms may exist between OT and RLN3 neurons, to regulate peptide release (Mairesse et al. 2015).

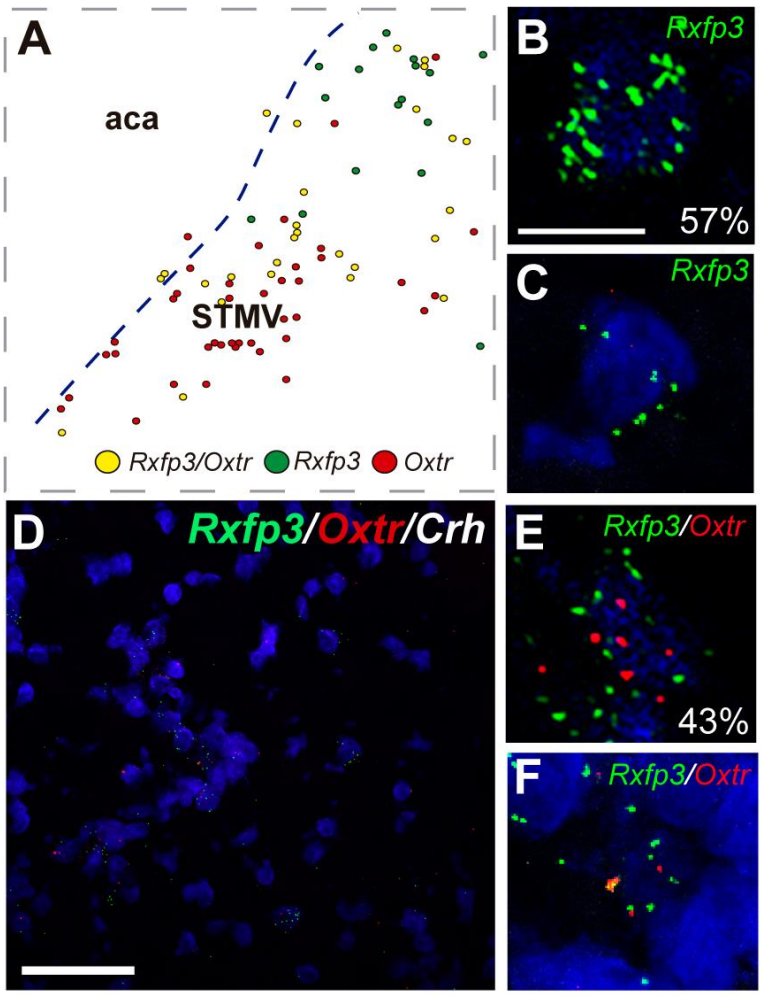


**Figure 4.14**. **Characterization and distribution of the *Rxfp3* mRNA positive neurons phenotype at the STMV** (**A**) Schematic showing *Rxfp3* distribution and colocalization with O*xtr* mRNA in STMV. (**D**) and representative images with quantification percentage of colocalization (**B**, **C, E and F**). Scale bar: 10µm (B), 100 µm (D).

In RXFP3-A2-treated rats, we also detected increased pERK levels in the STMV and OV nuclei, which are strongly interconnected with the cortical amygdala and the MeA (Gutiérrez-Castellanos et al. 2014; Cádiz-Moretti et al.

2014) and have been implicated in social interaction and social memory (Ferguson et al. 2001; Bannerman et al. 2004a; Takahashi et al. 2004; Kuhlmann et al. 2005). In these regions, *Rxfp3* mRNA was predominantly expressed by GABAergic neurons (80% *Slc32a1* mRNA-positive), and ~30% were *Oxtr* mRNA-positive. A major/minor proportion were *Oxtr* mRNA-positive (39% in the MePV and 16% in the MeAD, respectively) (**Table 4.2**). These findings suggest the RLN3/RXFP3 and OT/OXTR systems may interact in the ST. In this regard, OT gene knockout mice displayed a specific decrease in neuronal activation in ST after a social interaction and memory test (Ferguson et al. 2001).

Taken together, the current findings have demonstrated that RXFP3 is expressed by GABAergic neurons in the extended amygdala, consistent with reports in other brain areas (Richter et al. 2005; Blasiak et al. 2013; Albert-Gascó et al. 2017; Haidar et al. 2017), which implies an overall disinhibitory effect of the RLN3/RXFP3 system within the amygdala. Furthermore, the presence and proportions of *Rxfp3* and *Oxtr* mRNA-expressing neurons was broadly consistent across the different amygdaloid nuclei, suggesting a functional interaction between RXFP3 and OXTR signalling, which warrants further investigation. Notably, OT has been implicated in the elicitation of social memory consolidation (Ferguson et al. 2001; Gur et al. 2014). As such, our results suggest a role for RLN3/RXFP3 signalling in modulating social memory, which might occur via rapid (direct and/or indirect) alterations in pERK and related signalling in GABAergic/peptidergic neurons within specific areas of the extended amygdala. Moreover, RXFP3 activation might be capable of modifying (antagonising) the influence of OT/OXTR signalling on MeA and ST neurons, in regulating (promoting) social behaviour, but further studies are now required to clarify the nature and complexity of this interaction.

**Table 4.3**. Proportion of Oxtr neurons that express Rxfp3 mRNA.

| MePV |
|---|

| | Rxfp3/Oxtr | Total Oxtr |
|---|---|---|
| ***Rxfp3-Oxtr-Slc32a1*** | 22 | 66 |
| ***Rxfp3-Oxtr 1*** | 52 | 77 |
| ***Rxfp3-Oxtr 2*** | 33 | 48 |
| **MeAD** | | |
| ***Rxfp3-Oxtr-Slc32a1*** | **Rxfp3/Oxtr** | **Total Oxtr** |
| | 18 | 66 |
| ***OV*** | | |
| ***Rxfp3-Oxtr*** | **Rxfp3/Oxtr** | **Total Oxtr** |
| | 52 | 58 |
| ***STMV*** | | |
| ***Rxfp3-Oxtr*** | ***Rxfp3/Oxtr*** | ***Total Oxtr*** |
| | ***27*** | ***68*** |

# 5

# General discussion

## 5.1. Overall findings

Findings exposed confirm the impact of RLN3/RXFP3 signalling on short-term memory. Furthermore, we also revealed that short-term memory is modulated through direct activation of *Rxfp3* expressing neurons which coexpress vGAT and relevant phenotypes (PV ad OXTR) for each of the behaviours. Furthermore, RXFP3-A2 infused rats show increased ERK activation levels after spatial and social paradigms. Additionally, the use of ERK activation densities is a valid marker to measure the action and impact of RLN3/RXFP3 system. Finally, time stands out as a critical factor to consider when analysing RLN3/RXFP3 signalling impact on behaviour. All these findings have been carried out using different tools and techniques. These two behaviours get confined within the RLN3/RXFP3 signalling system and potentially modulated by NI RLN3 arising projections (**Fig 5.1**).

When analysing the effect of the RLN3/RXFP3 system over memory encoding and retrieval we used a pharmacological approach. To properly address this impact is important to fully delimit the process which is being modulated. From a conceptual theoretical view, short-term memory has been referred to memory storage in comparison to spatial working memory which refers to maintenance and manipulation of information influenced by attention (Baddeley 1992). Although conceptually different, animal studies have not been able to efficiently separate them and even show evidence for partial or complete overlaps (Davidson et al. 2006; Unsworth and Engle 2007).

In our studies, ERK activation was used as a marker. Areas to analyse were firstly delimited by western blot, which revealed substantial increases when compared to controls. Although this strategy was useful in order to find potential RLN3/RXFP3 modulated areas, some other areas might have been left out due to low resolution techniques. This could be de case, for both types of memories, at the hippocampus which on western blot analysis (data not shown) did not show differences compared to controls but ISH *Rxfp3* mRNA data reveals a high expression on dorsal and ventral hippocampus (Haidar et al. 2017). Another possibility is that RXFP3 activation on hippocampal neurons upregulates other types of MAPK (Kocan et al. 2014). Furthermore, ERK

activation as a specific marker for RLN3 action of on RXFP3 allowed us to pinpoint approximate time span of action. In addition, increased pERK density levels do not guarantee a direct RLN3/RXFP3 signalling effect. This was the case at the septal area where ChAT positive neurons were not *Rxfp3* mRNA expressing neurons and partially on amygdala and extended amygdala where pERK/*Rxfp3* neurons constituted ~50% in MeA and ~22% at ST. Specially remarkable is the case of STMV, where differences in ERK activation are high and consistent but colocalization with *Rxfp3* is low. This suggests an indirect ERK activation triggered by the RLN3/RXFP3 system on non-*Rxfp3* mRNA positive neurons. Altogether, despite the direct or indirect nature of ERK activation by RXFP3, the ability to identify RLN3/RXFP3 action in specific nuclei represents a highly valuable tool.

Common to both behavioural studies is the RXFP3 activation delivery system. On both cases, we choose to use icv infusions after cannula implantations as the safest and less invasive strategy to activate RXFP3. This model has the advantage of centrally activating all RXFP3 positive neurons in brain. Nonetheless, it might neglect specific neuronal function as it is not activated depending on specific circuits. In addition, this strategy raises questions regarding area activation specificity and brings by more complexity in result analysis. For instance, it proved challenging to discern specific area contribution to the same behaviour. Some consideration should be set out on the fact that not all targeted areas receive the same RXFP3-A2 concentration. However, given GPCRs sensitivity and RXFP3 specificity; concentrations do not need to be high to have a sufficient effect (Kocan et al. 2014).

ISH Rxfp3 data on both septum and amygdala reveals that the receptor is coexpressed in GABAergic neurons. Being RXFP3 an inhibitory GPCR (Blasiak et al. 2013; Kania et al. 2017), RXFP3 agonist would promote inhibition of GABAergic neurons. RLN3 is coexpressed with GABA (Ma et al. 2007) so, presumably it acts synergically to further inhibit target *Rxfp3/vGAT* mRNA expressing neurons. Furthermore, many of these *Rxfp3* expressing neurons coexpress OXTR or PV genes which are involved in memory storage and retrieval for social recognition memory and spatial memory. This fact is in

agreement with other neuropeptidergic systems which enhance amino acidic neurotransmitters action.

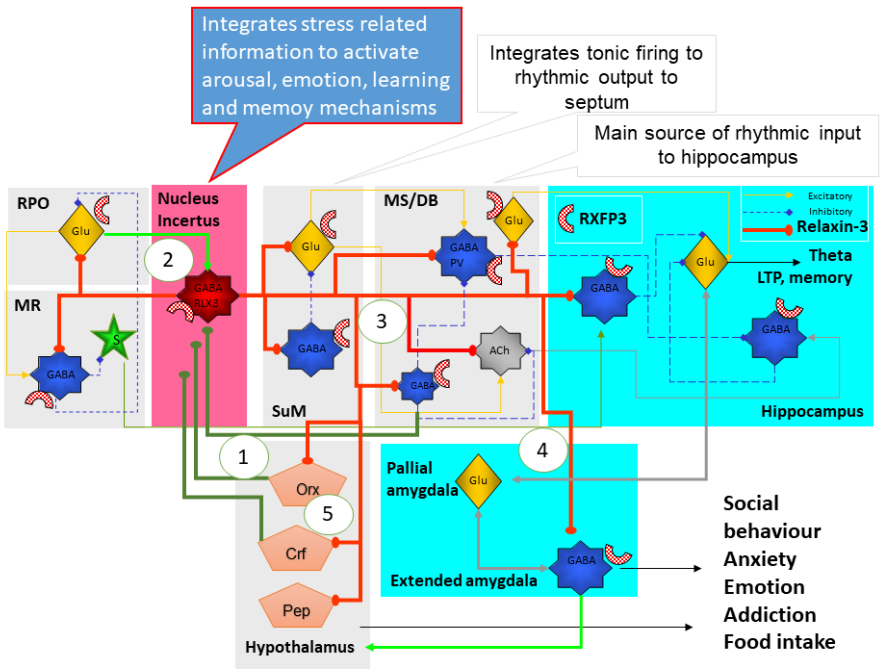


**Figure 5.1 General scheme describing RLN3 connections of nucleus incertus and its specific targets**. The NI receives hypothalamic projections (1) from corticotropin releasing factor (CRF) and orexin (Orx) peptidergic projections and also from GABAergic projections arising from the septal área. Projections arrive to NI from the reticularis pontis oralis (RPO) (2) which is responsible for driving theta from somatosensory stimulation. The NI then sends ascending connections (3) to the median raphe (MnR), supramammillary nucleus (SuM), medial septum and diagonal band (MS/DB) and hippocampus which are responsible for generating and modulating subcortically driven theta rhythm. NI projections also reach the extended amygdala (4) which might be responsible for emotionally driven behaviors including addictive behaviors, stress and anxiety and social stimuli processing. Some of these behaviors, like food intake can be directed from projections through hypothalamic nuclei (5) and might be mediated by other peptidergic systems (Pep).

Finally, results delimit a time range for RLN3/RXFP3 signalling action. Thus, 20 minutes after infusions was always effective to observe pERK activation but 90 minutes after infusions were only effective in the septal area. Likewise, 20 but not 90 minutes postinfusion caused an effect in social memory,

whereas 90 minutes postinfusion impaired spatial memory. It must be concluded that RLN3/RXFP3 time concrete periods can be area specific. Another possibility is that 20 minutes may reflect the end point in RXFP3-A2. If this was correct we would expect higher pERK levels at earlier times. This would explain why only around 30% of *Rxfp3* neurons colocalize with pERK. At 20 minutes and to solve this earlier points would result in higher percentage of *Rxfp3* coexpression with pERK.

## 5.2. Role of RLN3/RXFP3 system in spatial memory

Previous studies had already revealed RLN3/RXFP3 signalling impact on spatial working memory tested on a continuous 10 minutes spontaneous alternation test (Ma et al. 2009a; Haidar et al. 2017). Thus, they tested spatial working memory relying on the fact that rodent have innate capabilities to spontaneously alternate between arms avoiding arm repetitions and exploring novelty (Drew et al. 1973). On these studies results indicated that R3/I5 infusions on MS alone had no effect on spontaneous alternation. However, antagonist infusions impaired spontaneous alternation and combination of both reinstated it (Ma et al. 2009a). Thus, they concluded that R3/I5 infusions in the MS were necessary for spatial working memory. On the same studies infusions of R3/I5 also caused an increased theta rhythm related to spatial memory, increased attention and arousal processes.

On our testing of spatial memory we used a more classic approach using a two-trial delayed spontaneous alternation task (SADT). Encoding of memory would take place at the Familiarization phase, storage at the delay period (~90 min) and retrieval at the SADT. Considering RXFP3-A2 infused subjects have impaired spontaneous alternation plus novelty preference as they could not distinguish between novel and familiar arms we can confirm that RLN3/RXFP3 system impairs short-term memory. Given, that spontaneous alternation and novelty need information processing we could consider also a spatial working memory impairment. However, rodent behaviour interpretation is not always clear. Some authors in the literature would use the term spatial working memory to refer to the short-term storage of information (Olton and

Samuelson 1976; Olton et al. 1979; Honig 2018) and others would not consider SADT as a measure of spatial working memory. Thus, considering this hypothesis RXFP3-A2 infusions on a SADT paradigm would need no information manipulation and behaviour planning thus, only short-term memory would be getting impaired.

When analysing the specific nuclei correlates for spatial memory impairments, on a two trial spontaneous alternation task, we centred our study on the septal area. Given its profuse innervation and receptor expression it stand out as a major pivotal factor which could modulate spatial memory. From our results, we learned that RLN3/RXFP3 system clearly impacts on the MS/DB area. This effect is observed with an increase in ERK activated neurons. Nonetheless, in situ hybridization data from our posterior testing suggests that activation of ERK is of indirect nature. A possible explanation, is that RXFP3 positive neurons show pERK activation at earlier time point or other MAPK are more prominent for the RLN3/RXFP3 signalling at the MS (Van der Westhuizen et al. 2010; Kocan et al. 2014).

In addition, increased density of pERK/ChAT positive neurons in the MS after RXFP3-A2 infusion further highlight the importance of the RLN3/RXFP3 system in the regulation of the septohipocampal cholinergic pathway. Impairment of two trial delayed spontaneous alternation task is consistent with a cholinergic septohipocampal MS/DB inhibition. However, no *Rxfp3* mRNA positive neurons within the MS expressed *ChAT* and approximately 20% of them were *PV* mRNA positive. On the other hand, 50% of PV neurons expressed *Rxfp3* mRNA. Within the MS, only a small percentage of the RLN3/RXFP3 induced pERK was found in the MS-1 layer coexpressed with PV expressing neurons. This makes it still relevant for spatial memory consolidation. Additionally, RXFP3 activation in MS-2 and MS-3 septal layers, mostly populated with CR and CB positive neurons (Kiss et al. 1997) could be the key to understanding how these different neuronal phenotypes interact to regulate spatial memory.

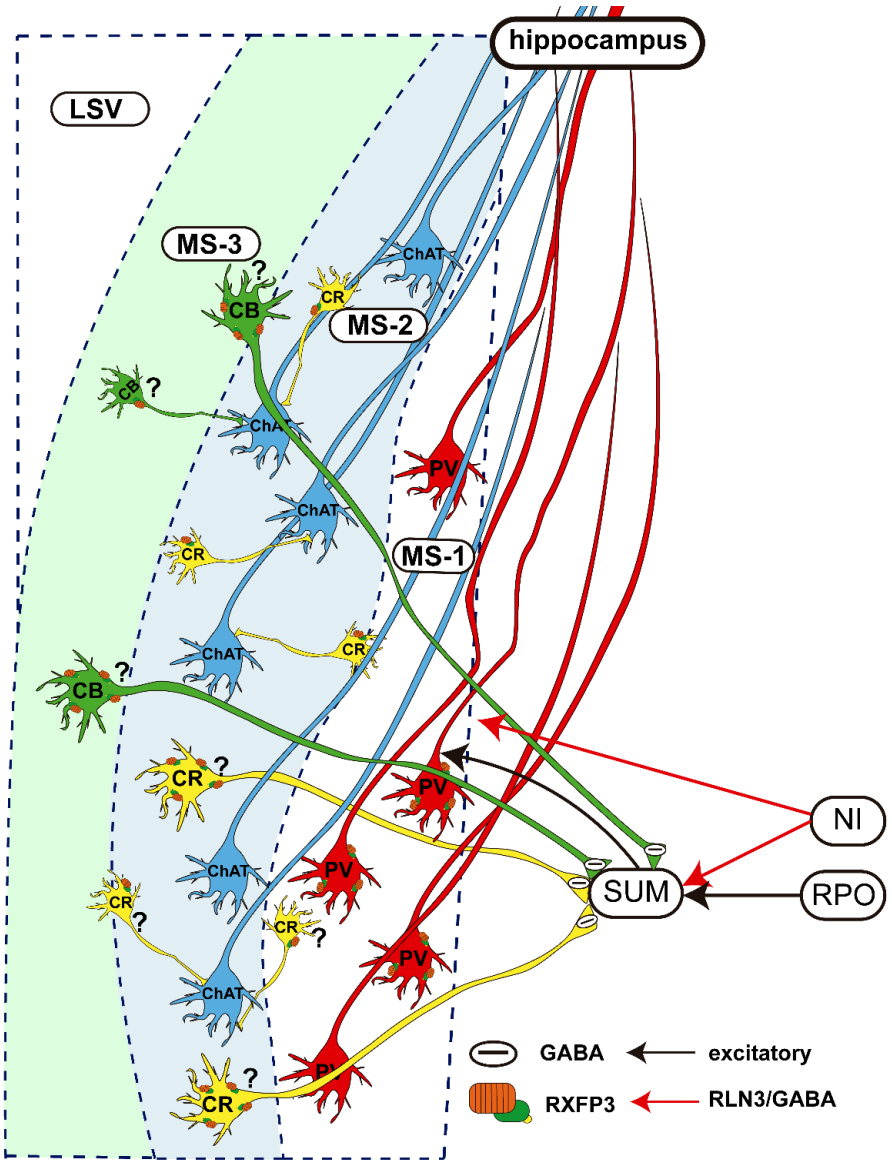


**Figure 5.2 RLN3/RXFP3 system role regulating MS/DB neuronal activity**. Impact over the septohippocampal pathway at MS-1 is shown with Rxfp3/PV neurons. Additionally, hypothetical Rxfp3 expression on GABA CR and CB positive neurons and interaction with inhibitory feedback on supramammillar nucleus (SUM) and/or ChAT neurons could result in impaired SAB on a two trial behavioural test. "?" indicate hypothetical Rxfp3/vGAT phenotype.

Not many studies have been carried out to study the specific function of these neurons. Classic anatomical studies showed CR, CB neurons coexpressing GABA project to the supramammillar nucleus (SUM) (Borhegyi and Freund 1998). In turn, SUM excitatory glutamatergic neurons project back to MS/DB promoting theta rhythm (Young et al. 2017; Ruan et al. 2017). Theta rhythm correlates with a class of movement that changes the rats location in an environment (Taube et al. 1990; O'Keefe and Recce 1993; Hirase et al. 1999; Buzsáki 2005). Furthermore, hippocampal neurons which are modulated by theta rhythm (TPD), theta-modulated place-by-direction cells code for both the location and head direction of animals (Cacucci et al. 2004). Our previous studies have shown that some septal CR positive neurons project back to the NI (Sánchez-Pérez et al. 2015). Altogether, RLN3/RXFP3 signalling on GABAergic neurons in MS-2 and MS-3 layers could act as a compensatory mechanism counteracting the PV neurons inhibition situated in the MS-1 (**Fig 5.2**). RLN3/RXFP3 system direct action in the hippocampus could further contribute to the observed RXFP3 agonist-induced behavioural defects.

## 5.3. Role of RLN3/RXFP3 system in social memory

No prior studies have linked the RLN3/RXFP3 system to social recognition memory. Social recognition memory is defined as the capability of remembering a familiar conspecific who have already met. Although this may make reference to circumstances like pair bonding, mating or pup careering our approach was centred on how RLN3/RXFP3 system modulates conspecific social memory after meeting another subject. The behavioural paradigm used in this work excluded sexual, exploratory biases, self-odor or maternal care as social stimuli which could vary the result. These other behaviours are relevant and also require social recognition memory (Winslow and Insel 2004; Young and Wang 2004; Coria-Avila et al. 2014)

RXFP3 effect on amygdala and extended amygdala neuronal activity was also evaluated using ERK activation densities within specific brain areas Similarly to what was shown in septum, ERK activation seem partly indirect

since we found many pERK positive neurons which did not express *Rxfp3* . Nevertheless, approximately half of total *Rxfp3* neurons in the MeA and 22% in the ST were positive for pERK. ERK have transient levels of phosphorylation, meaning that activated shift quickly to inactivated states (Wilsbacher et al. 1999).

On the other hand, vasopressin and oxytocin systems are well known modulators of social recognition memory (Winslow et al. 2000; Ferguson et al. 2001; Heinrichs and Domes 2008; Wang et al. 2015). We hypothesize that RLN3/RXFP3 system impact over OT/OXTR system alone can drastically affect social recognition memory impairing its encoding and later retrieval. The mechanism underlying RLN3/RXFP3-dependent SRM impairment and what areas have a stronger impact still remain unclear. However, we propose that the RLN3/RXFP3 signalling might be inhibiting the MeA-ST-LS pathway through inhibition of *Rxfp3/Oxtr* positive neurons at both MeA and ST (**Fig 5.3**)

The effects that we observed after RXFP3 agonist infusion can be explained considering that *Rxfp3* receptor is highly co-expressed with the *Oxtr*.

Thus, the proposed mechanism underling social memory regulation would imply OXTR/RXFP3/vGAT neurons in MeA, projecting and contacting ST local vGAT interneurons (Dong et al. 2001) (**Fig 5.3**). After activation with OT Inhibition of the GABAergic interneurons at ST would, in turn, disinhibit ST glutamatergic neurons which could directly or indirectly relay SRM information to the LS finally the information pass from the LS to ventral CA1 field where social recognition memory gets stored (Okuyama et al. 2016). This hypothesis is supported by previous c-Fos distribution on wild type and OT KO after novel social encounters. In these experiments, c-Fos immunolabelling at MeA and ST increased in wild type mice but not in OT KO mice (Ferguson et al. 2001).

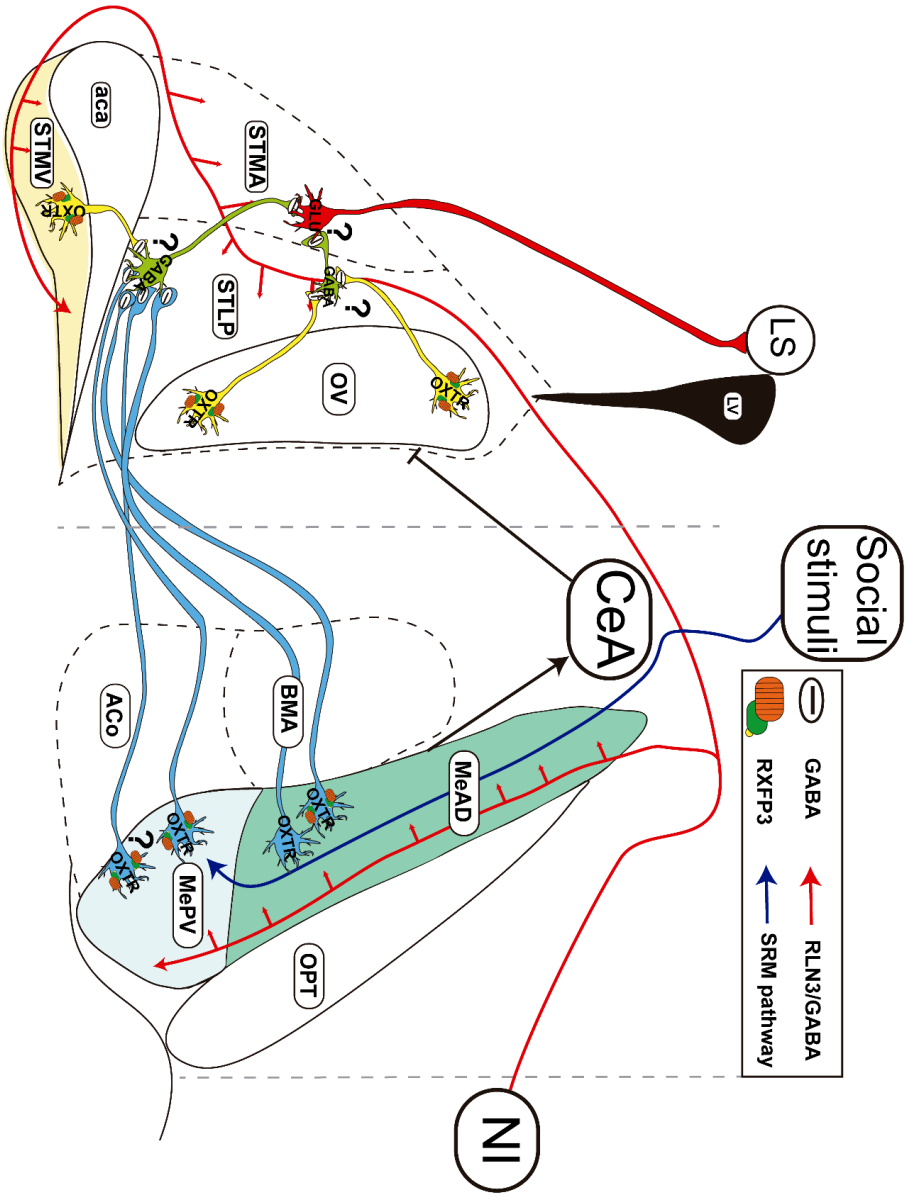


**Figure 5.3 RLN3/RXFP3 system impact over amygdala and extended amygdala.** medial amygdala and the bed nucleus of the stria terminalis (ST) scheme showing possible interactions between OXTR/vGAT/Rxfp3 mRNA positive neurons and ST. "?" indicate hypothetical pathway.

Furthermore, other areas could synergically be acting to impair SRM. In agreement with this, recent data revealed expression and inhibition of *Rxfp3* on approximately 90% of OT and AVP expressing neurons within the paraventricular nucleus (PVN) (Kania et al. 2017). PVN acts as one of the main sources of OT in the brain (Swaab et al. 1975; Hashimoto et al. 1985). This would ensure a complete blocking of the OT/OXTR system in the brain and favour and SRM impairment.

Further experiments to detect double pERK and OXTR mRNA neurons in this paradigm will be required to finally demonstrate this hypothesis

## 5.4. Future directions

All throughout our research we have been able to answer several aspects which define and confine RLN3/RXFP3 system modulatory action. However, these studies have raised new questions. In fact, the different components which modulate the overall behavioural outcome remain to be elucidated.

One of the main aspects we intend to enlighten is the specific contribution that different RLN3/RXFP3 regulated areas have on specific behaviours. For instance, icv strategy does not allow us to decipher what is the contribution of different areas. Similar concerns apply to social recognition memory regulation. In addition, finding a specific marker for RXFP3 activation would help to delimit both the optimal activation time span and better delimit areas of action. In order to do so RXFP3 conformational changes after activation would be a better strategy since RXFP3 shares signalling cascade with other GPCRs and tirosine kinases. Perhaps a more feasible alternative would be to make use of several markers at the same time to better delimit the peak time of action. For example, other MAPK which have been described in vitro to be activated by RXFP3 (Van der Westhuizen et al. 2010; Kocan et al. 2014)

Furthermore, if we focus on specific RXFP3 subphenotypes it would be really interesting to define its distinct functions. For instance, specific activation of RXFP3 on *PV*/*Rxfp3* positive neurons function may antagonise the effect of

*vGAT*/*Rxfp3* mRNA positive neurons. While *Rxfp3*/*vGAT* mRNA positive at MS-2 and MS-3 could inhibit SUM glutamatergic projecting neurons; and some local targeted projection neurons; in contrast to *Rxfp3*/*PV*/*vGAT* mRNA positive neurons at MS-1 which would inhibit PV positive neurons from the septohippocampal pathway.

From a behavioural standpoint social memory formation has different variants which still remain untested when RLN3/RXFP3 system is stimulated. For instance we do not know the effect over long-term social memory, motivated spatial behaviour or win-shift paradigms. In addition, social memory in rodents follows an intricate pathway from olfactory stimuli to memory consolidation at ventral CA1 field (Okuyama et al. 2016). Many of these areas, are strongly innervated by the RLN3 and express RXFP3 Furthermore, it is necessary to selectively activate specific phenotypes to see if other *Rxfp3* expressing phenotypes, other than OT/OXTR, directly affect social memory formation. Finally, some consideration should be made regarding the expression of *Rxfp3* in oxytocin and vasopressin positive neurons at the PVN as these neurons are crucial for social recognition memory (Landgraf et al. 1995; Ferguson et al. 2001; Lukas et al. 2013; Gur et al. 2014) and have been seen to be inhibited by RXFP3 activation *in vivo* (Kania et al. 2017).

For all these new applications it would be interesting to activate RXFP3 through a non-pharmacological approach. To use a viral strategy using receptors exclusively activated by designer drugs (DREADDs) driven by specific *Rxfp3* mRNA sub-phenotypes (E.g. *Rxfp3*/*OXTR* vs *Rxfp3*/-) or to inhibit RXFP3 expression using shRXFP3 (designed in our lab) would give insights into specific function and physiological function of RLN3/RXFP3 system. In parallel, specific activation of RLN3-NI projections would allow to study both spatial and social memory modulation in conditions nearer to physiological states. Even more interesting would be to see what impact dose NI-RLN3 projection activation and what stimuli is necessary to successfully act on areas like OV, CeA or PVN where RXFP3 is densely distributed but RLN3 fibres are scarce.

# 6

# Conclusions

The RLN3/RXFP3 system:

1) modulates spatial memory in rats.
2) central activation impairs short-term spatial memory in rats.
3) central activation increases the activation of ERK at the medial septum/diagonal band.
4) impact over the septal area takes place through the expression of RXFP3 in GABAergic neurons which at midline levels also express parvalbumin.
5) modulates social recognition memory but not social interaction in rats.
6) central activation impairs social recognition memory in rats.
7) central activation increases the activation of ERK at the medial amygdala and extended amygdala after a social behaviour paradigm
8) centrally activated pERK increased neurons express also in an increased ratio of neurons RXFP3.
9) impact over the amygdala and extended amygdala areas takes place through expression of RXFP3 in GABAergic and non-GABAergic neurons which partially also express the oxytocin receptor.

# 7

## Papel del sistema Relaxina-3/Receptor 3 de la familia de las relaxinas en la memoria espacial y el comportamiento social

## 7.1. Introducción

La regulación del comportamiento depende de diferentes sistemas anatómicos y fisiológicos. Entre estos sistemas fisiológicos están aquellos que promueven o inhiben circuitos comportamentales resultantes a través de regulación de acción rápida basada en aminoácidos y otros que modulan los anteriores a través de la regulación de acción lenta. Tanto la relaxina-3 (RLN3) como su receptor de mayor afinidad Receptor peptídico de la familia de las relaxinas 3 (RXFP3) pertenecen al segundo grupo. La RLN3 y RXFP3 presentan una distribución superpuesta en las diferentes áreas donde podemos encontrarlas con función espacio-temporal propia en diferentes paradigmas comportamentales. A pesar de que su impacto sobre el comportamiento se ha descrito desde su descubrimiento se requieren nuevos experimentos que clarifiquen el alcance y mecanismos en los que este sistema comportamental funciona. Por ejemplo, no se conocen los marcadores fenotípicos que comparte RXFP3, la regulación que puede estar ocurriendo con otros neuromoduladores o el rango total de comportamientos modulados.

La RLN3 fue descubierta en 2001 cuando se buscaban homólogos de relaxina en diferentes bases de datos (Bathgate et al. 2002). Dado que su expresión estaba mayoritariamente confinada al cerebro se la clasifico como un neuropéptido. El receptor por el que la RLN3 tiene mayor afinidad es RXFP3

(Bathgate et al. 2006). Este receptor también ha sido llamado GPCR135 (Liu et al. 2003) y receptor somatotain y angiotensin-like dada su similitud en estructura con el receptor de angiostestina AT1 y de somatostatina-5 (Matsumoto et al. 2000). Examinaciones ultraestructurales del cerebro de rata revelaron que la immunoreactividad (IR) de RLN3 está presente en el retículo endoplasmático, aparato de Golgi y soma celular y dentro de vesículas de núcleo denso en la sinapsis de los terminales nerviosos (Tanaka et al. 2005; Ma et al. 2009a). Estos hechos confirman a la RLN3 como un neurotransmisor.

La distribución de células RLN3 positivas en el cerebro ha sido estudiada en rata y ratón revelando una expresión intensa en una agrupación de células en una región conocida como nucleus incertus (NI) (Bathgate et al. 2002; Burazin et al. 2002; Tanaka et al. 2005; Ma et al. 2007; Smith et al. 2010).

Estructuras equivalentes al NI también se ha encontrado conservada en otras especies incluyendo el pez cebra (Donizetti et al. 2008) y macaco (Ma et al. 2009a). La conservación del NI y RLN3 en todas las diferentes especies sugiere una función importante. Posteriormente el uso de técnicas de trazado de alta resolución permitió descubrir que además de NI (~2000 neuronas), también otras áreas expresan el neuropéptido RLN3. Este es el caso del núcleo del rafé pontis (~350 neuronas), parte anterior del área gris periaqueductal (PAG) (~550 neuronas) y un área dorsal a la substancia nigra (~350 neuronas) (Tanaka et al. 2005). El conjunto de estas células RLN3 positivas mandan proyecciones a diferentes partes del cerebro entre las que destacan el área septal, amígdala, amígdala extendida e hipocampo ventral

Paralelamente estudios de hibridación in situ clásicos permitieron delimitar donde se expresa con mayor intensidad RXFP3. Las técnicas de hibridación in situ clásicas utilizan radioligandos que no proporcionan una resolución celular. Sin embargo, sí que permitieron delimitar con bastante exactitud la distribución del receptor en el cerebro. A su vez tests de unión entre RXFP3 y el agonista del receptor R3/I5 proporcionaron claves de cuál podría ser su función. De entre todas las áreas donde se expresa el receptor son especialmente interesante por su incidencia en varios comportamientos el area septal, amígdala, amígdala extendida e hipocampo (Ma et al. 2007; Ma et al. 2009a; Smith et al. 2010; Haidar et al. 2017).

De entre los comportamientos que el sistema RLN3/RXFP3 puede tener un impacto es de especial interés la memoria espacial dependiente de hipocampo. Esta fue descrita por primera vez en 1970 en experimentos electrofisiológicos que mostraban correlatos comportamentales entre una localización espacial y disparos neuronales (O'Keefe and Dostrovsky 1971; Ranck 1973). La memoria espacial hace referencia a memorias que almacenan información de las localizaciones del espacio que nos rodea (Morellini 2013). Una respuesta comportamental que utiliza memoria especial es la navegación; esta es la habilidad de viajar desde un lugar a otro. Biólogos comportamentales utilizan la navegación como media observable y medible de la memoria espacial. (McNaughton et al. 1996; Thompson and Varela 2001; McNaughton et al. 2006; Morellini 2013). Como otros tipos de memoria la memoria espacial

es un proceso basado en la experiencia que se codifica se almacena y finalmente se recupera cuando se requiere de la información (Atkinson and Shiffrin 1968; Baddeley and Warrington 1970; Milner 1972). La duración que la información queda almacenada determina si la memoria especial es de corto o bien largo-plazo (Eysenck 1988).

La mayoría de modelos animales que estudian la memoria especial analizan memoria de trabajo especial utilizando laberintos en T, en Y o radiales. La memoria espacial de trabajo es un concepto utilizado para hacer referencia a la memoria mientras está siendo utilizada para planificar y llevar a cabo un comportamiento. Específicamente, la memoria espacial de trabajo es un proceso cognitivo que incluye procesos atencionales, memoria a corto-plazo y procesamiento de la información (Baddeley 1992; Becker and Morris 1999). Todos los laberintos utilizados para analizar la memoria especial de trabajo hacen uso de la alternancia espontanea, es decir la tendencia que tienen los roedores que evitar volver a entrar en un brazo del laberinto que acaban de visitar. El razonamiento que correlación alternancia espontánea y memoria especial de trabajo es que no volver a entrar en un brazo que ya han entrado es porque recuerdan que han estado en ese brazo y por ello entran en el/los brazos por visitar. Sin embargo, algunos autores argumentan que la tendencia a explorar el último brazo decrece a causa un proceso de habituación y esto da lugar a la alternancia. Siguiendo esta hipótesis en este paradigma no tendría lugar la manipulación de la información necesario para hablar en memoria espacial de trabajo (Sanderson and Bannerman 2012). Desde este punto en adelante en nuestro paradigmas experimentales en laberintos en T interpretamos que estamos evaluando memoria especial de trabajo. Sin embargo, es plausible que la manipulación de información en estos paradigmas no ocurra y solo se analice memoria a corto plazo. El correlato en el hipocampo de este tipo de memoria son las “place cells” que al disparar delimitan localización en el espacio específicas (O’Keefe and Dostrovsky 1971; Ranck 1973).A su vez también existe el ritmo theta, una onda rítmica (7-12Hz) que tiene lugar en neuronas de CA1, CA3 y DG del hipocampo (Buzsáki 2002). La activación de “place cells” viene precedida por un relación en fase con el ritmo theta en el hipocampo (O’Keefe and Recce 1993). Mientras que las “place cells” correlacionan con una localización específica en el espacio (O’Keefe and

Dostrovsky 1971) el ritmo theta correlaciona con una clase de movimiento que cambia la localización en el espacio (Taube et al. 1990; O'Keefe and Recce 1993; Hirase et al. 1999; Buzsáki 2002) A su vez, neuronas hipocámpicas que son moduladas por el ritmo theta (TPD) codifican para la localización y dirección de cabeza de los animales (Cacucci et al. 2004).

La modulación mediante el sistema RLN3/RXFP3 de la memoria especial se piensa que tiene lugar mediante las proyecciones RLN3/GABA positivas desde el NI hasta el septum medial/banda diagonal y hacia el giro dentado del hipocampo (dorsal y ventral). Específicamente, las proyecciones RLN3/GABA sobre la vía septo-hipocámpica en el septum medial (Nuñez et al. 2006; Ma et al. 2009a; Ma et al. 2013; Martínez-Bellver et al. 2015; Martínez-Bellver et al. 2017), caracterizada por sus conexiones con neuronas parvalbumina y colinérgicas. La estimulación eléctrica del NI provoca oscilaciones del ritmo theta y lesiones del NI mientras se estimula en el núcleo reticularis pontis oralis lo abolen (Nuñez et al. 2006). Inyecciones del agonista R3/I5 directamente en el septum medial promovieron ritmo theta y no afectaron a la memoria especial de trabajo en un paradigma continuo de alternancia espontanea de 10 minutos (Ma et al. 2009a).

El rol del sistema RLN3/RXFP3 en memoria espacial ha sido estudiado con anterioridad. Sin embargo, el estudio tanto la memoria espacial de trabajo como la memoria espacial a corto plazo puede profundizarse aún más. Esto incluye testar nuevas variantes en el paradigma de memoria espacial y probar tiempos más largos de almacenaje.

Otro comportamiento que el sistema RLN3/RXFP3 tiene una alta probabilidad de estar implicado es el comportamiento social. El comportamiento social es presenta diferentes componentes los cuales son dependientes en gran mediad de amígdala. En nuestro caso nos centramos en la interacción social entre individuos conspecíficos y memoria de reconocimiento social (SRM). La SRM puede definirse como la habilidad de recordar a un sujeto que has conocido con anterioridad (Gheusi et al. 1994). En roedores, SRM, es mediada por estímulos olfativos percibidos a través de los bulbos olfativos principal (MOB) y accesorio (AOB) (Dulac and Torello 2003) cuya información es posteriormente enviada a la amígdala medial (MeA)

(Ferguson et al. 2001; Lukas et al. 2013; Gur et al. 2014). La MeA es crucial para SRM ya que recibe los estímulos sociales olfativos mediante proyecciones directas (Scalia and Winans 1975). Esta información es a su vez modula por los sistemas neuropeptídicos vasopresina en septum lateral (LS) y oxitocina (OT) en la MeA. El sistema OT/OXTR es especialmente importante ya que ratones KO para el gen de OT no tienen SRM, mientras que infusiones locales en MeA restablece la SRM (Everts and Koolhaas 1997; Winslow et al. 2000; Ferguson et al. 2001; Choleris et al. 2007; Veenema 2008). Ratones que tiene knockeados el gen de OT también muestran un descenso en la expresión de c-Fos en MeA, núcleo del lecho de la stria terminalis (ST) (Ferguson et al. 2001) comparado con vehículos después de un test de interacción social y memoria social (Ferguson et al. 2001; Richter et al. 2005).

El rol del sistema RLN3/RXFP3 en la modulación de comportamientos sociales no se ha estudiado hasta el momento. Sin embargo, las fibras de RLN3 son muy abundantes en la MeA y ST desde los niveles más rostrales a los más caudales (Santos et al. 2016). A sí mismo, estudios clásicos de ISH revelan que el gen de Rxfp3 se expresa abundantemente en MeA, ST e hipocampo (Sutton et al. 2004).

## 7.2. Objeto y objetivos de la investigación

Teniendo en cuenta las evidencias que sugieren que el sistema RLN3/RXFP3 puede estar implicado en la modulación de la memoria espacial y el comportamiento social consideramos dos hipótesis:

**Hipótesis 1**: El Sistema RLN3/RXFP3 tiene un impacto sobre la memoria espacial mediante sus proyecciones RLN3 positivas y expresión de RXFP3 en la región septal.

- **Objetivo 1**: Estudiar el impacto de la activación de RXFP3 sobre la región septal utilizando la fosforilación de ERK1/2 como marcador.
- **Objetivo 2:** Estudiar la distribución de las neuronas pERK1/2 positivas en núcleos específicos de la región septal.
- **Objetivo 3:** Estudiar cual es el efecto de la activación de RXFP3 sobre la memoria espacial.
- **Objetivo 4:** Estudiar la distribución y fenotipo del neuronas que expresan Rxfp3 en la región septal.

**Hipótesis 2:** El Sistema RLN3/RXFP3 tiene un impacto sobre el comportamiento social mediante sus proyecciones RLN3 positivas y expresión de RXFP3 en la amígdala y amígdala extendida.

- **Objetivo 1**: Estudiar el impacto de la activación de RXFP3 sobre la amígdala utilizando la fosforilación de ERK1/2 como marcador.
- **Objetivo 2**: Estudiar cual es el efecto de la activación de RXFP3 sobre la el comportamiento social.
- **Objetivo 3**: Estudiar la distribución de las neuronas pERK1/2 positivas en núcleos específicos de la amígdala y amígdala extendida.
- **Objetivo 4:** Estudiar la distribución de las neuronas pERK1/2 positivas en núcleos específicos de la amígdala y amígdala extendida expresan el Rxfp3 y en qué proporción.
- **Objetivo 5**: Estudiar la distribución y fenotipo del neuronas que expresan Rxfp3 en amígdala y amígdala extendida.

## 7.3. Planteamiento y metodología

### 7.3.1. Grupos experimentales de memoria espacial y Paradigma de interacción y memoria social en un laberinto de tres habitaciones.

Para comprobar el impacto que el sistema RLN3/RXFP3 tiene sobre la memoria espacial y sobre el comportamiento social realizamos infusiones intracerebroventriculares del agonista de RXFP3, RXFP3-A2. Para ello se implantaron cánulas en uno de los ventrículos laterales mediante una operación estereotáxica. Una semana después de la operación, a través de la cánula implantada a las ratas se las infusión o bien un 1 µL del péptido RXFP3-A2 (5 µg/µL) o vehículo (aCSF) a un ritmo de 0.5 µL/min mediante un inyector Harvard syringe injector (Harvard PHD 2000 Syringe Pump; Harvard Apparatus, Holliston, MA, USA).

El agonista RXFP3-A2 ([R3A(11–24, C15 → A)B]; tiene una alta afinidad por el receptor de la RLN3, RXFP3 (Shabanpoor et al. 2012). A lo largo de todo el estudio se utilizaron diferentes grupos experimentales. Para el análisis de memoria espacial existían tres grupos experimentales; grupo naive sin ningún tipo de cirugía, grupos vehículo o sham y RXFP3-A2 con una cirugía en uno de los ventrículos laterales. Estos tres grupos se utilizaron para los análisis de immunoblots, paradigma de alternancia en laberinto en T y estudios de colocalización mediante immunoflourescencias.

Para el estudio de la distribución del RNAm del gen de *Rxfp3* y sus fenotipos en las diferentes regiones del área septal solo había un grupo naive. Finalmente, para comprobar el impacto del sistema RLN3/RXFP3 sobre el comportamiento social existían dos grupos control; naive y vehículo (con operación icv); y dos grupos experimentales. Los dos grupos experimentales tenían infusiones del agonista RXFP3-A2 en un punto diferente del paradigma de interacción social y memoria social en un laberinto de tres habitaciones. El primer grupo se le infusionaba ante de comprobar la interacción social y por ello se le denomino A2-Soc. El segundo grupo experimental se les infusionaba el agonista antes de comprobar la preferencia y SRM y por ello se los denomino A2-Pref.

### 7.3.2. Paradigma de alternancia espontánea en un laberinto en T

Tanto las ratas del grupo vehículo como las del grupo RXFP3-A2 fueron habituadas al experimentador durante la semana anterior al paradigma comportamental. En el día del paradigma experimental y del sacrificio, los animales fueron habituados durante 30 minutos a la habitación donde se realizó el paradigma previo a las infusiones (vehículo ó RXFP3-A2). 5 minutos después de las infusiones las ratas se les dejo explorar libremente el laberinto T durante 5 minutos con uno de los brazos cortos cerrados (fase de familiarización)

A lo largo de todo el experimento el brazo cerrado fue balanceado entre los diferentes sujetos testados, de forma que se alternaba el brazo cerrado cada dos casos (un vehículo, un RXFP3-A2) para así evitar sesgos. El brazo cerrado es posteriormente denominado como brazo “novel” y el brazo abierto como “familiar”. Después de la familiarización las ratas regresaron a su caja durante 90 minutos. Paso este tiempo, se las dejo explorar libremente durante 3 minutos el laberinto en T con todos los brazos abiertos para así evaluar la tenencia entre los brazos familiar y novel.

### 7.3.3. Hibridación in situ (ISH) Multiplex – distribución septal de RNAm del gen Rxfp3

La distribución de las neuronas del gen Rxfp3 y su fenotipo colinérgico o GABAérgico mediante hibridación in situ RNAscope multiplex. RNAscope® es un herramienta comercial proporcionada por Advanced Cell Diagnostics (ACD, Newark, CA, USA). Esta técnica incluye la incubación de secciones congeladas de cerebro post-fijado con hasta 3 sondas. Una sonda típica contiene hasta 20 pares ZZ que cubren un total de ~1000 pares de base del RNAm diana.

Para comprobar que las sondas de RNAm no tienen uniones inespecíficas se realizan verificaciones in sílico y se validan para seleccionar oligonucleótidos con temperaturas óptimas para la hibridación bajo las condiciones de RNAscope (Wang et al. 2012).

La ratas se anestesiaron con pentobarbitone (100 mg/kg i.p), decapitadas, y se extrajeron los cerebros con rapidez, congelaron en hielo seco. Los cerebros se encastraron en OCT Embedding gel (Tissue-Tek® OCT, Optimum Cutting Temperature, Sakura Finetek USA Inc., Torrance, CA, USA) y almacenados a -80ºC. Antes de cortar los cerebros se atemperaron los cerebros a -20ºC por 2 h y cortaron con un criostato (Cryocut CM 1800, Leica Microsystems, North Ryde, NSW, Australia). Las secciones coronales (16 µm) se cortaron y montaron mediante calor en portaobjetos Superfrost-Plus Slides (Fisher Scientific, Hampton, NH, USA, Cat#12-550-15).

Las secciones se fijaron en paraformaldehido (PFA) durante 16 min a 4ºC, lavadas en PBS, deshidratadas in en concentraciones de alcohol crecientes (50%, 70% and 100%). Una vez deshidratadas las secciones se almacenaron en etanol al 100% a -20ºC durante toda la noche. Al día siguiente, los portaobjetos se secaron a temperatura ambiente, se dibujó una barrera hidrofóbica alrededor de las secciones (ImmEdge hydrophobic PAP pen, Vector Laboratories, Burlingame, CA, USA; Cat #310018). Las secciones se incubaron con pretratamiento de proteasas-4 (ACD, Cat #322340) durante 16 minutos. Después de lavar las secciones con PBS se incubaron las diferentes combinaciones de sondas durante 2h a 40ºC siempre siendo una de las sondas Rxfp3 (ACD, #316181). Después de la incubación las secciones se lavaron con wash buffer (ACD, Cat#310091) y la señal se amplifico con los productos de amplificación-ACD según el protocolo proporcionado por la compañía. Después de los lavados con wash buffer, las secciones se trataron con DAPI (ACD, #320851), cubrieron con medio de montaje para fluorescencia (Fluoromount-G, Southern Biotech, Birmingham, AL, USA, Cat# 17985-10), y guardados a -20ºC hasta su visualización.

### 7.3.4. Paradigma de interacción y memoria social en un laberinto de tres habitaciones

Todas las ratas fueron habituadas durante la semana posterior a las cirugías y previamente a los experimentos comportamentales. En el día del test comportamental y sacrificio las ratas se habituaron durante 30 minutos a la habitación donde se testo el comportamiento antes de las infusiones. El paradigma comportamental se realizó en un laberinto de tres habitaciones en

tres fases, habituación, test de interacción social y test de preferencia social. Seguido de 5 minutos, en los que se habituó a los animales al laberinto, las ratas se les permitió explorar libremente el laberinto durante 10 minutos o bien a un sujeto conspecífico o un objeto inanimado (“Sociability Test”). Posteriormente, en el “Preference Test cada rata tuvo como opción explorar un conspecífico familiar (del Sociability test) y una conspecífico novel durante 10 minutos. A lo largo de todo el experimento las habitaciones (derecha o izquierda) en el que se encontraba el sujeto novel, ratas y objetos se balanceo en todos los casos.

Tanto el agonista RXFP3-A2 como el aCSF se infusionaron 20 minutos antes de cada test. El tiempo explorando cada una de las habitaciones se monitorizo para luego sacrificar a cada una de las ratas inmediatamente después del “Preference test”. Los datos en ambos tests se expresaron como “preference index” que se calculó como el tiempo oliendo de los sujetos menos el tiempo oliendo el objeto (Sociability Test) o el tiempo oliendo el sujeto novel menso el tiempo oliendo el sujeto familiar conspecífico (Preference test).

## 7.4. Discusión General

### 7.4.1. Hallazgos generales

Los resultados expuestos confirman un impacto del sistema RLN3/RXFP3 en la memoria a corto plazo. Es más, también revela que la memoria a corto plazo es modulada a través de la activación directa de las neuronas Rxfp3 que coexpresan vGAT y otros fenotipos relevantes (PV y OXTR) para los comportamientos estudiados. Así mismo sujetos con infusiones del agonista RXFP3-A2 tienen densidades aumentadas de activación de ERK después de un paradigma de memoria espacial y social. Estos estudios también validan el uso de la densidad de pERK como medida de acción del sistema RLN3/RXFP3. Finalmente, el tiempo es un factor crítico a tener en cuenta cuando se analiza la acción del sistema RLN3/RXFP3 sobre el comportamiento.

Para el análisis del efecto del sistema RLN3/RXFP3 sobre la codificación de la memoria utilizamos una aproximación farmacológica. Para

analizar correctamente el proceso que pretendíamos estudiar había antes que definirlo y delimitarlo correctamente. Desde un punto de vista conceptual y teórico, la memoria a corto plazo está definida por un mantenimiento de la información por un tiempo finito. Por otra parte la memoria de trabajo requiere además de un mantenimiento una modificación o manipulación de esta memoria. Esta proceso es a su vez afectado por la atención (Baddeley 1992). Aunque la memoria a corto plazo y la memoria de trabajo son conceptualmente diferentes modelos animales no han sido capaces de separarlos eficientemente. Los resultados y evidencias apuntan más en algunos casos a un solapamiento de ambos procesos (Davidson et al. 2006; Unsworth and Engle 2007).

En nuestros estudios utilizamos la activación de ERK como marcador del sistema RLN3/RXPF3. Primero se delimitaron las áreas a analizar mediante western blots que revelaron un incremento sustancial en la activación de ERK

Esta estrategia aunque fue la adecuada, porque permitió encontrar áreas potencialmente moduladas por RLN3/RXFP3, por otra parte puede haber dejado algunas áreas por detectar dada la baja resolución espacio-temporal de la técnica. Este podría ser el caso del hipocampo que mediante el análisis de western blot, después infusiones de agonista, no mostraban diferencias en la densidad de pERK pero sí que se ha descrito un expresión alta de RXFP3 tanto en el hipocampo ventral como dorsal (Haidar et al. 2017). Otra posibilidad es que la activación de RXFP3 en el hipocampo de lugar a un aumento en la activación de otra MAPK diferente a ERK (Kocan et al. 2014). A su vez la activación de ERK también nos permitió delimitar el tiempo aproximado de acción. El aumento de la densidad de pERK por infusiones de RXFP3-A2 ha demostrado no tener por qué guardar una relación directa con el sistema RLN3/RXFP3. Esto sugiere que la activación de ERK pese a ser un efecto causado por la activación de RXFP3-A2 no todos los casos son directos. Este era el caso en el área septal donde pese aumentar la densidad de pERK en neuronas colinérgicas, estas no expresaban el receptor de RLN3. Al analizar cuan directo era el efecto en amígdala vimos que sí que era parcialmente directo con ~50% en MeA y un ~22% en ST. De especial

relevancia es el caso de STMV donde las diferencias en la activación de ERK son muy altas y sin embargo la colocalización con Rxfp3 es muy baja. Esto sugiere en este caso un activación de ERK indirecta pero provocada por el sistema RLN3/RXFP3 en neuronas pERK positivas y RNAm *Rxfp3* negativas. En resumen a pesar de la naturaleza directa o indirecta del aumento de pERK en sujetos con infusiones de agonistas, la capacidad de detectar e identificar núcleos específicos sobre los que actúa el sistema RLN3/RXFP3 es una herramienta que tiene un alto valor.

Común a ambos tests comportamentales es la activación de RXFP3 mediante infusiones icv. En ambos casos las infusiones se realizaron una semana después de implantar las cánulas mediante cirugías estereotáxicas por ser la estrategia más segura y menos invasiva para activar RXFP3. Este modelo tiene la ventaja de activar de manera central todas las neuronas RXFP3 positivas del cerebro. Por contra, puede que esta estrategia este negando el efecto especifico que algunas de estas neuronas tengan en circuitos específicos. A su vez, plantea nuevas preguntas sobre la contribución específica de cada una de estas áreas a los comportamientos bajo estudio. Este análisis ha sido de interpretación especialmente complicada dado que en ambos tipos de memoria están implicadas varias áreas que se interconectan entre ellas formando circuitos altamente complejos. También es importante considerar que dada la distribución de RXFP3-A2 no todas las áreas Rxfp3 positivas bajo estudio tienen la misma potencialidad de recibir el péptido RLN3. Sin embargo, puede que este hecho este compensado mediante la alta sensibilidad de los receptor GPCR y específicamente RXFP3, que no requieren altas concentraciones para tener un suficiente efecto resultante (Kocan et al. 2014).

Por su parte los resultados de hibridación in situ, revelan que el receptor Rxfp3 esta coexpresado en neuronas GABAérgicas. Dado que RXFP3 es un receptor metabotrópico y demuestra que inhibe neuronas in vivo (Blasiak et al. 2013; Kania et al. 2017), la activación de RXFP3 promovería la inibición de neuronas GABAérgicas. Las fibras de RLN3 coexpresan a su vez GABA (Ma et al. 2007) así que presumiblemente ambos sistemas actúan sinérgicamente para aumentar el efecto inhibitorio sobre las neuronas

Rxfp3/vGAT positivas tanto del área septal como de amígdala. Muchas de estas neuronas a su vez coexpreasn otros marcadores como OXTR o PV que están implicados en el almacenaje y recuperación de memoria social y espacial. Este hecho es concordante con otros sistemas neuropeptidérgicos que también sirven para potenciar la acción de neurotransmisores aminoacídicos de acción rápida.

Finalmente, los resultados establecen un rango temporal de acción para la señalización de RLN3/RXFP3. Análisis de los resultados 20 minutos después de las infusiones de agonista siempre fue un tiempo eficiente para observar un aumento en la activación de ERK. Sin embargo, a 90 minutos solo era apreciable una diferencia en la activación de ERK en el área septal. De manera similar infusiones a 20 pero no a 90 minutos causaron un efecto en la memoria de reconocimiento social, así como 90 minutos después de infusiones impedían la codificación de memoria espacial. Podemos concluir que el tiempo específico de acción del sistema RLN3/RXFP3 tiene cierto componente específico de área. Otra posibilidad, teniendo en cuenta que el aumento de activación de ERK observado en septum a 90 minutos es indirecto, puede que 20 minutos sea el punto final de activación RXFP3-A2 dependiente. De ser así esperaríamos densidades más altas de pERK a tiempos más cercanos a la infusión. Esto explicaría porque en amígdala a 20 minutos la colocalización de pERK con Rxfp3 es solo de un 30% y muchas neuronas Rxfp3 positivas no son también pERK positivas.

### 7.4.2. Rol del sistema RLN3/RXFP3 en la memoria espacial

Estudios previos ya habían revelado el impacto que tiene el sistema RLN3/RXFP3 sobre la memoria especial de trabajo en un paradigma de continuo de alternancia espontanea de 10 minutos (Ma et al. 2009a; Haidar et al. 2017). Así pues testaron la memoria espacial de trabajo basándose en el hecho de que si los roedores alternan entre brazos en un laberinto es porque recuerdan el último brazo que han visitado, evitando brazos ya visitados (Drew et al. 1973). En estos estudios los resultados indicaron que infusiones del agonista R3/I5 directamente en el septum medial no tenían ningún efecto en la

alternancia espontanea. Sin embargo, infusiones del antagonista impedían la correcta alternancia espontanea entre brazos que al infusionar el agonista volvía a nivel basales comparables a los grupos control (Ma et al. 2009a). Así pues, concluyeron que infusiones de R3/I5 en el septum medial provocaban la no codificación de la memoria especial de trabajo. En los mismos estudios infusiones de R3/I5 también causaron un aumento del ritmo theta relacionado con memoria espacial y procesos atencionales.

En nuestro paradigma comportamental decidimos tomar una estrategia más clásica con una tarea de alternancia espontanea en dos pruebas (SADT) con un tiempo entre ellas. Mientras que la codificación de la memoria tendría lugar en la fase de familiarización, el almacenaje en el tiempo entre pruebas (~90 minutos) y la recuperación de la memoria en la segunda prueba o SADT. Teniendo en cuenta que los sujetos infusionados con RXFP3-A2 no codifican la alternancia espontánea y no diferencian entre el brazo novel y familiar confirmamos que el sistema RLN3/RXFP3 impide la codificación de memoria espacial a corto plazo.

Dado que la alternancia espontanea requiere de modificación de la información almacenada, consideramos que también afectaba a la memoria espacial de trabajo. Sin embargo, la interpretación del comportamiento animal y sus correlatos en el comportamiento humano no son siempre claros y algunos autores interpretan que en modelos animales no existe una distinción entre ambos procesos cognitivos (Olton and Samuelson 1976; Olton et al. 1979; Honig 2018) a su vez también se ha descrito en la literatura otros que no considerarían nuestro modelo de SADT como un paradigma que evalué memoria espacial de trabajo. Teniendo en cuenta esta última hipótesis las infusiones de RXFP3-A2 en un paradigma de SADT no requeriría manipulación de información ni planificación en el comportamiento y por tanto solo afectaría a la memoria espacial a corto plazo.

### 7.4.3. Rol del Sistema RLN3/RXFP3 en la memoria de reconocimiento social

Ningún estudio comportamental anterior ha relacionado el sistema RLN3/RXFP3 con la memoria de reconocimiento social. La memoria de

reconocimiento social puede ser definida como la capacidad de recordar a un conspecífico familiar que se ha conocido con anterioridad. Esto hace referencia a un rango extenso de comportamientos desde comportamientos sexuales, cuidado de crías y otros comportamientos maternales. Todos estos comportamientos son muy relevantes para el comportamiento social y potencialmente modulables por el sistema RLN3/RXFP3(Winslow and Insel 2004; Young and Wang 2004; Coria-Avila et al. 2014). Sin embargo, nuestro trabajo se ha centrado en el reconocimiento de un sujeto igual eliminando variables como sexo, olores propios, edad o relación parental.

Para evaluar el efecto de la activación de RXFP3 sobre la amígdala y amígdala extendida también se utilizó la activación de ERK. Esto permitió definir partes dentro de la amígdala y amígdala extendida que presentaban aumentos en la densidad de activación de ERK. Parte del total del aumento de densidad de pERK es indirecto ya que encontramos muchas neuronas pERK positivas que no expresan el receptor. Aun así más de la mitad de las neuronas pERK positivas de MeA y en un 0.2 de los casos en ST son Rxfp3 positivas. Esto puede ser explicado porque los estados de fosforilación de ERK son transitorios y por ello pasan de estados activos a inactivos en muy poco tiempo (Wilsbacher et al. 1999). Por otra parte, los sistemas vasopresina y oxitocina son moduladores de la memoria de reconocimiento social (Winslow et al. 2000; Ferguson et al. 2001; Heinrichs and Domes 2008; Wang et al. 2015) y por tanto la inhibición por parte del sistema RLN3/RXFP3 de estos dos sistemas tendría un efecto directo sobre la no codificación de SRM.

## 7.5. Conclusiones

El sistema RLN3/RXFP3:

1) modula la memoria espacial en ratas.
2) activado centralmente impide la codificación de la memoria espacial a corto plazo.
3) activado centralmente aumenta la activación de ERK en el septum medial/banda diagonal.
4) tiene un impacto sobre el área septal mediante neuronas que expresan RXFP3 y GABA y que son en la línea media también expresan parvalbumina.
5) modula la memoria de reconocimiento social pero no la interacción social en ratas.
6) activado centralmente impide la codificación de la memoria de reconocimiento social.
7) activado centralmente aumenta la activación de ERK en la amígdala medial y amígdala extendida después de un paradigma de interacción social.
8) activado centralmente presenta una ratio aumentada de neuronas pERK positivas que también expresan RXFP3.
9) Tiene un impacto sobre la amígdala y amígdala extendida a través la expresión de RXFP3 en neuronas GABAérgicas y no GABAérgicas que parcialmente también expresan el receptor de oxytocina.

## 7.6. Futuras líneas de investigación

A lo largo de toda nuestra investigación hemos sido capaces de contestas diferentes aspectos que definen y delimitan al sistema RLN3/RXFP3 y cómo funciona su acción moduladora. Sin embargo, estos estudios plantean nuevas preguntas. De hecho los diferentes componentes que modulan el comportamiento resultante aun no quedan del todo claros.

Uno de los aspectos principales que pretendemos clarificar es la contribución específica e individual que cada una de las áreas reguladas por RLN3/RXFP3 tiene sobre comportamientos específicos. Por ejemplo, dado que elegimos como estrategia realizar infusiones ICV esto no nos permite descifrar la contribución especifica tanto en a la memoria espacial como a la memoria de reconocimiento social. Asimismo, encontrar un marcador específico de la activación de RXFP3 permitiría delimitar con mayor exactitud el tiempo óptimo de detección del sistema y las áreas de mayor acción. Para hacerlo sería más acertado recurrir a algún marcador que detectara cambios conformacionales específicos de RXFP3 ya que las vías de señalización del receptor de RLN3 son compartidas por muchos otros GPCRs y receptores tirosin kinasa. Tal vez, una alternativa más factible seria utilizar varios marcadores simultáneamente para delimitar de manera más eficiente el punto óptimo de acción del sistema. Por ejemplo, se podrían utilizar otras MAPK que in vitro se activan (Van der Westhuizen et al. 2010; Kocan et al. 2014)

De igual modo, la activación *in vivo* de subfenotipos de neuronas RXFP3 positivas permitirá diferenciar las funciones específicas de cada una de las poblaciones Rxfp3 positivas. Así pues, la activación exclusiva de Rxfp3 en neuronas PV/Rxfp3 cerca de la línea media del septum medial puede revelar si existe una acción antagónica sobre la acción de las neuronas Rxfp3/vGAT positivas de regiones laterales del septum medial y viceversa. La inhibición de neuronas Rxfp3/vGAT positivas distribuidas en MS-2 y MS-3 puede tener como consecuencia la desinhibición de neuronas glutamatérgicas de proyección en SUM lo que promueve el ritmo theta, relacionado con memoria espacial. Por otra parte, la activación de Rxfp3 en neuronas Rxfp3/PV positivas inhibiría

estas neuronas teniendo como resultado la inhibición de parte de la vida septohipocampica.

Desde un punto de vista comportamental la formación de memoria social tiene diferentes variantes que tras la activación del sistema RLN3/RXFP3 aún están por testar. Por ejemplo, no conocemos el efecto que tiene el sistema sobre memoria social a largo-plazo, en comportamiento espacial motivado o de ganancia y cambio (win-shift behaviours). Así mismo, en roedores la memoria de reconocimiento social sigue una vía intrincada desde el estímulo inicial olfativo hasta que se consolida en CA1 ventral del hipocampo (Okuyama et al. 2016). Muchas de estas áreas están inervadas por fibras de RLN3 y tienen un alto grado de expresión de RXPF3. En estas áreas es necesario selectivamente activar fenotipos Rxfp3 positivos para ver si otros fenotipos alternativos a neuronas Rxfp3/Oxtr también contribuyen en la modulación de la memoria de reconocimiento social. Finalmente, se debería tomar en consideración las neuronas oxitocin y vasopresin positivas del núcleo paraventricular del hipotálamo como fuente de estos neuropéptidos ya que son cruciales para la memoria de reconocimiento social (Landgraf et al. 1995; Ferguson et al. 2001; Lukas et al. 2013; Gur et al. 2014) y se ha comprado mediante estudios electrofisiológicos que RXFP3 hiperpolariza estas neuronas in vivo (Kania et al. 2017).

Para llevar a cabo todas estas nuevas aplicaciones sería interesante poder activar RXFP3 mediante una aproximación no farmacológica. Es decir, mediante el uso de una estrategia basado en partículas víricas. El uso combinado de receptores activados exclusivamente por drogas de diseño artificial (DREADDs) expresados en subfenotipos de Rxfp3 (ej. Rxfp3/OXTR vs Rxfp3/-) a la vez que en otras regiones se inhibe la expresión de Rxfp3 utilizando shRXFP3 (diseñados en nuestro laboratorio) proporcionarían importantes detalles de cómo funcionan regiones específicas reguladas por el sistema RLN3/RXFP3 en condiciones cercanas a las fisiológicas. En paralelo otros estudios que activen específicamente las neuronas RLN3 positivas del NI permitiría estudiar que dosis de estimulación es necesaria para activar RXFP3 en áreas donde no se observan fibras RLN3 positivas como es el caso de OV, CeA o PVN y si esta activación tiene lugar por transmisión por volumen.

# 8

# Bibliography

Acsády L, Katona I, Martínez-Guijarro FJ, et al (2000) Unusual target selectivity of perisomatic inhibitory cells in the hilar region of the rat hippocampus. J Neurosci 20:6907–19. doi: https://doi.org/10.1523/JNEUROSCI.20-18-06907.2000

Ahn HJ, Hernandez CM, Levenson JM, et al (2008) c-Rel, an NF- B family transcription factor, is required for hippocampal long-term synaptic plasticity and memory formation. Learn Mem 15:539–549. doi: 10.1101/lm.866408

Albert-Gascó H, García-Avilés Á, Moustafa S, et al (2017) Central relaxin-3 receptor (RXFP3) activation increases ERK phosphorylation in septal cholinergic neurons and impairs spatial working memory. Brain Struct Funct 222:449–463. doi: 10.1007/s00429-016-1227-8

Albert-Gascó H, Ma S, Ros-Bernal F, et al (2018) GABAergic neurons in the rat medial septal complex express relaxin-3 receptor (RXFP3) mRNA. Front Neuroanat 11:133. doi: 10.3389/fnana.2017.00133

Alheid GF (2006) Extended Amygdala and Basal Forebrain. Ann N Y Acad Sci 985:185–205. doi: 10.1111/j.1749-6632.2003.tb07082.x

Alheid GFF, Beltramino CAA, de Olmos JSS, et al (1998) The neuronal organization of the supracapsular part of the stria terminalis in the rat: the dorsal component of the extended amygdala. Neuroscience 84:967–996. doi: 10.1016/S0306-4522(97)00560-5

Amaral DG, Scharfman HE, Lavenex P (2007) The dentate gyrus: fundamental neuroanatomical organization (dentate gyrus for dummies). Prog Brain Res 163:3–22. doi: 10.1016/S0079-6123(07)63001-5

Antonucci F, Alpar A, Kacza J, et al (2012) Cracking Down on Inhibition: Selective Removal of GABAergic Interneurons from Hippocampal Networks. J Neurosci 32:1989–2001. doi: 10.1523/JNEUROSCI.2720-11.2012

Arakawa H (2017) Involvement of serotonin and oxytocin in neural mechanism regulating amicable social signal in male mice: Implication for impaired recognition of amicable cues in BALB/c strain. Behav Neurosci 131:176–

191. doi: 10.1037/bne0000191

Atkinson RC, Shiffrin RM (1968) Human Memory: A Proposed System and its Control Processes. Psychol Learn Motiv 2:89–195. doi: 10.1016/S0079-7421(08)60422-3

Baddeley A (1992) Working memory. Science 255:556–559. doi: http://dx.doi.org/10.1126/science.1736359

Baddeley AD, Warrington EK (1970) Amnesia and the distinction between long- and short-term memory. J Verbal Learning Verbal Behav 9:176–189. doi: 10.1016/S0022-5371(70)80048-2

Banerjee A, Shen P-JJ, Ma S, et al (2010) Swim stress excitation of nucleus incertus and rapid induction of relaxin-3 expression via CRF1 activation. Neuropharmacology 58:145–155. doi: 10.1016/j.neuropharm.2009.06.019

Bannerman D., Rawlins JN., McHugh S., et al (2004a) Regional dissociations within the hippocampus—memory and anxiety. Neurosci Biobehav Rev 28:273–283. doi: 10.1016/j.neubiorev.2004.03.004

Bannerman DM, Matthews P, Deacon RMJ, Rawlins JNP (2004b) Medial septal lesions mimic effects of both selective dorsal and ventral hippocampal lesions. Behav Neurosci 118:1033–1041. doi: 10.1037/0735-7044.118.5.1033

Bassant M-HH, Simon A, Poindessous-Jazat F, et al (2005) Medial septal GABAergic neurons express the somatostatin sst2A receptor: functional consequences on unit firing and hippocampal theta. J Neurosci 25:2032–2041. doi: 10.1523/JNEUROSCI.4619-04.2005

Bathgate R a D, Oh MHY, Ling WJJ, et al (2013) Elucidation of relaxin-3 binding interactions in the extracellular loops of RXFP3. Front Endocrinol (Lausanne) 4:1–10. doi: 10.3389/fendo.2013.00013

Bathgate RA, Ivell R, Sanborn BM, et al (2006) International Union of Pharmacology LVII: recommendations for the nomenclature of receptors for relaxin family peptides. Pharmacol Rev 58:7–31. doi: 10.1124/pr.58.1.9

Bathgate RA, Samuel CS, Burazin TC, et al (2002) Human relaxin gene 3 (H3) and the equivalent mouse relaxin (M3) gene. Novel members of the relaxin peptide family. J Biol Chem 277:1148–1157. doi: 10.1074/jbc.M107882200

Baxter MG, Murray EA (2002) The amygdala and reward. Nat Rev Neurosci 3:563–573. doi: 10.1038/nrn875

Becker JT, Morris RG (1999) Working Memory(s). Brain Cogn 41:1–8. doi: 10.1006/brcg.1998.1092

Benarroch EE (2015) The amygdala: functional organization and involvement in neurologic disorders. Neurology 84:313–324. doi: 10.1212/WNL.0000000000001171

Billova S, Galanopoulou AS, Seidah NG, et al (2007) Immunohistochemical expression and colocalization of somatostatin, carboxypeptidase-E and prohormone convertases 1 and 2 in rat brain. Neuroscience 147:403–418. doi: 10.1016/j.neuroscience.2007.04.039

Blasiak A, Blasiak T, Lewandowski MH, et al (2013) Relaxin-3 innervation of the intergeniculate leaflet of the rat thalamus - neuronal tract-tracing and in vitro electrophysiological studies. Eur J Neurosci 37:1284–1294. doi: 10.1111/ejn.12155; 10.1111/ejn.12155

Bonnet L, Comte A, Tatu L, et al (2015) The role of the amygdala in the perception of positive emotions: “intensity detector”. Front Behav Neurosci 9:178. doi: 10.3389/fnbeh.2015.00178

Borhegyi Z, Freund TF (1998) Dual projection from the medial septum to the supramammillary nucleus in the rat. Brain Res Bull 46:453–9. doi: 10.1016/S0361-9230(98)00038-0

Borhegyi Z, Varga V, Szilágyi N, et al (2004) Phase segregation of medial septal GABAergic neurons during hippocampal theta activity. J Neurosci 24:8470–8479. doi: 10.1523/jneuroscience.1413-04.2004

Brito GNO, Thomas GJ (1981) T-maze alternation, response patterning, and septo-hippocampal circuitry in rats. Behav Brain Res 3:319–340. doi: 10.1016/0166-4328(81)90003-6

Brown RE, McKenna JT (2015) Turning a Negative into a Positive: Ascending GABAergic Control of Cortical Activation and Arousal. Front Neurol 6:135. doi: 10.3389/fneur.2015.00135

Burazin TC, Bathgate RA, Macris M, et al (2002) Restricted, but abundant, expression of the novel rat gene-3 (R3) relaxin in the dorsal tegmental region of brain. J Neurochem 82:1553–1557. doi: https://doi.org/10.1046/j.1471-4159.2002.01114.x

Buzsáki G (2002) Theta oscillations in the hippocampus. Neuron 33:325–340.

Buzsáki G (2005) Theta rhythm of navigation: link between path integration and landmark navigation, episodic and semantic memory. Hippocampus 15:827–840. doi: 10.1002/hipo.20113

Cacucci F, Lever C, Wills TJ, et al (2004) Theta-Modulated Place-by-Direction Cells in the Hippocampal Formation in the Rat. J Neurosci 24:8265–8277. doi: 10.1523/JNEUROSCI.2635-04.2004

Cádiz-Moretti B, Otero-García M, Martínez-García F, Lanuza E (2014) Afferent projections to the different medial amygdala subdivisions: a retrograde tracing study in the mouse. Brain Struct Funct 22:1033–1065. doi: 10.1007/s00429-014-0954-y

Calvez J, de Ávila C, Matte L-O, et al (2016) Role of relaxin-3/RXFP3 system in stress-induced binge-like eating in female rats. Neuropharmacology 102:207–215. doi: 10.1016/j.neuropharm.2015.11.014

Cammarota M, Bevilaqua LR, Ardenghi P, et al (2000) Learning-associated activation of nuclear MAPK, CREB and Elk-1, along with Fos production, in the rat hippocampus after a one-trial avoidance learning: abolition by NMDA receptor blockade. Brain Res Mol Brain Res 76:36–46. doi: 10.1523/JNEUROSCI.20-12-04563.2000

Choleris E, Little SR, Mong JA, et al (2007) Microparticle-based delivery of oxytocin receptor antisense DNA in the medial amygdala blocks social recognition in female mice. Proc Natl Acad Sci U S A 104:4670–4675. doi: 10.1073/pnas.0700670104

Colmers WF, Lukowiak K, Pittman QJ (1988) Neuropeptide Y action in the rat

hippocampal slice: site and mechanism of presynaptic inhibition. J Neurosci 8:3827–37. doi: 10.1523/JNEUROSCI.08-10-03827.1988

Colom L V, Castaneda MT, Reyna T, et al (2005) Characterization of medial septal glutamatergic neurons and their projection to the hippocampus. Synapse 58:151–164. doi: 10.1002/syn.20184

Coria-Avila GA, Manzo J, Garcia LI, et al (2014) Neurobiology of social attachments. Neurosci Biobehav Rev 43:173–182. doi: 10.1016/j.neubiorev.2014.04.004

Dantzer R, Bluthe R-M, Koob GF, Le Moal M (1987) Modulation of social memory in male rats by neurohypophyseal peptides. Psychopharmacology (Berl) 91:363–368. doi: 10.1007/BF00518192

Davidson MC, Amso D, Anderson LC, Diamond A (2006) Development of cognitive control and executive functions from 4 to 13 years: evidence from manipulations of memory, inhibition, and task switching. Neuropsychologia 44:2037–2078. doi: 10.1016/j.neuropsychologia.2006.02.006

Davis MC, Green MF, Lee J, et al (2014) Oxytocin-augmented social cognitive skills training in schizophrenia. Neuropsychopharmacology 39:2070–2077. doi: 10.1038/npp.2014.68

Davis S, Vanhoutte P, Pages C, et al (2000) The MAPK/ERK cascade targets both Elk-1 and cAMP response element-binding protein to control long-term potentiation-dependent gene expression in the dentate gyrus in vivo. J Neurosci 20:4563–4572.

de Ávila C, Chometton S, Lenglos C, et al (2018) Differential effects of relaxin-3 and a selective relaxin-3 receptor agonist on food and water intake and hypothalamic neuronal activity in rats. Behav Brain Res 336:135–144. doi: 10.1016/j.bbr.2017.08.044

Dong H-W, Petrovich GD, Swanson LW (2001) Topography of projections from amygdala to bed nuclei of the stria terminalis. Brain Res Rev 38:192–246. doi: 10.1016/S0165-0173(01)00079-0

Donizetti A, Grossi M, Pariante P, et al (2008) Two neuron clusters in the stem

of postembryonic zebrafish brain specifically express relaxin-3 gene: first evidence of nucleus incertus in fish. Dev Dyn 237:3864–3869. doi: 10.1002/dvdy.21786

Dreifuss JJ (1975) A review on neurosecretory granules: their contents and mechanisms of release. Ann N Y Acad Sci 248:184–201. doi: https://doi.org/10.1111/j.1749-6632.1975.tb34185.x

Drew WG, Miller LL, Baugh EL (1973) Effects of ?9-THC, LSD-25 and scopolamine on continuous, spontaneous alternation in the Y-maze. Psychopharmacologia 32:171–182. doi: 10.1007/BF00428688

Dulac C, Torello AT (2003) Sensory systems: Molecular detection of pheromone signals in mammals: from genes to behaviour. Nat Rev Neurosci 4:551–562. doi: 10.1038/nrn1140

Dutar P, Bassant MH, Senut MC, Lamour Y (1995) The septohippocampal pathway: structure and function of a central cholinergic system. Physiol Rev 75:393–427. doi: 10.1152/physrev.1995.75.2.393

Everts HG, Koolhaas JM (1997) Lateral septal vasopressin in rats: role in social and object recognition? Brain Res 760:1–7. doi: https://doi.org/10.1016/S0006-8993(97)00269-2

Eysenck MW (1988) Models of memory: information processing. Psychopharmacol Ser 6:3–11.

Fadda F, Melis F, Stancampiano R (1996) Increased hippocampal acetylcholine release during a working memory task. Eur J Pharmacol 307:R1-2.

Faridar A, Jones-Davis D, Rider E, et al (2014) Mapk/Erk activation in an animal model of social deficits shows a possible link to autism. Mol Autism 5:57. doi: 10.1186/2040-2392-5-57

Farooq U, Kumar JR, Rajkumar R, Dawe GS (2016) Electrical microstimulation of the nucleus incertus induces forward locomotion and rotation in rats. Physiol Behav 160:50–58. doi: 10.1016/j.physbeh.2016.03.033

Ferguson JN, Aldag JM, Insel TR, Young LJ (2001) Oxytocin in the medial

amygdala is essential for social recognition in the mouse. J Neurosci 21:8278–8285.

Fitz NF, Gibbs RB, Johnson DA (2008) Selective lesion of septal cholinergic neurons in rats impairs acquisition of a delayed matching to position T-maze task by delaying the shift from a response to a place strategy. Brain Res Bull 77:356–60. doi: 10.1016/j.brainresbull.2008.08.016

Ford B, Holmes CJ, Mainville L, Jones BE (1995) GABAergic neurons in the rat pontomesencephalic tegmentum: codistribution with cholinergic and other tegmental neurons projecting to the posterior lateral hypothalamus. J Comp Neurol 363:177–196. doi: 10.1002/cne.903630203

Fox AS, Oler JA, Tromp DPMM, et al (2015) Extending the amygdala in theories of threat processing. Trends Neurosci 38:319–329. doi: 10.1016/j.tins.2015.03.002

Freund TF, Antal M (1988) GABA-containing neurons in the septum control inhibitory interneurons in the hippocampus. Nature 336:170–173. doi: 10.1038/336170a0

Freund TF, Buzsáki G (1998) Interneurons of the hippocampus. Hippocampus 6:347–470. doi: 10.1002/(SICI)1098-1063(1996)6:4<347::AID-HIPO1>3.0.CO;2-I

Freund TF, Gulyas AI (1997) Inhibitory control of GABAergic interneurons in the hippocampus. Can J Physiol Pharmacol 75:479–487. doi: 10.3389/fnins.2012.00165

Fuhrmann F, Justus D, Sosulina L, et al (2015) Locomotion, Theta Oscillations, and the Speed-Correlated Firing of Hippocampal Neurons Are Controlled by a Medial Septal Glutamatergic Circuit. Neuron 86:1253–1264. doi: 10.1016/j.neuron.2015.05.001

Ganella DE, Ma S, Gundlach AL (2013) Relaxin-3/RXFP3 signaling and neuroendocrine function - A perspective on extrinsic hypothalamic control. Front Endocrinol (Lausanne) 4:1–11. doi: 10.3389/fendo.2013.00128

Gangadharan G, Shin J, Kim S-W, et al (2016a) Medial septal GABAergic projection neurons promote object exploration behavior and type 2 theta

rhythm. Proc Natl Acad Sci U S A 113:6550–5. doi: 10.1073/pnas.1605019113

Gangadharan G, Shin J, Kim S-W, et al (2016b) Medial septal GABAergic projection neurons promote object exploration behavior and type 2 theta rhythm. Proc Natl Acad Sci U S A 113:6550–6555. doi: 10.1073/pnas.1605019113

Gheusi G, Bluthé R-M, Goodall G, Dantzer R (1994) Social and individual recognition in rodents: Methodological aspects and neurobiological bases. Behav Processes 33:59–87. doi: 10.1016/0376-6357(94)90060-4

Gibbs RB, Johnson DA (2007) Cholinergic lesions produce task-selective effects on delayed matching to position and configural association learning related to response pattern and strategy. Neurobiol Learn Mem 88:19–32. doi: 10.1016/j.nlm.2007.03.007

Giese KP, Mizuno K (2013) The roles of protein kinases in learning and memory. Learn Mem 20:540–552. doi: 10.1101/lm.028449.112

Givens B, Olton DS (1994) Local modulation of basal forebrain: effects on working and reference memory. J Neurosci 14:3578–3587.

Givens BS, Olton DS (1990) Cholinergic and GABAergic modulation of medial septal area: effect on working memory. Behav Neurosci 104:849–855. doi: 10.1037/0735-7044.104.6.849

Gobrogge KL, Liu Y, Young LJ, Wang Z (2009) Anterior hypothalamic vasopressin regulates pair-bonding and drug-induced aggression in a monogamous rodent. Proc Natl Acad Sci U S A 106:19144–19149. doi: 10.1073/pnas.0908620106

Goto M, Swanson LW, Canteras NS (2001) Connections of the nucleus incertus. J Comp Neurol 438:86–122. doi: 10.1002/cne.1303

Green MF, Horan WP, Lee J (2015) Social cognition in schizophrenia. Nat Rev Neurosci 16:620–631. doi: 10.1038/nrn4005

Gritti I, Henny P, Galloni F, et al (2006) Stereological estimates of the basal forebrain cell population in the rat, including neurons containing choline

acetyltransferase, glutamic acid decarboxylase or phosphate-activated glutaminase and colocalizing vesicular glutamate transporters. Neuroscience 143:1051–1064. doi: 10.1016/j.neuroscience.2006.09.024

Gritti I, Manns ID, Mainville L, Jones BE (2003) Parvalbumin, calbindin, or calretinin in cortically projecting and GABAergic, cholinergic, or glutamatergic basal forebrain neurons of the rat. J Comp Neurol 458:11–31. doi: 10.1002/cne.10505

Gulyas AI, Hajos N, Katona I, Freund TF (2003) Interneurons are the local targets of hippocampal inhibitory cells which project to the medial septum. Eur J Neurosci 17:1861–1872. doi: 10.1046/j.1460-9568.2003.02630.x

Gupta R, Koscik TR, Bechara A, Tranel D (2011) The amygdala and decision-making. Neuropsychologia 49:760–766. doi: 10.1016/j.neuropsychologia.2010.09.029

Gur R, Tendler A, Wagner S (2014) Long-Term Social Recognition Memory Is Mediated by Oxytocin-Dependent Synaptic Plasticity in the Medial Amygdala. Biol Psychiatry 76:377–386. doi: 10.1016/j.biopsych.2014.03.022

Gutiérrez-Castellanos N, Pardo-Bellver C, Martínez-García F, Lanuza E (2014) The vomeronasal cortex - afferent and efferent projections of the posteromedial cortical nucleus of the amygdala in mice. Eur J Neurosci 39:141–158. doi: 10.1111/ejn.12393

Haidar M, Guèvremont G, Zhang C, et al (2017) Relaxin-3 inputs target hippocampal interneurons and deletion of hilar relaxin-3 receptors in “floxed-RXFP3” mice impairs spatial memory. Hippocampus 27:529–546. doi: 10.1002/hipo.22709

Halls ML, van der Westhuizen ET, Bathgate R a D, Summers RJ (2007) Relaxin family peptide receptors--former orphans reunite with their parent ligands to activate multiple signalling pathways. Br J Pharmacol 150:677–691. doi: 10.1038/sj.bjp.0707140

Hangya B, Borhegyi Z, Szilagyi N, et al (2009) GABAergic neurons of the medial septum lead the hippocampal network during theta activity. J

Neurosci 29:8094–8102. doi: 10.1523/jneurosci.5665-08.2009

Happé F, Conway JR (2016) Recent progress in understanding skills and impairments in social cognition. Curr Opin Pediatr 28:736–742. doi: 10.1097/MOP.0000000000000417

Hashimoto H, Fukui K, Noto T, et al (1985) Distribution of vasopressin and oxytocin in rat brain. Endocrinol Jpn 32:89–97.

Hatalski CG, Guirguis C, Baram TZ (1998) Corticotropin releasing factor mRNA expression in the hypothalamic paraventricular nucleus and the central nucleus of the amygdala is modulated by repeated acute stress in the immature rat. J Neuroendocrinol 10:663–669.

Heinrichs M, Domes G (2008) Neuropeptides and social behaviour: effects of oxytocin and vasopressin in humans. Prog Brain Res 170:337–350. doi: 10.1016/S0079-6123(08)00428-7

Henderson Z, Lu C, Janzsó G, et al (2010) Distribution and role of Kv3. 1b in neurons in the medial septum diagonal band complex. Neuroscience 166:952–969. doi: 10.1016/j.neuroscience.2010.01.020

Hepler D, Olton D, Wenk G, Coyle J (1985) Lesions in nucleus basalis magnocellularis and medial septal area of rats produce qualitatively similar memory impairments. J Neurosci 5:866–873.

Hirase H, Czurkó A, Csicsvari J, Buzsáki G (1999) Firing rate and theta-phase coding by hippocampal pyramidal neurons during “space clamping”. Eur J Neurosci 11:4373–4380.

Hitti FL, Siegelbaum SA (2014) The hippocampal CA2 region is essential for social memory. Nature 508:88–92. doi: 10.1038/nature13028

Honig WK (2018) Studies of Working Memory in the Pigeon. 211–248. doi: 10.4324/9780203710029-8

Hosken IT, Sutton SW, Smith CM, Gundlach AL (2015) Relaxin-3 receptor (Rxfp3) gene knockout mice display reduced running wheel activity: Implications for role of relaxin-3/RXFP3 signalling in sustained arousal. Behav Brain Res 278:167–175. doi: 10.1016/j.bbr.2014.09.028

Huh CYL, Goutagny R, Williams S (2010) Glutamatergic neurons of the mouse medial septum and diagonal band of Broca synaptically drive hippocampal pyramidal cells: relevance for hippocampal theta rhythm. J Neurosci 30:15951–15961. doi: 10.1523/jneurosci.3663-10.2010

Hurlemann R, Patin A, Onur OA, et al (2010) Oxytocin enhances amygdala-dependent, socially reinforced learning and emotional empathy in humans. J Neurosci 30:4999–5007. doi: 10.1523/JNEUROSCI.5538-09.2010

Impey S, Obrietan K, Storm DR (1999) Making new connections: role of ERK/MAP kinase signaling in neuronal plasticity. Neuron 23:11–40.

Jan LY, Jan YN (1982) Peptidergic transmission in sympathetic ganglia of the frog. J Physiol 327:219–46.

Johnson DA, Zambon NJ, Gibbs RB (2002) Selective lesion of cholinergic neurons in the medial septum by 192 IgG-saporin impairs learning in a delayed matching to position T-maze paradigm. Brain Res 943:132–141.

Justice NJ, Yuan ZF, Sawchenko PE, Vale W (2008) Type 1 corticotropin-releasing factor receptor expression reported in BAC transgenic mice: implications for reconciling ligand-receptor mismatch in the central corticotropin-releasing factor system. J Comp Neurol 511:479–96. doi: 10.1002/cne.21848

Kania A, Gugula A, Grabowiecka A, et al (2017) Inhibition of oxytocin and vasopressin neuron activity in rat hypothalamic paraventricular nucleus by relaxin-3-RXFP3 signalling. J Physiol 595:3425–3447. doi: 10.1113/JP273787

Kania A, Lewandowski MH, Błasiak A (2014) Relaxin-3 and relaxin family peptide receptors--from structure to functions of a newly discovered mammalian brain system. Postepy Hig Med Dosw (Online) 68:851–864.

Kelsey JE, Vargas H (1993) Medial septal lesions disrupt spatial, but not nonspatial, working memory in rats. Behav Neurosci 107:565–574.

Kemp IR, Kaada BR (1975) The relation of hippocampal theta activity to arousal, attentive behaviour and somato-motor movements in

unrestrained cats. Brain Res 95:323–342. doi: 10.1016/0006-8993(75)90110-9

Kirk IJ (1998) Frequency modulation of hippocampal theta by the supramammillary nucleus, and other hypothalamo-hippocampal interactions: mechanisms and functional implications. Neurosci Biobehav Rev 22:291–302.

Kiss J, Maglóczky Z, Somogyi J, Freund T. (1997) Distribution of calretinin-containing neurons relative to other neurochemically-identified cell types in the medial septum of the rat. Neuroscience 78:399–410. doi: 10.1016/S0306-4522(96)00508-8

Kiss J, Patel AJ, Baimbridge KG, Freund TF (1990) Topographical localization of neurons containing parvalbumin and choline acetyltransferase in the medial septum-diagonal band region of the rat. Neuroscience 36:61–72. doi: 10.1016/0306-4522(90)90351-4

Kitabatake Y, Hikida T, Watanabe D, et al (2003) Impairment of reward-related learning by cholinergic cell ablation in the striatum. Proc Natl Acad Sci 100:7965–7970. doi: 10.1073/pnas.1032899100

Kocan M, Sarwar M, Hossain M a., et al (2014) Signalling profiles of H3 relaxin, H2 relaxin and R3(BΔ23-27)R/I5 acting at the relaxin family peptide receptor 3 (RXFP3). Br J Pharmacol 171:2827–2841. doi: 10.1111/bph.12623

Köhler C, Eriksson LG (1984) An immunohistochemical study of somatostatin and neurotensin positive neurons in the septal nuclei of the rat brain. Anat Embryol (Berl) 170:1–10.

Köhler C, Srebro B (1980) Effects of lateral and medial septal lesions on exploratory behavior in the albino rat. Brain Res 182:423–440. doi: 10.1016/0006-8993(80)91199-3

Korotkova T, Ponomarenko A, Monaghan CK, et al (2017) Reconciling the different faces of hippocampal theta: The role of theta oscillations in cognitive, emotional and innate behaviors. Neurosci Biobehav Rev. doi: 10.1016/j.neubiorev.2017.09.004

Korzan WJ, Summers TR, Ronan PJ, et al (2001) The role of monoaminergic nuclei during aggression and sympathetic social signaling. Brain Behav Evol 57:317–327.

Kubota Y, Inagaki S, Shiosaka S, et al (1983) The distribution of cholecystokinin octapeptide-like structures in the lower brain stem of the rat: an immunohistochemical analysis. Neuroscience 9:587–604. doi: 10.1016/0306-4522(83)90176-8

Kuei C, Sutton S, Bonaventure P, et al (2007) R3(BΔ23–27)R/I5 Chimeric Peptide, a Selective Antagonist for GPCR135 and GPCR142 over Relaxin Receptor LGR7. J Biol Chem 282:25425–25435. doi: 10.1074/jbc.M701416200

Kuhlmann S, Piel M, Wolf OT (2005) Impaired Memory Retrieval after Psychosocial Stress in Healthy Young Men.

Landgraf R, Gerstberger R, Montkowski A, et al (1995) V1 vasopressin receptor antisense oligodeoxynucleotide into septum reduces vasopressin binding, social discrimination abilities, and anxiety-related behavior in rats. J Neurosci 15:4250–4258.

Leão RN, Targino ZH, Colom L V, Fisahn A (2015) Interconnection and synchronization of neuronal populations in the mouse medial septum/diagonal band of Broca. J Neurophysiol 113:971–80. doi: 10.1152/jn.00367.2014

Lee LC, Rajkumar R, Dawe GS (2014) Selective lesioning of nucleus incertus with corticotropin releasing factor-saporin conjugate. Brain Res 1543:179–190. doi: 10.1016/j.brainres.2013.11.021

Lee S-H, Dan Y (2012) Neuromodulation of brain states. Neuron 76:209–22. doi: 10.1016/j.neuron.2012.09.012

Lenglos C, Mitra A, Guèvremont G, Timofeeva E (2014) Regulation of expression of relaxin-3 and its receptor RXFP3 in the brain of diet-induced obese rats. Neuropeptides 48:119–132. doi: 10.1016/J.NPEP.2014.02.002

Leranth C, Carpi D, Buzsaki G, Kiss J (1999) The entorhino-septo-

supramammillary nucleus connection in the rat: morphological basis of a feedback mechanism regulating hippocampal theta rhythm. Neuroscience 88:701–718. doi: 10.1016/S0306-4522(98)00245-0

Leranth C, Frotscher M (1989) Organization of the septal region in the rat brain: Cholinergic-GABAergic interconnections and the termination of hippocampo-septal fibers. J Comp Neurol 289:304–314. doi: 10.1002/cne.902890210

Leranth C, Kiss J (1996) A population of supramammillary area calretinin neurons terminating on medial septal area cholinergic and lateral septal area calbindin-containing cells are aspartate/glutamatergic. J Neurosci 16:7699–710.

Leung LS, Yim CY (1986) Intracellular records of theta rhythm in hippocampal CA1 cells of the rat. Brain Res 367:323–327. doi: 10.1016/0006-8993(86)91611-2

Leutgeb S, Leutgeb JK, Moser M-B, Moser EI (2005) Place cells, spatial maps and the population code for memory. Curr Opin Neurobiol 15:738–746. doi: 10.1016/J.CONB.2005.10.002

Li Y, Kim J (2015) Neuronal expression of CB2 cannabinoid receptor mRNAs in the mouse hippocampus. Neuroscience 311:253–267. doi: 10.1016/j.neuroscience.2015.10.041

Liu C, Chen J, Kuei C, et al (2005) Relaxin-3/insulin-like peptide 5 chimeric peptide, a selective ligand for G protein-coupled receptor (GPCR)135 and GPCR142 over leucine-rich repeat-containing G protein-coupled receptor 7. Mol Pharmacol 67:231–40. doi: 10.1124/mol.104.006700

Liu C, Eriste E, Sutton S, et al (2003) Identification of Relaxin-3/INSL7 as an Endogenous Ligand for the Orphan G-protein-coupled Receptor GPCR135. J Biol Chem 278:50754–50764. doi: 10.1074/jbc.M308995200

Ludwig M, Leng G (2006) Dendritic peptide release and peptide-dependent behaviours. Nat Rev Neurosci 7:126–136. doi: 10.1038/nrn1845

Ludwig M, Sabatier N, Bull PM, et al (2002) Intracellular calcium stores regulate activity-dependent neuropeptide release from dendrites. Nature 418:85–

89. doi: 10.1038/nature00822

Lukas M, Toth I, Veenema AH, Neumann ID (2013) Oxytocin mediates rodent social memory within the lateral septum and the medial amygdala depending on the relevance of the social stimulus: Male juvenile versus female adult conspecifics. Psychoneuroendocrinology 38:916–926. doi: 10.1016/j.psyneuen.2012.09.018

Ma S, Blasiak A, Olucha-Bordonau FE, et al (2013) Heterogeneous responses of nucleus incertus neurons to corticotrophin-releasing factor and coherent activity with hippocampal theta rhythm in the rat. J Physiol 591:3981–4001. doi: 10.1113/jphysiol.2013.254300

Ma S, Bonaventure P, Ferraro T, et al (2007) Relaxin-3 in GABA projection neurons of nucleus incertus suggests widespread influence on forebrain circuits via G-protein-coupled receptor-135 in the rat. Neuroscience 144:165–190. doi: 10.1016/j.neuroscience.2006.08.072

Ma S, Olucha-Bordonau FE, Hossain A, et al (2009a) Modulation of hippocampal theta oscillations and spatial memory by relaxin-3 neurons of the nucleus incertus. Learn Mem 16:730–742. doi: 10.1101/lm.1438109

Ma S, Sang Q, Lanciego JL, Gundlach AL (2009b) Localization of relaxin-3 in brain of Macaca fascicularis: identification of a nucleus incertus in primate. J Comp Neurol 517:856–872. doi: 10.1002/cne.22197

Ma S, Smith CM, Blasiak A, Gundlach AL (2017) Distribution, physiology and pharmacology of relaxin-3/RXFP3 systems in brain. Br J Pharmacol 174:1034–1048. doi: 10.1111/bph.13659

Mairesse J, Gatta E, Reynaert M-L, et al (2015) Activation of presynaptic oxytocin receptors enhances glutamate release in the ventral hippocampus of prenatally restraint stressed rats. Psychoneuroendocrinology 62:36–46. doi: 10.1016/j.psyneuen.2015.07.005

Mamad O, McNamara HM, Reilly RB, Tsanov M (2015) Medial septum regulates the hippocampal spatial representation. Front Behav Neurosci

9:166. doi: 10.3389/fnbeh.2015.00166

Manseau F, Danik M, Williams S (2005) A functional glutamatergic neurone network in the medial septum and diagonal band area. J Physiol 566:865–884. doi: 10.1113/jphysiol.2005.089664

Martínez-Bellver S, Cervera-Ferri A, Luque-García A, et al (2017) Causal relationships between neurons of the nucleus incertus and the hippocampal theta activity in the rat. J Physiol 595:1775–1792. doi: 10.1113/JP272841

Martínez-Bellver S, Cervera-Ferri A, Martínez-Ricós J, et al (2015) Regular theta-firing neurons in the nucleus incertus during sustained hippocampal activation. Eur J Neurosci 41:1049–67. doi: 10.1111/ejn.12934

Maski K, Holbrook H, Manoach D, et al (2015) Sleep Dependent Memory Consolidation in Children with Autism Spectrum Disorder. Sleep 38:1955–1963. doi: 10.5665/sleep.5248

Matsumoto M, Kamohara M, Sugimoto T, et al (2000) The novel G-protein coupled receptor SALPR shares sequence similarity with somatostatin and angiotensin receptors. Gene 248:183–9.

Mattson MP, Camandola S (2001) NF-κB in neuronal plasticity and neurodegenerative disorders. J Clin Invest 107:247–254. doi: 10.1172/JCI11916

McGowan BM, Stanley SA, White NE, et al (2007) Hypothalamic mapping of orexigenic action and Fos-like immunoreactivity following relaxin-3 administration in male Wistar rats. Am J Physiol Metab 292:913–919. doi: 10.1152/ajpendo.00346.2006

McGowan BMC, Stanley SA, Smith KL, et al (2005) Central Relaxin-3 Administration Causes Hyperphagia in Male Wistar Rats. Endocrinology 146:3295–3300. doi: 10.1210/en.2004-1532

McNaughton BL, Barnes CA, Gerrard JL, et al (1996) Deciphering the hippocampal polyglot: the hippocampus as a path integration system. J Exp Biol 199:173–85.

McNaughton BL, Battaglia FP, Jensen O, et al (2006) Path integration and the neural basis of the “cognitive map.” Nat Rev Neurosci 7:663–678. doi: 10.1038/nrn1932

Meadows KL, Byrnes EM (2015) Sex- and age-specific differences in relaxin family peptide receptor expression within the hippocampus and amygdala in rats. Neuroscience 284:337–348. doi: 10.1016/j.neuroscience.2014.10.006

Milner B (1972) Disorders of learning and memory after temporal lobe lesions in man. Clin Neurosurg 19:421–46.

Morales FR, Roig J a, Monti JM, et al (1971) Septal unit activity and hippocampal EEG during the sleep-wakefulness cycle of the rat. Physiol Behav 6:563–567. doi: 10.1016/0031-9384(71)90206-X

Morellini F (2013) Spatial memory tasks in rodents: what do they model? Cell Tissue Res 354:273–286. doi: 10.1007/s00441-013-1668-9

Mysin IE, Kitchigina VF, Kazanovich Y (2015) Modeling synchronous theta activity in the medial septum: key role of local communications between different cell populations. J Comput Neurosci 39:1–16. doi: 10.1007/s10827-015-0564-6

Nerad L, McNaughton N (2006) The septal EEG suggests a distributed organization of the pacemaker of hippocampal theta in the rat. Eur J Neurosci 24:155–166. doi: 10.1111/j.1460-9568.2006.04902.x

Nordmann JJ, Morris JF (1984) Method for quantitating the molecular content of a subcellular organelle: hormone and neurophysin content of newly formed and aged neurosecretory granules. Proc Natl Acad Sci U S A 81:180–4.

Nuñez a., Cervera-Ferri A, Olucha-Bordonau F, et al (2006) Nucleus incertus contribution to hippocampal theta rhythm generation. Eur J Neurosci 23:2731–2738. doi: 10.1111/j.1460-9568.2006.04797.x

O’Keefe J (1976) Place units in the hippocampus of the freely moving rat. Exp Neurol 51:78–109. doi: 10.1016/0014-4886(76)90055-8

O'Keefe J, Dostrovsky J (1971) The hippocampus as a spatial map. Preliminary evidence from unit activity in the freely-moving rat. Brain Res 34:171–5.

O'Keefe J, Recce ML (1993) Phase relationship between hippocampal place units and the EEG theta rhythm. Hippocampus 3:317–330. doi: 10.1002/hipo.450030307

Okada K, Nishizawa K, Kobayashi T, et al (2015) Distinct roles of basal forebrain cholinergic neurons in spatial and object recognition memory. Sci Rep 5:13158. doi: 10.1038/srep13158

Okuyama T, Kitamura T, Roy DS, et al (2016) Ventral CA1 neurons store social memory.

Olton DS, Becker JT, Handelmann GE (1979) Hippocampus, space, and memory. Behav Brain Sci 2:313–322. doi: 10.1017/S0140525X00062713

Olton DS, Samuelson RJ (1976) Remembrance of places passed: Spatial memory in rats. J Exp Psychol Anim Behav Process 2:97–116. doi: 10.1037/0097-7403.2.2.97

Olucha-Bordonau FE, Fortes-Marco L, Otero-García M, et al (2014) The amygdala structure and function. In: Paxinos G (ed) The rat nervous system. IV Edition. pp 441–490

Olucha-Bordonau FE, Otero-García M, Sánchez-Pérez AM, et al (2012) Distribution and targets of the relaxin-3 innervation of the septal area in the rat. J Comp Neurol 520:1903–1939. doi: 10.1002/cne.23018

Olucha-Bordonau FE, Teruel V, Barcia-González J, et al (2003) Cytoarchitecture and efferent projections of the nucleus incertus of the rat. J Comp Neurol 464:62–97. doi: 10.1002/cne.10774

Osborne PG (1994) A GABAergic mechanism in the medial septum influences cortical arousal and locomotor activity but not a previously learned spatial discrimination task. Neurosci Lett 173:63–66. doi: 10.1016/0304-3940(94)90150-3

Otsubo H, Onaka T, Suzuki H, et al (2010) Centrally administered relaxin-3 induces Fos expression in the osmosensitive areas in rat brain and

facilitates water intake. Peptides 31:1124–1130. doi: 10.1016/j.peptides.2010.02.020

Pan WX, McNaughton N (1997) The medial supramammillary nucleus, spatial learning and the frequency of hippocampal theta activity. Brain Res 764:101–108.

Paxinos GG, Watson C (2014) The Rat Brain in Stereotaxic Coordinates. Academic Press, San Dicego

Pellissier LP, Gandía J, Laboute T, et al (2017) μ opioid receptor, social behaviour and autism spectrum disorder: reward matters. Br J Pharmacol. doi: 10.1111/bph.13808

Peng S, Zhang Y, Zhang J, et al (2010) ERK in learning and memory: a review of recent research. Int J Mol Sci 11:222–232. doi: 10.3390/ijms11010222

Pereira CW, Santos FN, Sanchez-Perez AM, et al (2013) Electrolytic lesion of the nucleus incertus retards extinction of auditory conditioned fear. Behav Brain Res 247:201–210. doi: 10.1016/j.bbr.2013.03.025; 10.1016/j.bbr.2013.03.025

Poucet B (1989) Object exploration, habituation, and response to a spatial change in rats following septal or medial frontal cortical damage. Behav Neurosci 103:1009–1016. doi: 10.1037/0735-7044.103.5.1009

Pro-Sistiaga P, Mohedano-Moriano A, Ubeda-Bañon I, et al (2007) Convergence of olfactory and vomeronasal projections in the rat basal telencephalon. J Comp Neurol 504:346–362. doi: 10.1002/cne.21455

Raghavachari S, Kahana MJ, Rizzuto DS, et al (2001) Gating of human theta oscillations by a working memory task. J Neurosci 21:3175–3183. doi: 21/9/3175 [pii]

Ragozzino ME, Unick KE, Gold PE (1996) Hippocampal acetylcholine release during memory testing in rats: augmentation by glucose. Proc Natl Acad Sci U S A 93:4693–4698.

Rajkumar R, Wu Y, Farooq U, et al (2016) Stress activates the nucleus incertus and modulates plasticity in the hippocampo-medial prefrontal cortical

pathway. Brain Res Bull 120:83–90. doi: 10.1016/j.brainresbull.2015.10.010

Ramanan N, Shen Y, Sarsfield S, et al (2005) SRF mediates activity-induced gene expression and synaptic plasticity but not neuronal viability. Nat Neurosci 8:759–767. doi: 10.1038/nn1462

Ranck JB (1973) Studies on single neurons in dorsal hippocampal formation and septum in unrestrained rats. I. Behavioral correlates and firing repertoires. Exp Neurol 41:461–531.

Rasia-Filho AA, Londero RG, Achaval M (2000) Functional activities of the amygdala: an overview. J Psychiatry Neurosci 25:14–23.

Richter K, Wolf G, Engelmann M (2005) Social recognition memory requires two stages of protein synthesis in mice. Learn Mem 12:407–413. doi: 10.1101/lm.97505

Risold PY, Swanson LW (1997) Chemoarchitecture of the rat lateral septal nucleus. Brain Res Brain Res Rev 24:91–113.

Robinson J, Manseau F, Ducharme G, et al (2016) Optogenetic activation of septal glutamatergic neurons drive hippocampal theta rhythms. J Neurosci 36:3016–3023. doi: 10.1523/jneurosci.2141-15.2016

Roland JJ, Stewart AL, Janke KL, et al (2014) Medial septum-diagonal band of Broca (MSDB) GABAergic regulation of hippocampal acetylcholine efflux is dependent on cognitive demands. J Neurosci 34:506–14. doi: 10.1523/JNEUROSCI.2352-13.2014

Rosengren KJ, Lin F, Bathgate RAD, et al (2006) Solution Structure and Novel Insights into the Determinants of the Receptor Specificity of Human Relaxin-3. J Biol Chem 281:5845–5851. doi: 10.1074/jbc.M511210200

Ruan M, Young CK, McNaughton N (2017) Bi-Directional Theta Modulation between the Septo-Hippocampal System and the Mammillary Area in Free-Moving Rats. Front Neural Circuits 11:62. doi: 10.3389/fncir.2017.00062

Ryan PJ, Buchler E, Shabanpoor F, et al (2013a) Central relaxin-3 receptor

(RXFP3) activation decreases anxiety- and depressive-like behaviours in the rat. Behav Brain Res 244:142–151. doi: 10.1016/j.bbr.2013.01.034; 10.1016/j.bbr.2013.01.034

Ryan PJ, Kastman HE, Krstew E V., et al (2013b) Relaxin-3/RXFP3 system regulates alcohol-seeking. Proc Natl Acad Sci U S A 110:20789–20794. doi: 10.1073/pnas.1317807110

Ryan PJ, Ma S, Olucha-Bordonau FE, Gundlach AL (2011) Nucleus incertus-An emerging modulatory role in arousal, stress and memory. Neurosci Biobehav Rev 35:1326–1341. doi: 10.1016/j.neubiorev.2011.02.004

Sánchez-Pérez AM, Arnal-Vicente I, Santos FN, et al (2015) Septal projections to the nucleus incertus: Bidirectional pathways for modulation of hippocampal function. J Comp Neurol 523:565–588. doi: 10.1002/cne.23687

Sanchez-Perez AM, Garcia-Aviles A, Albert Gasco H, et al (2012) [Effects of methylphenidate on anxiety]. Rev Neurol 55:499–506.

Sanderson DJ, Bannerman DM (2012) The role of habituation in hippocampus-dependent spatial working memory tasks: Evidence from GluA1 AMPA receptor subunit knockout mice. Hippocampus 22:981–994. doi: 10.1002/hipo.20896

Santos FN, Pereira CW, Sánchez-Pérez AM, et al (2016) Comparative distribution of relaxin-3 inputs and calcium-binding protein-positive neurons in rat amygdala. Front Neuroanat 10:36. doi: 10.3389/fnana.2016.00036

Scalia F, Winans SS (1975) The differential projections of the olfactory bulb and accessory olfactory bulb in mammals. J Comp Neurol 161:31–55. doi: 10.1002/cne.901610105

Schiller D, Eichenbaum H, Buffalo EA, et al (2015) Memory and Space: Towards an Understanding of the Cognitive Map. J Neurosci 35:13904–13911. doi: 10.1523/JNEUROSCI.2618-15.2015

Schindelin J, Arganda-Carreras I, Frise E, et al (2012) Fiji: an open-source platform for biological-image analysis. Nat Methods 9:676–682. doi:

10.1038/nmeth.2019

Seese RR, Maske AR, Lynch G, Gall CM (2014) Long-term memory deficits are associated with elevated synaptic ERK1/2 activation and reversed by mGluR5 antagonism in an animal model of autism. Neuropsychopharmacology 39:1664–1673. doi: 10.1038/npp.2014.13

Servan A, Brunelin J, Poulet E (2017) The effects of oxytocin on social cognition in borderline personality disorder. Encephale. doi: 10.1016/j.encep.2017.11.001

Seymour B, Dolan R (2008) Emotion, Decision Making, and the Amygdala. Neuron 58:662–671. doi: 10.1016/j.neuron.2008.05.020

Shabanpoor F, Akhter Hossain M, Ryan PJ, et al (2012) Minimization of Human Relaxin-3 Leading to High-Affinity Analogues with Increased Selectivity for Relaxin-Family Peptide 3 Receptor (RXFP3) over RXFP1. J Med Chem 55:1671–1681. doi: 10.1021/jm201505p

Sherwood OD (2004) Relaxin's Physiological Roles and Other Diverse Actions. Endocr Rev 25:205–234. doi: 10.1210/er.2003-0013

Shojo H, Kaneko Y (2000) Characterization and Expression of Oxytocin and the Oxytocin Receptor. Mol Genet Metab 71:552–558. doi: 10.1006/MGME.2000.3094

Simon AP, Poindessous-Jazat F, Dutar P, et al (2006) Firing properties of anatomically identified neurons in the medial septum of anesthetized and unanesthetized restrained rats. J Neurosci 26:9038–9046. doi: 10.1523/JNEUROSCI.1401-06.2006

Smith CM, Hosken IT, Sutton SW, et al (2012) Relaxin-3 null mutation mice display a circadian hypoactivity phenotype. Genes, Brain Behav 11:94–104. doi: 10.1111/j.1601-183X.2011.00730.x

Smith CM, Shen PJ, Banerjee A, et al (2010) Distribution of relaxin-3 and RXFP3 within arousal, stress, affective, and cognitive circuits of mouse brain. J Comp Neurol 518:4016–4045. doi: 10.1002/cne.22442

Smith SM, Vale WW (2006) The role of the hypothalamic-pituitary-adrenal axis

in neuroendocrine responses to stress. Dialogues Clin Neurosci 8:383–395.

Sotty F, Danik M, Manseau F, et al (2003) Distinct electrophysiological properties of glutamatergic, cholinergic and GABAergic rat septohippocampal neurons: novel implications for hippocampal rhythmicity. J Physiol 551:927–943. doi: 10.1113/jphysiol.2003.046847

Sperk G, Hamilton T, Colmers WF (2007) Neuropeptide Y in the dentate gyrus. In: Progress in brain research. pp 285–297

Stumpf C, Petsche H, Gogolak G (1962) The significance of the rabbit's septum as a relay station between the midbrain and the hippocampus II. The differential influence of drugs upon both the septal cell firing pattern and the hippocampus theta activity. Electroencephalogr Clin Neurophysiol 14:212–219. doi: 10.1016/0013-4694(62)90031-7

Sutton SW, Bonaventure P, Kuei C, et al (2005) G-protein-coupled receptor (GPCR)-142 does not contribute to relaxin-3 binding in the mouse brain: Further support that relaxin-3 is the physiological ligand for GPCR135. Neuroendocrinology 82:139–150. doi: 10.1159/000091267

Sutton SW, Bonaventure P, Kuei C, et al (2004) Distribution of G-protein-coupled receptor (GPCR)135 binding sites and receptor mRNA in the rat brain suggests a role for relaxin-3 in neuroendocrine and sensory processing. Neuroendocrinology 80:298–307. doi: 10.1159/000083656

Swaab DF, Nijveldt F, Pool CW (1975) Distribution of oxytocin and vasopressin in the rat supraoptic and paraventricular nucleus. J Endocrinol 67:461–463. doi: 10.1677/JOE.0.0670461

Sweatt JD (2001) The neuronal MAP kinase cascade: a biochemical signal integration system subserving synaptic plasticity and memory. J Neurochem 76:1–10.

Sweeney JE, Lamour Y, Bassant MH (1992) Arousal-dependent properties of medial septal neurons in the unanesthetized rat. Neuroscience 48:353–362. doi: 10.1016/0306-4522(92)90495-N

Takahashi T, Ikeda K, Ishikawa M, et al (2004) Social stress-induced cortisol

elevation acutely impairs social memory in humans. Neurosci Lett 363:125–130. doi: 10.1016/J.NEULET.2004.03.062

Tanaka M, Iijima N, Miyamoto Y, et al (2005) Neurons expressing relaxin 3/INSL 7 in the nucleus incertus respond to stress. Eur J Neurosci 21:1659–1670. doi: 10.1111/j.1460-9568.2005.03980.x

Taube JS, Muller RU, Ranck JB, et al (1990) Head-direction cells recorded from the postsubiculum in freely moving rats. II. Effects of environmental manipulations. J Neurosci 10:436–447. doi: 10.1523/jneurosci.2635-04.2004

Terenzi MG, Ingram CD (2005) Oxytocin-induced excitation of neurones in the rat central and medial amygdaloid nuclei. Neuroscience 134:345–354. doi: 10.1016/j.neuroscience.2005.04.004

Thomas GJ, Gash DM (1986) Differential effects of posterior septal lesions on dispositional and representational memory. Behav. Neurosci. 100:712–719.

Thompson E, Varela FJ (2001) Radical embodiment: neural dynamics and consciousness. Trends Cogn Sci 5:418–425.

Toth K, Borhegyi Z, Freund TF (1993) Postsynaptic targets of GABAergic hippocampal neurons in the medial septum-diagonal band of broca complex. J Neurosci 13:3712–3724.

Toth K, Freund TF, Miles R (1997) Disinhibition of rat hippocampal pyramidal cells by GABAergic afferents from the septum. J Physiol 500 ( Pt 2:463–474.

Trainor BC, Crean KK, Fry WHD, Sweeney C (2010) Activation of extracellular signal-regulated kinases in social behavior circuits during resident-intruder aggression tests. Neuroscience 165:325–336. doi: 10.1016/j.neuroscience.2009.10.050

Trezza V, Campolongo P, Vanderschuren LJMJ (2011) Evaluating the rewarding nature of social interactions in laboratory animals. Dev Cogn Neurosci 1:444–458. doi: 10.1016/J.DCN.2011.05.007

Tsanov M (2015) Septo-hippocampal signal processing: breaking the code. Prog Brain Res 219:103–20. doi: 10.1016/bs.pbr.2015.04.002

Ujfalussy B, Kiss T (2006) How do glutamatergic and GABAergic cells contribute to synchronization in the medial septum? J Comput Neurosci 21:343–357. doi: 10.1007/s10827-006-9082-x

Unsworth N, Engle RW (2007) On the division of short-term and working memory: An examination of simple and complex span and their relation to higher order abilities. Psychol Bull 133:1038–1066. doi: 10.1037/0033-2909.133.6.1038

Van den Pol AN (2012) Neuropeptide transmission in brain circuits. Neuron 76:98–115. doi: 10.1016/j.neuron.2012.09.014

Van der Westhuizen ET, Christopoulos A, Sexton PM, et al (2010) H2 relaxin is a biased ligand relative to H3 relaxin at the relaxin family peptide receptor 3 (RXFP3). Mol Pharmacol 77:759–772. doi: 10.1124/mol.109.061432

Van der Westhuizen ET, Sexton PM, Bathgate RA, Summers RJ (2005) Responses of GPCR135 to human gene 3 (H3) relaxin in CHO-K1 cells determined by microphysiometry. Ann N Y Acad Sci 1041:332–337. doi: 10.1196/annals.1282.053

Van der Westhuizen ET Van Der, Werry TD, Sexton PM, Summers RJ (2007) The Relaxin Family Peptide Receptor 3 Activates Extracellular Signal-Regulated Kinase 1 / 2 through a Protein Kinase C-Dependent Mechanism. Mol Pharmacol 71:1618–1629. doi: 10.1124/mol.106.032763.growth

Vandecasteele M, Varga V, Berényi A, et al (2014) Optogenetic activation of septal cholinergic neurons suppresses sharp wave ripples and enhances theta oscillations in the hippocampus. Proc Natl Acad Sci 111:13535–13540. doi: 10.1073/pnas.1411233111

Varga V, Hangya B, Kranitz K, et al (2008) The presence of pacemaker HCN channels identifies theta rhythmic GABAergic neurons in the medial septum. J Physiol 586:3893–3915. doi: 10.1113/jphysiol.2008.155242

Veenema AH (2008) Central vasopressin and oxytocin release: regulation of complex social behaviours. Prog Brain Res 170:261–276. doi: 10.1016/S0079-6123(08)00422-6

Vertes RP (2005) Hippocampal theta rhythm: a tag for short-term memory. Hippocampus 15:923–935. doi: 10.1002/hipo.20118

Vertes RP, Kocsis B (1997) Brainstem-diencephalo-septohippocampal systems controlling the theta rhythm of the hippocampus. Neuroscience 81:893–926.

Vinogradova OS (1995) Expression, control, and probable functional significance of the neuronal theta-rhythm. Prog Neurobiol 45:523–583. doi: 10.1016/0301-0082(94)00051-I

Vögler O, Barceló JM, Ribas C, Escribá P V. (2008) Membrane interactions of G proteins and other related proteins. Biochim Biophys Acta - Biomembr 1778:1640–1652. doi: 10.1016/j.bbamem.2008.03.008

Vuilleumier P, Sander D (2008) Trust and valence processing in the amygdala. Soc Cogn Affect Neurosci 3:299–302. doi: 10.1093/scan/nsn045

Wang F, Flanagan J, Su N, et al (2012) RNAscope. J Mol Diagnostics 14:22–29. doi: 10.1016/j.jmoldx.2011.08.002

Wang H, Su N, Wang L-C, et al (2014) Quantitative ultrasensitive bright-field RNA in situ hybridization with RNAscope. In: Methods in molecular biology (Clifton, N.J.). pp 201–212

Wang Y, Zhao S, Wu Z, et al (2015) Oxytocin in the regulation of social behaviours in medial amygdala-lesioned mice via the inhibition of the extracellular signal-regulated kinase signalling pathway. Clin Exp Pharmacol Physiol 42:465–474. doi: 10.1111/1440-1681.12378

Wei B, Huang Z, He S, et al (2012) The onion skin-like organization of the septum arises from multiple embryonic origins to form multiple adult neuronal fates. Neuroscience 222:110–123. doi: 10.1016/j.neuroscience.2012.07.016

Williams DL, Goldstein G, Minshew NJ (2006) The profile of memory function

in children with autism. Neuropsychology 20:21–29. doi: 10.1037/0894-4105.20.1.21

Wilsbacher JL, Goldsmith EJ, Cobb MH (1999) Phosphorylation of MAP kinases by MAP/ERK involves multiple regions of MAP kinases. J Biol Chem 274:16988–16994. doi: 10.1074/JBC.274.24.16988

Winslow JT, Ferguson JN, Young LJ, et al (2000) Social amnesia in mice lacking the oxytocin gene. Nat Genet 25:284–288. doi: 10.1038/77040

Winslow JT, Insel TR (2004) Neuroendocrine basis of social recognition. Curr Opin Neurobiol 14:248–253. doi: 10.1016/j.conb.2004.03.009

Wu M, Shanabrough M, Leranth C, Alreja M (2000) Cholinergic excitation of septohippocampal GABA but not cholinergic neurons: implications for learning and memory. J Neurosci 20:3900–3908.

Yoder RM, Pang KC (2005) Involvement of GABAergic and cholinergic medial septal neurons in hippocampal theta rhythm. Hippocampus 15:381–392. doi: 10.1002/hipo.20062

Young CK, Ruan M, McNaughton N (2017) A Critical Assessment of Directed Connectivity Estimates with Artificially Imposed Causality in the Supramammillary-Septo-Hippocampal Circuit. Front Syst Neurosci 11:72. doi: 10.3389/fnsys.2017.00072

Young LJ, Wang Z (2004) The neurobiology of pair bonding. Nat Neurosci 7:1048–1054. doi: 10.1038/nn1327

Yuan M, Meyer T, Benkowitz C, et al (2017) Somatostatin-positive interneurons in the dentate gyrus of mice provide local- and long-range septal synaptic inhibition. Elife. doi: 10.7554/eLife.21105

Zaborszky L, Duque A, Gielow M, et al (2014) Organization of the basal forebrain cholinergic projection system: specific or diffuse? In: The Rat Nervous System: Fourth Edition. pp 491–507

Zaborszky L, van den Pol AN, Gyengesi E (2012) The basal forebrain cholinergic projection system in mice. In: The Mouse Nervous System. pp 684–718

Zhang C, Chua BE, Yang A, et al (2015) Central relaxin-3 receptor (RXFP3) activation reduces elevated, but not basal, anxiety-like behaviour in C57BL/6J mice. Behav Brain Res 292:125–132. doi: 10.1016/j.bbr.2015.06.010

Zhang H, Lin SC, Nicolelis MA (2011) A distinctive subpopulation of medial septal slow-firing neurons promote hippocampal activation and theta oscillations. J Neurophysiol 106:2749–2763. doi: 10.1152/jn.00267.2011; 10.1152/jn.00267.2011

# 9

# Appendices

## 9.1. Supplementary Figures

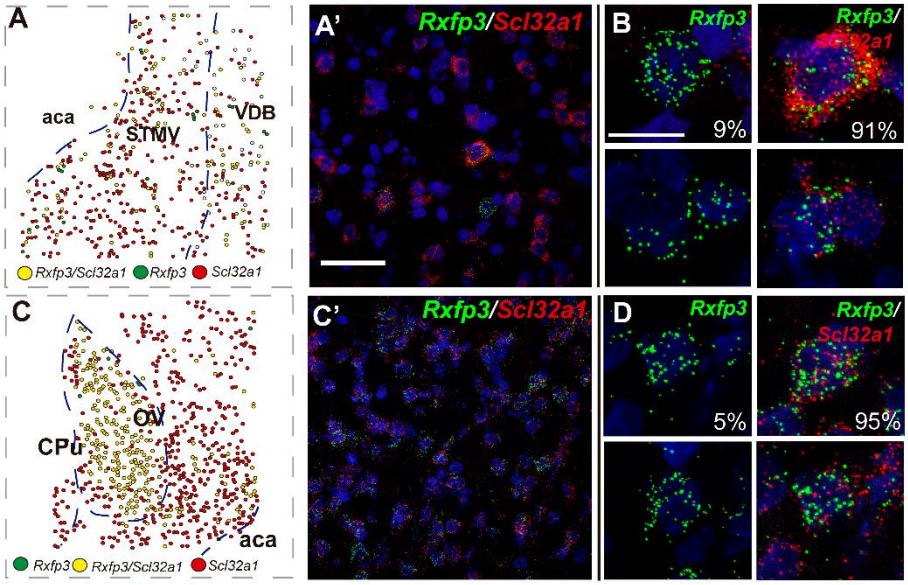


**Supplementary Figure 1 Characterisation of the neurochemical phenotype of *Rxfp3* mRNA-positive neurons in STMV an STOV**. (**A**) Schematic illustrating *Rxfp3* distribution and co-expression with O*xtr* mRNA in STMV (**A′and B**) Representative fluorescent images. Representative images of fluorescent ISH and quantification of co-expression percentages indicated (lower right corner). (**C**) Schematic illustrating *Rxfp3* mRNA distribution and co-expression with *Oxtr and Slc32a1* mRNAs in the MePV. (**C′** and **D**). Scale barS: 100 µm (A′), 10µm (B)

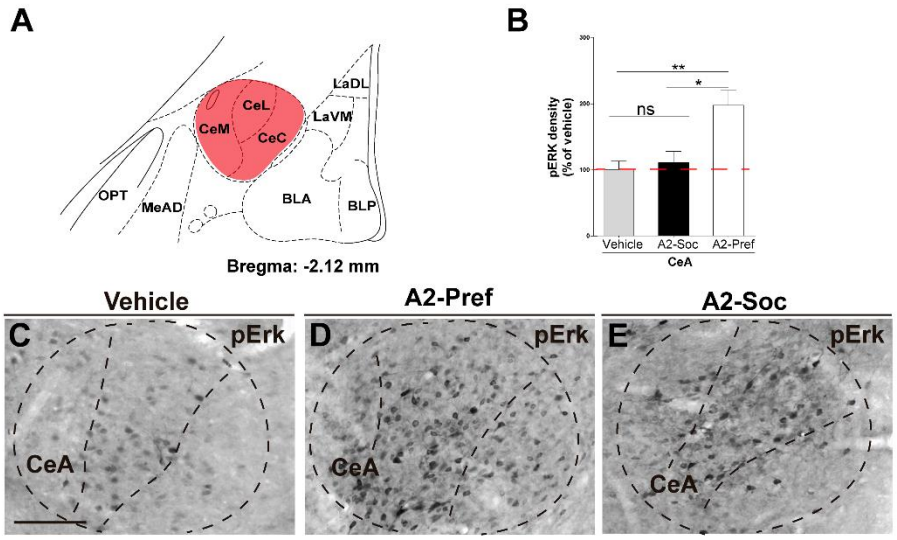


**Supplementary Figure 2. pERK immunostaining in the CeA after social encounters**. **(A)** Schematic illustrating the CeA sub-nuclei analysed. (**B**) Density of pERK-stained neurons was significantly increased in A2-Pref rats compared to vehicle treated rats (dashed red line). Representative images of pERK immunostaining in the CeA of **(C)** vehicle, **(D)** A2-Pref and **(E)** A2-Soc group rats. *p < 0.05; **p < 0.01. Scale bar: 100 µm (C).

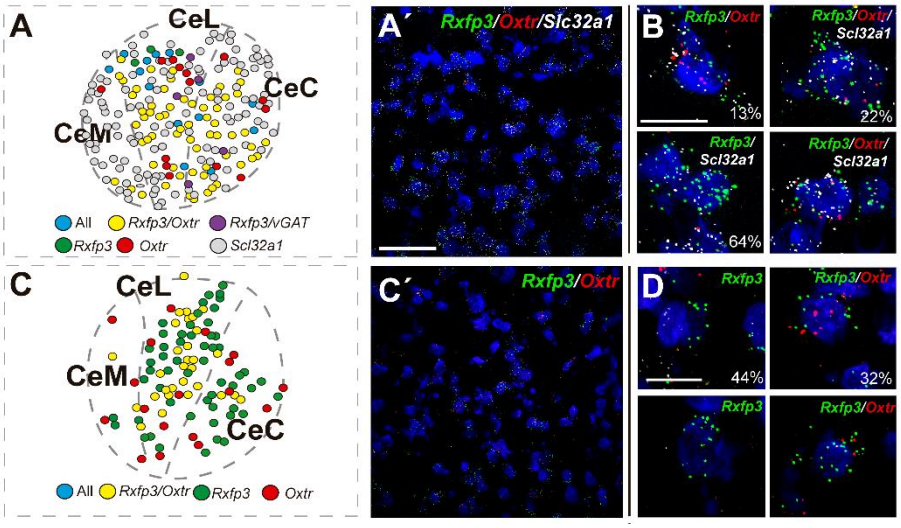


**Supplementary Figure 3. Characterisation of the neurochemical phenotype of *Rxfp3* mRNA-positive neurons in CeA**. (**A**) Schematic illustrating *Rxfp3* mRNA distribution and co-expression with *Oxtr* and *Slc32a1* mRNA in CeA. (**A'**and **B**) Representative fluorescent images. Representative images of fluorescent ISH and quantification of co-expression percentages indicated (lower right corner). Scale bar: 100 µm (A'), 10µm (B)

## 9.2. Publications

Brain Struct Funct
DOI 10.1007/s00429-016-1227-8

ORIGINAL ARTICLE

# Central relaxin-3 receptor (RXFP3) activation increases ERK phosphorylation in septal cholinergic neurons and impairs spatial working memory

Héctor Albert-Gascó[1] · Álvaro García-Avilés[1] · Salma Moustafa[1] · Sandra Sánchez-Sarasua[1] · Andrew L. Gundlach[2,3] · Francisco E. Olucha-Bordonau[1] · Ana M. Sánchez-Pérez[1]

Received: 30 November 2015 / Accepted: 12 April 2016


Abstract The medial septum/diagonal band (MS/DB) is a relay region connecting the hypothalamus and brainstem with the hippocampus, and both the MS/DB and dorsal/ventral hippocampus receive strong topographic GABA/peptidergic projections from the nucleus incertus of the pontine tegmentum. The neuropeptide relaxin-3, released by these neurons, is the cognate ligand for a Gi/o protein-coupled receptor, RXFP3, which is highly expressed within the MS/DB, and both cholinergic and GABAergic neurons in this region of rat brain receive relaxin-3 positive terminals/boutons. Comprehensive in vitro studies have demonstrated that the cell signaling pathways altered by RXFP3 stimulation, include inhibition of forskolin-activated cAMP levels and activation of ERK phosphorylation. In this study we investigated whether intracerebroventricular (icv) injection of RXFP3-A2, a selective relaxin-3 receptor agonist, altered ERK phosphorylation levels in the MS/DB of adult male rats. We subsequently assessed the neurochemical phenotype of phosphorylated (p) ERK-positive neurons in MS/DB after icv RXFP3-A2 administration by dual-label immunostaining for pERK and neuronal markers for cholinergic and GABAergic neurons. Central RXFP3-A2 injection significantly increased levels of pERK immunoreactivity (IR) in MS/DB at 20 and 90 min post-injection, compared to vehicle and naive levels. In addition, RXFP3-A2 increased the number of cells expressing pERK-IR in the MS/DB at 90 (but not 20) min post-injection in cholinergic (but not GABAergic) neurons, which also expressed putative RXFP3-IR. Moreover, icv injection of RXFP3-A2 impaired alternation in a delayed spontaneous T-maze test of spatial working memory. The presence of RXFP3-like IR and the RXFP3-related activation of the MAPK/ERK pathway in MS/DB cholinergic neurons identifies them as a key target of ascending relaxin-3 projections with implications for the acute and chronic modulation of cholinergic neuron activity and function by relaxin-3/RXFP3 signaling.

**Keywords** Calcium-binding proteins Choline acetyltransferase GABA neurons MAPK/ERK pathway Nucleus incertus Septum · Working spatial memory RXFP3-like immunoreactivity

Francisco E. Olucha-Bordonau and Ana M. Sánchez-Perez contributed equally to this work.

& Ana M. Sánchez-Pérez
sanchean@uji.es

Francisco E. Olucha-Bordonau
folucha@uji.es

[1] Department of Medicine, School of Medical Sciences, University Jaume I, 12071 Castellón de la Plana, Spain

[2] The Florey Institute of Neuroscience and Mental Health, Parkville, VIC 3052, Australia

[3] Florey Department of Neuroscience and Mental Health, The University of Melbourne, Melbourne, VIC 3010, Australia

## Introduction

The septal area is involved in the regulation of behavioural processes of arousal, attention and spatial navigation/exploration, particularly via connections from the medial septum/diagonal band (MS/DB) to the hippocampus (Vertes and Kocsis 1997). Arousal, attention and locomotion related to navigation and exploration and mnemonic processes in humans (Morales et al. 1971; Bannerman et al. 2004) are functionally associated with hippocampal theta rhythm, a synchronous 4-12 Hz oscillation of primarily principal neurons and with place cell configuration (Kemp

Published online: 05 May 2016

frontiers in Neuroanatomy

ORIGINAL RESEARCH
published: 17 January 2018
doi: 10.3389/fnana.2017.00133

# GABAergic Neurons in the Rat Medial Septal Complex Express Relaxin-3 Receptor (RXFP3) mRNA

Hector Albert-Gascó [1,2‡], Sherie Ma [2,3†‡], Francisco Ros-Bernal [1], Ana M. Sánchez-Pérez [1], Andrew L. Gundlach [2,3§] and Francisco E. Olucha-Bordonau [1*§]

[1] Unitat Predepartamental de Medicina, Facultat de Ciències de la Salut, Universitat Jaume I, Castellón, Spain, [2] The Florey Institute of Neuroscience and Mental Health, Parkville, VIC, Australia, [3] Florey Department of Neuroscience and Mental Health, The University of Melbourne, Melbourne, VIC, Australia

OPEN ACCESS

Edited by:
Jose L. Lanciego,
Universidad de Navarra, Spain

Reviewed by:
Margarita Lucía Rodrigo-Angulo,
Universidad Autonoma de Madrid, Spain
Ursula H. Winzer-Serhan,
Texas A&M Health Science Center, United States
Carlos Crespo,
Universitat de València, Spain

*Correspondence:
Francisco E. Olucha-Bordonau
folucha@uji.es

†Present address:
Sherie Ma,
Drug Discovery Biology, Monash Institute of Pharmaceutical Sciences, Monash University, Parkville, VIC, Australia

‡These authors have contributed equally to this work.
§These authors jointly supervised this research.

Received: 12 September 2017
Accepted: 18 December 2017
Published: 17 January 2018

Citation:
Albert-Gascó H, Ma S, Ros-Bernal F, Sánchez-Pérez AM, Gundlach AL and Olucha-Bordonau FE (2018) GABAergic Neurons in the Rat Medial Septal Complex Express Relaxin-3 Receptor (RXFP3) mRNA. Front. Neuroanat. 11:133. doi: 10.3389/fnana.2017.00133

The medial septum (MS) complex modulates hippocampal function and related behaviors. Septohippocampal projections promote and control different forms of hippocampal synchronization. Specifically, GABAergic and cholinergic projections targeting the hippocampal formation from the MS provide bursting discharges to promote theta rhythm, or tonic activity to promote gamma oscillations. In turn, the MS is targeted by ascending projections from the hypothalamus and brainstem. One of these projections arises from the nucleus incertus in the pontine tegmentum, which contains GABA neurons that co-express the neuropeptide relaxin-3 (Rln3). Both stimulation of the nucleus incertus and septal infusion of Rln3 receptor agonist peptides promotes hippocampal theta rhythm. The $G_{i/o}$-protein-coupled receptor, relaxin-family peptide receptor 3 (RXFP3), is the cognate receptor for Rln3 and identification of the transmitter phenotype of neurons expressing RXFP3 in the septohippocampal system can provide further insights into the role of Rln3 transmission in the promotion of septohippocampal theta rhythm. Therefore, we used RNAscope multiplex in situ hybridization to characterize the septal neurons expressing Rxfp3 mRNA in the rat. Our results demonstrate that Rxfp3 mRNA is abundantly expressed in vesicular GABA transporter (vGAT) mRNA- and parvalbumin (PV) mRNA-positive GABA neurons in MS, whereas ChAT mRNA-positive acetylcholine neurons lack Rxfp3 mRNA. Approximately 75% of Rxfp3 mRNA-positive neurons expressed vGAT mRNA (and 22% were PV mRNA-positive), while the remaining 25% expressed Rxfp3 mRNA only, consistent with a potential glutamatergic phenotype. Similar proportions were observed in the posterior septum. The occurrence of RXFP3 in PV-positive GABAergic neurons gives support to a role for the Rln3-RXFP3 system in septohippocampal theta rhythm.

Keywords: arousal, ChAT, emotion, GABA, hippocampus, nucleus incertus, relaxin-3, theta rhythm

Abbreviations: ChAT, choline acetyl transferase; HDB, horizontal diagonal band; LS, lateral septum; LSD, lateral septum dorsal; LSI, lateral septum intermediate; LSV, lateral septum ventral; LV, lateral ventricle; MS, medial septum; NI, nucleus incertus; nNOS, neuronal nitric oxide synthase; PV, parvalbumin; Rln3, relaxin-3; Rxfp3, relaxin-family peptide receptor 3; SFi, septofimbrial nucleus; SFO, subfornical organ; TS, triangular septum; VDB, vertical diagonal band; vGAT (slc32a1), vesicular GABA transporter.